Available online at www.sciencedirect.com
ScienceDirect
Coordination Chemistry Reviews 250 (2006) 2952–2986
COORDINATION CHEMISTRY REVIEWS
www.elsevier.com/locate/ccr

Review

Anion coordination chemistry in aqueous solution of polyammonium receptors

Enrique García-España [a,*], Pilar Díaz [a], José M. Llinares [a], Antonio Bianchi [b]

[a] *Instituto de Ciencia Molecular, Universidad de Valencia, Institutos de Paterna, Apartado de Correos 22085, 46071 Valencia, Spain*
[b] *Dipartimento di Chimica, Università degli Studi di Firenze, Via della Lastruccia, 3-50019 Sesto Fiorentino, Italy*

Received 7 February 2006; accepted 26 May 2006
Available online 3 June 2006

Contents

Abstract

The behavior of polyamines as receptors of selected families of anions in water is explored. First metallocyanide interaction with saturated polyammonium hosts is analyzed both in solution and in the solid state. The utility of potentiometry, multinuclear NMR, microcalorimetry and cyclic voltammetry to describe solution features of this chemistry is described for selected systems. Sulfate, phosphate, polyphosphate and nucleotide interactions with large polyammonium receptors are then reviewed. Hydrogen bond formation is discussed from a thermodynamic point of view. The influence of the presence of aromatic fragments within the structure on the binding strength is discussed. Factors affecting ATP hydrolytic cleavage by macrocyclic polyammonium receptors is revisited. Metal complexes are analyzed as anion receptors through formation of mixed complexes. Finally, an example of the influence of anion in crystal growing is provided.

Keywords: Polyamines; Macrocycles; Metallocyanides; Sulfate; Polyphosphates; Nucleotides; Metal complexes

1. Introduction

Supramolecular chemistry, the chemistry beyond the molecule, gained its entity with the pioneering work of C.

* Corresponding author. Tel.: +34 96 3544879; fax: +34 96 3544003.
E-mail address: Enrique.garcia-es@uv.es (E. García-España).

0010-8545/$ – see front matter © 2006 Elsevier B.V. All rights reserved.
doi:10.1016/j.ccr.2006.05.018

Pedersen, J.-M. Lehn and D.J. Cram in the 1960–1970 decade [1–5]. The concepts and language of this chemical discipline, which were in part borrowed from biology and coordination chemistry, can be at a large extent attributed to the scientific creativity of Lehn [6–8]. Recognition, translocation, catalysis and self-organization are considered as the four corner stones of supramolecular chemistry. Recognition does not only contemplate the well-known transition metals (classical coordination chemistry) but also spherical metal ions, organic cations, neutral and anionic species. Anions have a great relevance from a biological point of view since over 70% of all cofactors and substrates involved in biology are of anionic nature. Anion coordination chemistry came up as a scientific topic also with the conceptual development of supramolecular chemistry [8–10].

Interestingly enough, the birth of the first recognized synthetic halide receptors occurred practically at the same time than the discovery by Charles Pedersen of the crown ethers. While C. Pedersen submitted to JACS its first paper on crown ethers on April 1967 entitled "Cyclic Polyamines and their Complexes with Metal Salts" [1], Park and Simmons, which were working in the same company than Pedersen, submitted their paper on the complexes formed by bicyclic diammonium receptors with chloride entitled "*Macrobicyclic Amines. III. Encapsulation of Halide ions by in, in-1, (k + 2)-diazabicyclo[k.l.m]alkane-ammonium ions*" also to JACS in November of the same year [11]. These cage-type receptors were called katapinands taking after the Greek term describing the swallowing up of the anionic species towards the interior of the cavity. However, while the investigations on crown ethers rapidly evolved and many of these compounds were prepared and its chemistry widely explored, the studies on anion coordination chemistry remained at this initial stage and were not further developed until J.-M. Lehn and his coworkers retook this point in the late 1970s and beginning of the 1980s [12–18]. These efforts were then followed by a reduced number of groups [19–21]. Nowadays, the number of research groups and scientific papers dealing with anions is very high [22–28] and has become a very lively topic within supramolecular chemistry as is reflected by the different reviews included in this issue.

The work we are going to summarize dates back to the early 1980s when some of us started our work on anion coordination analyzing the interaction of metallocyanide anions with synthetic polyammonium receptors in pure water (see Section 2). Although the review will start precisely with this work, it does not follow a chronological order. The receptors studied will be saturated polyammonium compounds either of cyclic or open-chain nature and cyclophane or heterocyclophane compounds. We will analyze their interaction with different anions either as free-receptors or in the form of metal complexes. It has to be emphasized that all the results included in the review refer to pure water as a solvent.

1.1. Anion properties

Anions present characteristic properties that have to be taken into account in order to prepare adequate receptors. First, anions are large when compared with metal ions. For instance, F^- which is the smallest anion displays an ionic radius ($r_{F^-} = 135$ pm) close to potassium ($r_{K^+} = 133$ pm) which can be considered as a middle-sized cation. The second aspect concerns the variety of shapes that anions have covering spherical (F^-, Cl^-, etc.), triangular (NO_3^-, HCO_3^-, etc.), tetrahedral (SO_4^{2-}, phosphate, ReO_4^-), square planar ($PdCl_4^{2-}$, $[Pt(CN)_4]^{2-}$), octahedral (PF_6^-, $[Fe(CN)_6]^{4-}$) or even the more complex shapes that many biologically relevant adopt like polyacarboxylates (citrate, malonate, succinate, etc.), nucleotides (AMP, ADP and ATP) and dinucleotides (NAD^+, NADH). In this sense, it is interesting to recall the anionic nature of the biologic polymers DNA and RNA that are recognized or self-recognized in key steps of life. The third particularity of anions regards their high hydration energies in comparison with metal ions of similar charge density. This characteristic, which is related to their hydrogen bonding ability, makes more energetically demanding its complexation in water in relation to spherical metal ions. It is important to remark that water is the solvent of life and provides an environment with which leaving systems are continuously exchanging nutrients and raw materials. Another very obvious but frequently ignored anion characteristic is the limited pH range of existence of many anions. If anions are conjugated bases of protic acids, they will bear protonation processes and their negative charge will depend on their basicity constants. A very simple example is provided by phosphate which presents in water stepwise constants of 11.5, 7.7 and 2.1 for its first, second and third protonation steps, respectively [29]. Therefore, phosphate will only exist as a trivalent anion in a very basic pH range while at neutral pH will be as a mixture of the monovalent and divalent forms. This property can be advantageously used for discriminating between anions of different basicity. A final characteristic of interest when designing receptors for anions is the fact that anions are coordinatively saturated species. Thus, only charge to charge or more or less weak intermolecular forces like hydrogen-bonding, π–π-stacking or hydrophobic effects can be used for their recognition. However, since anions are Lewis bases appropriately, designed Lewis acids can also be used for interacting with them. Different, boron, tin or silica-based receptors have been used for this purpose. Recently, metalloreceptors in which the metal ions constitute corners of different structures have also been employed as anion receptors [30,31]. Finally, classical coordination complexes are potential anion receptors provided they have coordinatively unsaturated sites. This point links anion coordination with metal coordination chemistry through ternary metal complex formation and is the mechanism of choice for many enzymes dealing with the activation of small molecules or anions. Carbonic anhydrase or phosphatases are examples of this behavior.

1.2. Considerations on the basicity and conformation of the receptors

The feature distinguishing anions from all other guest species is their negative charge. Therefore, charge is the prime property to be addressed when building anion receptors [10,32]. One

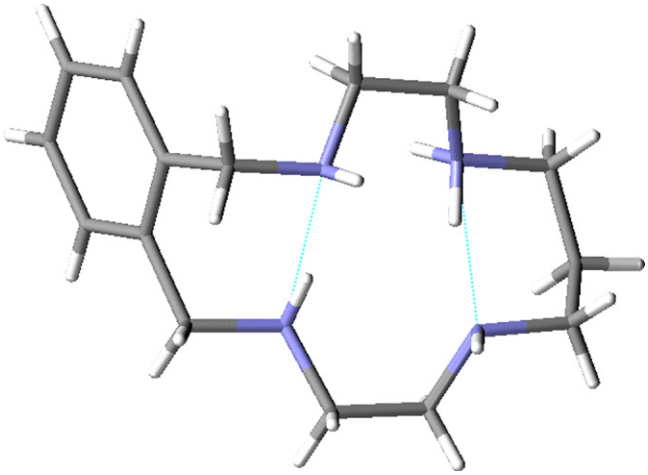

Fig. 1. Stick representation of the $H_2(oB232)^{2+}$ cation showing intramolecular hydrogen-bonding [36].

way to do this is through oppositely charged receptors having an appropriate disposition of charged centers. In the biological world the side chains of basic amino acids like lysine and arginine play this role, the first one offering an amino group which is protonated at neutral pH while the second one provides a permanently charged site. Lysine residues also participate in the binding of CO_2 to the surface of haemoglobin forming elusive carbamate groups and facilitating its transport from the tissues to the lungs and its expulsion.

In charged synthetic macrocycles it is important to know not only which is the actual protonation degree at a given pH value, but also which is the distribution of the charged centers [33]. Upon protonation polyammomium receptors stiffen achieving more organized or rigid structures. One well-known example comes from the crystal structure of the diprotonated or tetraprotonated forms of the cyclic tetraamine 1,4,8,11-tetraazacyclotetradecane (cyclam). In $H_2(cyclam)^{2+}$ the amine groups all show the *in-in* conformation favoring the formation of intramolecular hydrogen bonds between adjacent non-protonated and protonated amine groups, whereas in $H_4cyclam^{4+}$ all the ammonium groups display an *out* conformation so that the positive charges are as far away as possible between them [34,35]. Similar structural features to those of $H_2(cyclam)^{2+}$ are found in the crystals structure of $H_2(oB232)^{2+}$ (2,5,9,12-tetraaza[14]*ortho*cyclophane) in which intramolecular hydrogen bonding between adjacent non-protonated and protonated hydrogen bonds is also observed (see Fig. 1) [36].

These characteristics can be extended to the so-called large polyazacycloalkanes. The adjective large was coined to describe macrocyclic polyamines containing more than six amine groups [37]. Protonation introduces rigidity into the receptor since positive charges placed in adjacent nitrogens will tend to adopt *anti* conformations in order to minimize electrostatic repulsions becoming the macrocyclic shape more circular. The degree of rigidity depends also on the length of the hydrocarbon chains between the amine groups. The amount of electrostatic repulsion between ammonium groups separated by propylenic chains is markedly lower than when the separation is by ethylenic

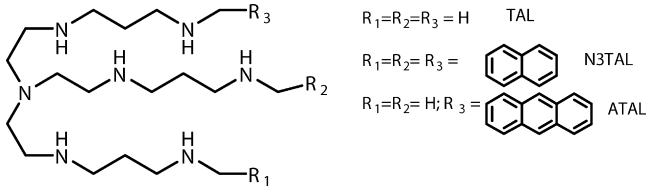

Chart 1.

chains. The next section includes further discussion on this crucial aspect.

Tripodal ligands have proved to be interesting receptors for anions [38–43]. Recently, we have prepared receptors of this class in which the three arms of the classical tripodal polyamine tris(aminoethyl)amine(tren) has been enlarged with propylamino bridges and different fluorophoric groups (receptors TAL, N3TAL and ATAL in Chart 1) [44,45].

Again in these receptors the protonation state should define the conformation adopted by the ligand being much more open when the amine groups in the arms are protonated.

The dichotomy rigid versus foldable or flexible ligands is an interesting point to be considered when designing receptors for anions [10,46]. Rigid hosts having complementary disposed anchoring groups for a given anion should provide the highest affinity and selectivity. The energetic cost for adapting to the anionic species has already been paid in the synthetic work. More flexible or foldable receptors which can adapt to the stereochemical requirements of a given anion along the complexation event should however pay the energetic cost for such reorganization (Fig. 2).

Nevertheless, the more flexible a receptor is the more self-adaptive will be and consequently the energetic cost to be paid for matching the stereochemical and electronic features of the target species will be lower. Therefore, in the design of a receptor one has also to take into account the purpose or function that wants to achieve. For instance, in order to have high rates and turnovers in catalytic processes, flexible self-adaptive receptors which do not bind too strongly to the target species are often preferred.

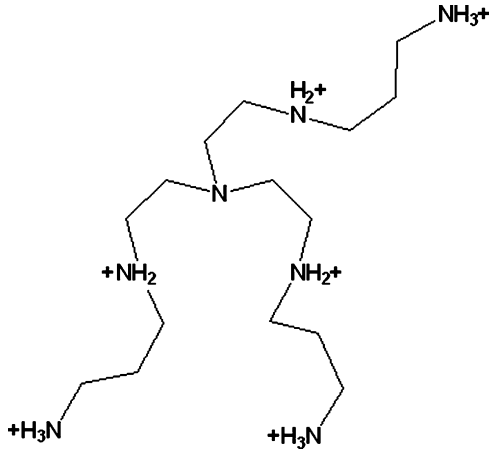

Fig. 2. Schematic representation of the open-conformation of hexaprotonated polyamine TAL.

2. Interaction with anionic complexes: supercomplex formation

The interaction of the series of large polyazacycloalkanes [21]aneN$_7$, [24]aneN$_8$, [27]aneN$_9$, [30]aneN$_{10}$, [33]aneN$_{11}$ and [36]aneN$_{12}$ (Chart 2) in their protonated forms with a series of metallocyanides and other anionic metal complexes was examined by different techniques [47–54]. The resulting supramolecular species formed are called supercomplexes or complexes of second coordination sphere in which the polyammonium species is placed in the second coordination sphere interacting electrostatically and through hydrogen bonding and other weak forces with the complex anion.

The use of metallocyanides as substrates for the interaction with ammonium receptor is not casual. These anions offer very simple ways of analyzing the influence on host–guest affinity of negative charge increases while other factors like shape and geometry are kept essentially constant. Apart from solvation effects, the only noticeable change when moving from $[Fe(CN)_6]^{3-}$ to $[Fe(CN)_6]^{4-}$ is the different net charge of both anions. In the same way, exchanging $[Fe(CN)_6]^{3-}$ by $[Co(CN)_6]^{3-}$ should be non-significant from a recognition point of view; both anions are octahedral and have a very close size.

On the other hand, the $[Fe(CN)_6]^{3-}/[Fe(CN)_6]^{4-}$ redox couple is very useful due to its quasi-reversible behavior [15,18]. This simple electrochemical behavior permits to derive stability constants by an alternative method to pH-metric titration, which is the most widely used technique in this area. It is always advisable to use more than one independent technique in order to have reliable descriptions of the anion–receptor systems.

Fig. 3 gathers a representation of the logarithms of the stepwise stability constants against the number of protons (p) for the equilibria $M(CN)_6^{(n-6)} + H_pL^{p+} \leftrightarrows [M(CN)_6](H_pL)^{(n+p-6)}$ (n = metal ion charge) for the interaction of $[Fe(CN)_6]^{4-}$ and

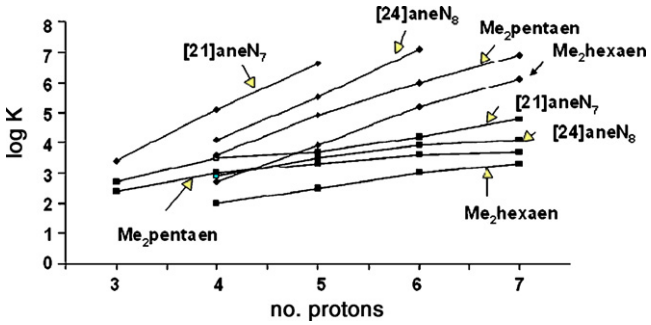

Fig. 3. Plot of the logarithms of the stability constants for the equilibria $M(CN)_6^{(n-6)} + H_pL^{p+} \leftrightarrows [M(CN)_6](H_pL)^{(n+p-6)}$ (n = metal ion charge) vs. the number (p) of positive charges in the receptor for the interaction of $[Fe(CN)_6]^{4-}$ (diamonds) and $[Co(CN)_6]^{3-}$ (squares) with the polyammonium receptors [21]aneN$_7$, [24]aneN$_8$, Me$_2$hexaen and Me$_2$heptaen [53]. Reproduced by permission of The Royal Society of Chemistry.

$[Co(CN)_6]^{3-}$ with the polyammonium receptors [21]aneN$_7$, [24]aneN$_8$ and its open-chain counterparts Me$_2$hexaen and Me$_2$heptaen (Chart 2). The open-chain counterparts were selected so that they had the same number of carbon and nitrogen atoms and same class of amine groups than their cyclic counterparts [55].

Such a plot shows that: (i) the stepwise constants for a given receptor increase as it does the protonation degree (positive charge) of the receptor, (ii) for a given protonation degree of the receptor the highest stability is displayed by the receptor with the highest charge density; smaller ligands show higher constants than the larger ones and cyclic ligands show higher constants than the corresponding open-chain counterparts: [21]aneN$_7$ > [24]aneN$_8$ > Me$_2$hexaen > Me$_2$heptaen and (iii) the stability constants of the adducts species formed by $[Fe(CN)_6]^{4-}$ are higher than those formed by $[Co(CN)_6]^{3-}$; the

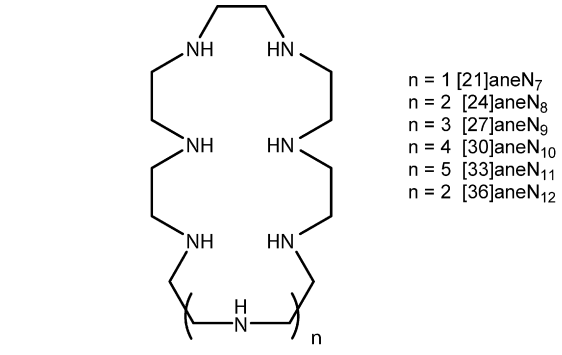

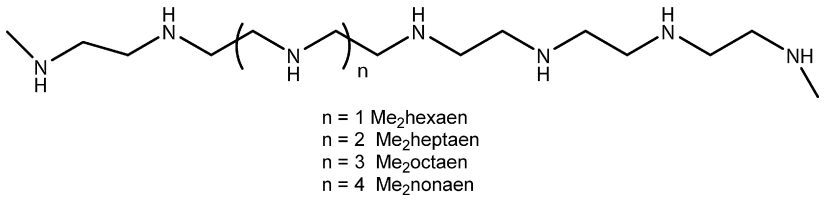

Chart 2.

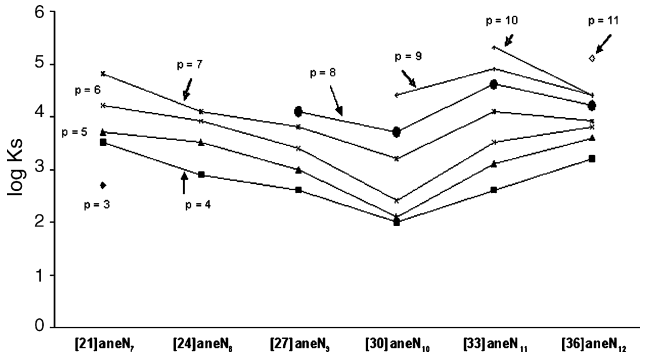

Fig. 4. Plot of the variation of the constants for the equilibria $[Co(CN)_6]^{3-} + H_p([3k]aneN_k)^{p+} \leftrightarrows [Co(CN)_6](H_p([3k]aneN_k))^{(3-p)}$ [52]. Reprinted with permission from Ref. [52]. Copyright 1992 American Chemical Society.

slopes of the lines joining the different protonation degrees in every system are higher for the $[Fe(CN)_6]^{4-}$ complexes than for the $[Co(CN)_6]^{3-}$ ones and also the systems with macrocyclic receptors show higher slopes than those with open-chain ligands.

All these data confirm that the main driving force in metallocyanide-polyammonium receptor interactions are charge–charge interactions, makes it difficult to modulate the selective discrimination of one guest over another. However, a representation of the constants for the equilibria $[Co(CN)_6]^{3-} + H_p([3k]aneN_k)^{p+} \leftrightarrows [Co(CN)_6](H_p([3k]aneN_k))^{(3-p)}$ shows that typically the constants for a given protonation degree p steadily decrease when going from a macrocycle to the next one in size until [30]aneN$_{10}$ is reached. From thereon an increase in stability is observed (Fig. 4). This change in the pattern could be attributed to an inclusion of the anion within the macrocyclic cavity favoring thus shorter charge–charge interactions and formation of stronger hydrogen bonds.

Inclusion of the macrocycle inside the cavity of the macrocycle was also postulated by early work performed by the groups of Lehn in Strasbourgh and Balzani in Bolonia on the interaction of $[Co(CN)_6]^{3-}$ with the polyammonium receptors [32]aneN$_8$ and [24]aneN$_6$ containing all propylenic chains between the nitrogen atoms [56,57]. These authors observed that the quantum yield of the light-induced aquation reaction of $[Co(CN)_6]^{3-}$ was reduced to one-third of the initial value in the presence of the octaprotonated receptor $H_8([32]aneN_8)^{8+}$ suggesting that inclusion of $[Co(CN)_6]^{3-}$ into the macrocycle through the equatorial plane had occurred.

$$[Co(CN)_6]^{3-} + H_3O^+ \rightarrow [Co(CN)_5(H_2O)]^{2-} + HCN$$

The four CN^- groups in the enclosed equatorial plane would be hydrogen bonded to the ammonium groups of the macrocycle and would not be exchanged by water molecules upon light excitation (Fig. 5).

These analyses have permitted to draw structural conclusions for a number of systems [58]. Reduction by 1/2 of the quantum yield would stand for an interaction of the polyammonium host and the metallocyanide through one of its triangular faces while reduction by 1/3 would imply interaction through one of its edges. Such studies have allowed, for instance, to assume that the interaction between $[Co(CN)_6]^{3-}$ and the tetraprotonated cyclophane 2,6,9,13-tetraza[14]*para*cyclophane (*p*B323, Chart 3) or hexaprotonated $H_6([24]aneN_6)^{6+}$ involves one face of the octahedron.

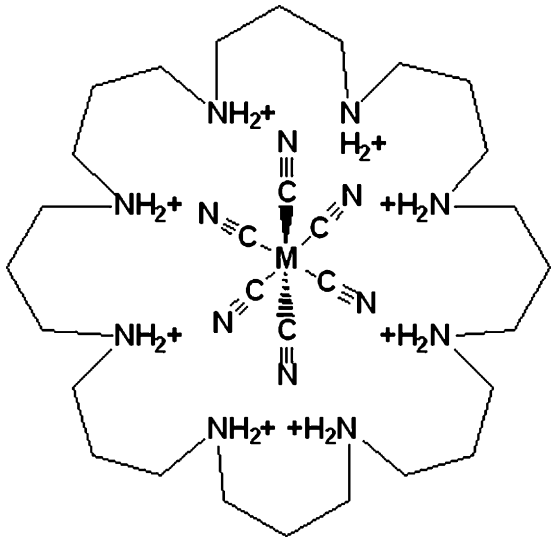

Fig. 5. Schematic drawing of the inclusion of the equatorial plane of octahedral metallocyanides in the macrocyclic hole of $H_8([32]aneN_8)^{8+}$ [56,57].

Similar results were obtained for the interaction of $[Co(CN)_6]^{3-}$ with the open-chain terminally dibenzylated receptor B2222B (Chart 3) containing five amine groups between the aryl moieties [59].

On the other hand, photochemical studies can provide values of the stability constants for the formation of the adduct species. Interaction of *p*B323 or of the dibenzylated ligands B2B-B2222B (Chart 3) with $[Co(CN)_6]^{3-}$ leads to a quenching of the emission of the aromatic moiety which has a static nature [54]. In this case, the association constants can be obtained by means of the equation:

$$K_{as} = \frac{(I_0 - I)\varepsilon^{p+}_{H_pL}}{I[Q]\varepsilon^{p+}_{H_pL} \cdot Q}$$

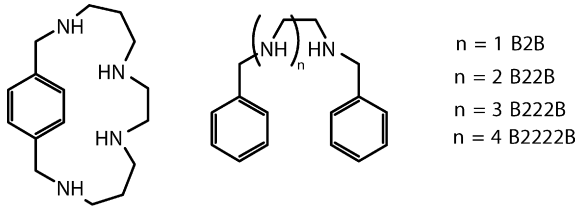

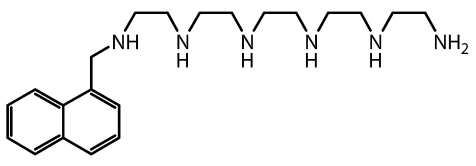

Chart 3.

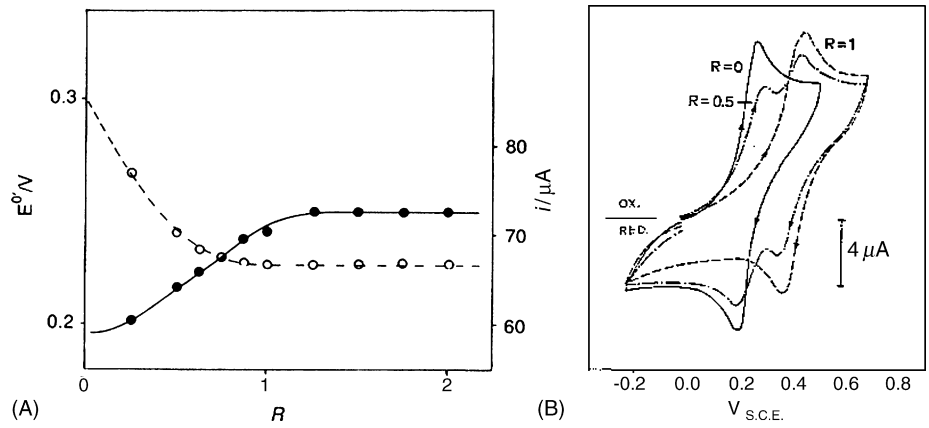

Fig. 6. (A) Typical effects of the addition of a polyammonium receptor (H_pL^{p+}) on the cyclic voltammogram of $[Fe(CN)_6]^{4-}$. R is the mole ratio receptor:metallocyanide [53]. Reproduced by permission of The Royal Society of Chemistry. (B) Representation of the variation of peak potential (continuous line) and peak current (dashed line) vs. R for a system polyammonium receptor H_pL^{p+}–$[Fe(CN)_6]^{4-}$. Reprinted with permission from Ref. [49]. Copyright 1987 American Chemical Society.

where $\varepsilon^{p+}_{H_pL}$ and $\varepsilon^{p+} \cdot Q_b$ are, respectively, the molar absorptivities of the emissive species and of the adducts formed between the emissive species and the quencher, I the fluorescence-emission intensity for a given amount of quencher and I_0 is the fluorescence maximum intensity. Interestingly enough, the values of the constants obtained for the interaction of tetraprotonated $H_4(pB323)^{4+}$ with $[Co(CN)_6]^{3-}$ either by means of pH-metric titrations or steady-state fluorescence measurements are in good agreement and are higher than those obtained for the large azacycloalkanes with the same protonation degrees [49,60].

When dealing with receptors in which naphthylmethyl units were bound to the ends of a polyamine chain (see receptor N22222 in Chart 3) it was possible to carry out the photoexcitation of hexacyanocobaltate by direct irradiation of the naphthalene unit. Therefore, this system might be considered as a molecular photoreactor, the host acting as an antenna which photosensitizes the aquation reaction in the guest species [61].

As above noted, the use of $[Fe(CN)_6]^{4-}$ permits to analyze the systems by cyclic voltamperometry. Fig. 6 shows the typical behavior of these systems.

Addition of the receptor to an aqueous solution of $[Fe(CN)_6]^{4-}$ yields an anodic shift of the voltammogram until a certain mole ratio R = receptor: $[Fe(CN)_6]^{4-}$, normally 1 is reached (Fig. 6B). From a plot of the variations of the peak potentials versus R it is possible to deduce the stoichiometry of the formed supercomplex. Contrarily, the effect of supercomplex formation is a decrease on the peak intensity due to the formation of the higher molecular weight adducts species [53].

Distribution diagrams of the species existing in equilibria calculated from the stability constants determined pH-metrically coupled with plots of the variation of anodic peak currents and formal potentials show plateaus in the values of the latter two variables in the zones where single species predominate in solution (Fig. 7).

Application of classical voltammetric and polarographic methods permits to calculate the stability constants for the formation of $[Fe(CN)_6]^{3-}$ adducts. Similar determinations are not possible by means of pH-metric methods due to the very rapid aquation process of the oxidized anion.

Table 1 shows that, as it could be expected for anions displaying same charge, geometry and size, the values of the stability constants for the systems $[Fe(CN)_6]^{3-}$–polyammonium receptors are very close to those obtained by pH-metry for the systems $[Co(CN)_6]^{3-}$–polyammonium receptors.

Another point of interest regards the monomeric or polymeric nature of the adducts formed in aqueous solution. Application of the molar ratio method [62] to the electrochemical data indicated that the adduct species $[Fe(CN)_6]^{4-}$:H_pL^{p+} formed in aqueous solution had always a monomeric character and 2:2 or higher aggregates were not observed [63]. This discrete nature of the species formed in solution has not a necessary correspondence in the solid state. One of the first supercomplex structures determined by single crystal X-ray diffraction corresponded to a solid of chemical formula $[H_8([30]aneN_{10})][Co(CN)_6]_2Cl_2 \cdot 10H_2O$ which evolved from slow evaporation of aqueous solutions of

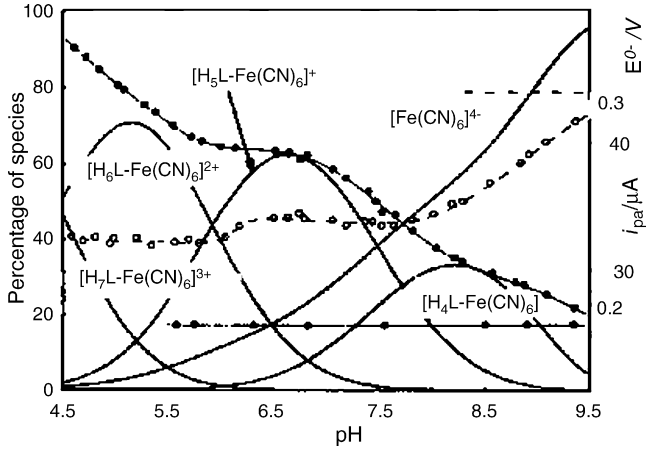

Fig. 7. Distribution diagram in the species existing in equilibria in the system $[Fe(CN)_6]^{4-}$:Me$_2$heptaen and anodic peak currents (dashed lines, open circles) and formal potentials (continuous lines, solid circles) of the couple $[Fe(CN)_6]^{3-}$–$[Fe(CN)_6]^{4-}$ [53]. Reproduced by permission of The Royal Society of Chemistry.

Table 1
Logarithms of the equilibrium constants for the supercomplex formation between $[Fe(CN)_6]^{3-}$ and the polyamines [21]aneN$_7$ and [24]aneN$_8$ calculated from cyclic voltammetry data

Reaction[a]	[21]aneN$_7$		[24]aneN$_8$	
	$[Fe(CN)_6]^{3-}$	$[Co(CN)_6]^{3-}$	$[Fe(CN)_6]^{3-}$	$[Co(CN)_6]^{3-}$
$A + H_3L \leftrightarrows H_3LA$	2.8	2.7		
$A + H_4L \leftrightarrows H_4LA$	3.4	3.5	2.9	2.9
$A + H_5L \leftrightarrows H_5LA$	3.8	3.7	3.8	3.5
$A + H_6L \leftrightarrows H_6LA$			4.4	3.9

The corresponding values for $[Co(CN)_6]^{3-}$ calculated by pH-metric techniques are included by means of comparison [53].
[a] Charges omitted.

$K_3[Co(CN)_6]$ and [30]aneN$_{10}$·10HCl (Fig. 8) [48]. The crystal structure consisted of octaprotonated macrocycles and two types of hexacyanocobaltate anions placed outside the macrocyclic hole. One of the hexacyanocobaltate anions is hydrogen bonded through four of its six cyanide groups with consecutive macrocycles forming a sort of chain-like structure. The second type of hexacyanocobaltate anions are interconnecting macrocycles of different chains by means of two long hydrogen bonds. The macrocycle adopts an elongated elliptical shape which is mainly due to repulsions between the positively charged ammonium groups. Interestingly enough, if this structure were kept in solution the metallocyanides along a single chain would provide also a diminution of 2/3 in the quantum yield of the photoexcited aquation reaction, four out of the six cyanide groups would be stabilized by hydrogen bonds.

In order to get further insight into the characteristics of these interactions and into the inclusive nature of the supercomplexes formed, the studies were extended to other kinds of anion complexes [48]. The interaction of hexachloroplatinate(IV) anions $PtCl_6^{2-}$ and the macrocycle [30]aneN$_{10}$ was studied in solution by means of ^{195}Pt NMR spectroscopy. The pH of study was very acidic (HCl 0.1 M) in order to prevent the migration of the polyazamacrocycle from the second to the first coordination sphere of platinum. The presence of the polycharged receptor causes an upfield shift of the ^{195}Pt NMR signal with respect to the signal of solvated $PtCl_6^{2-}$.

The shift in the ^{195}Pt signal reaches a constant value (Fig. 9) for molar ratios $R = [H_{10}([30]aneN_{10})^{10+}]/[PtCl_6^{2-}] > 1$ due to the formation of 1:1 metal complexes. However, another inflection is observed for R = 0.5 suggesting formation of supercomplexes of 2:1 anion:receptor stoichiometry.

The crystal structure of $[H_{10}([30]aneN_{10})][PtCl_6)]_2Cl_6 \cdot 2H_2O$ (Fig. 10) consists of a complex hydrogen bond network which implies the hydrogens of the protonated nitrogen atoms of the receptor, $PtCl_6^{2-}$ anions, chloride anions and water molecules. One of the chloride anions is placed over the macrocyclic hole forming trifurcated hydrogen bonds with three adjacent ammonium groups. The overall shape of the macrocycle is more circular than that previously mentioned for the octaprotonated form. Again it is interesting to empha-

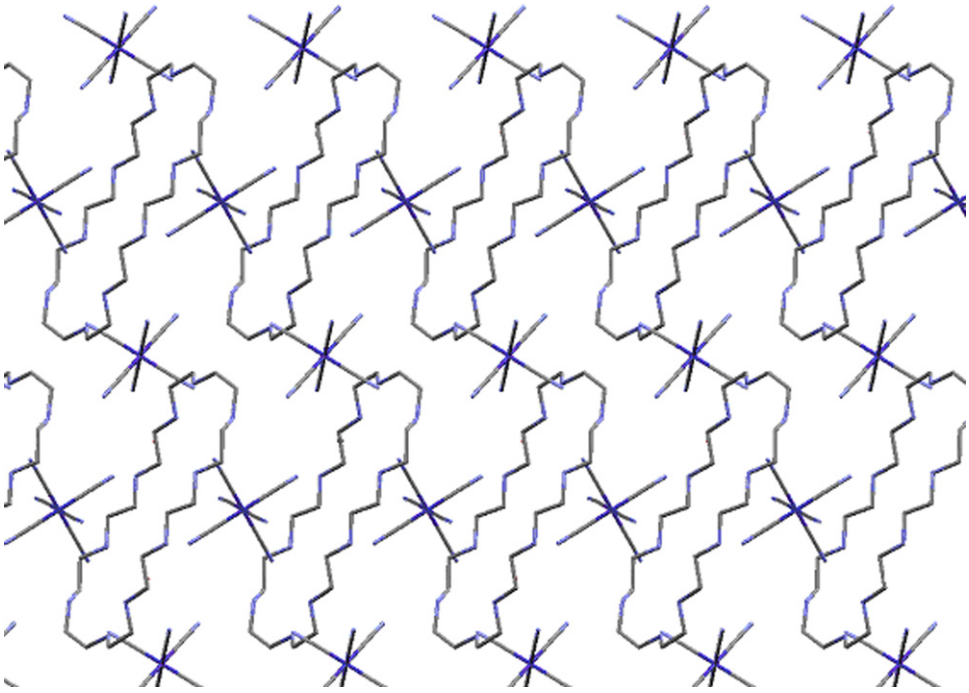

Fig. 8. Portion of the crystal structure of $[H_8([30]aneN_{10})][Co(CN)_6)]_2Cl_2 \cdot 10H_2O$ showing the two types of hexacyanocobaltate(III) anions [48].

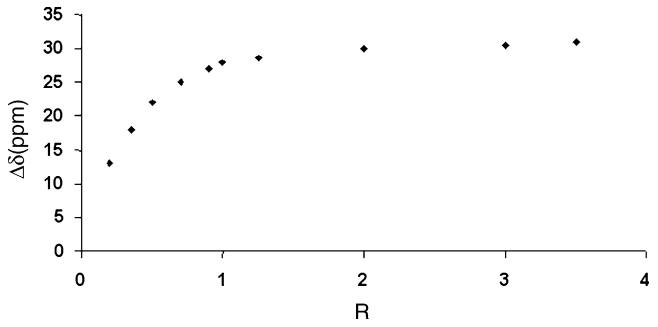

Fig. 9. Plot of the variation in the ^{195}Pt NMR chemicals shifts of $PtCl_6^{2-}$ upon addition of increasing amounts of $[H_{10}([30]aneN_{10})]^{10+}$. R = $[H_{10}([30]aneN_{10})^{10+}]/[PtCl_6]^{2-}$. Reprinted with permission from Ref. [52]. Copyright 1987 American Chemical Society.

size that the complex anions are placed outside the macrocyclic hole.

One can imagine that the octahedral shape and the size of $PtCl_6^{2-}$ could hinder its inclusion into the macrocycle. However, at least in the solid state, inclusion was also not detected for the square planar anion $[Pt(CN)_4]^{2-}$ even if all calculations and models suggested that there was enough free room for this process to occur. The crystal structure of the solid $[H_{10}([30]aneN_{10})][Pt(CN)_4)_5]\cdot 2H_2O$ showed again an array of hydrogen bonds involving the protonated macrocycle and the metallocyanide anions whose cyanide groups point directly towards the macrocyclic cavity (Fig. 11).

Due to the stronger and more inert character of the Pt–CN bond, it was possible to study these systems by means of pH-metric techniques detecting the formation of 1:1 adduct species. A noticeable increase in stability was observed in going from $[30]aneN_{10}$ to the larger $[33]aneN_{11}$ suggesting possible inclusion of the anion within the macrocyclic hole.

As it can be noticed, there is not agreement between the stoichiometries in the solid state and in solution. ^{195}Pt NMR studies

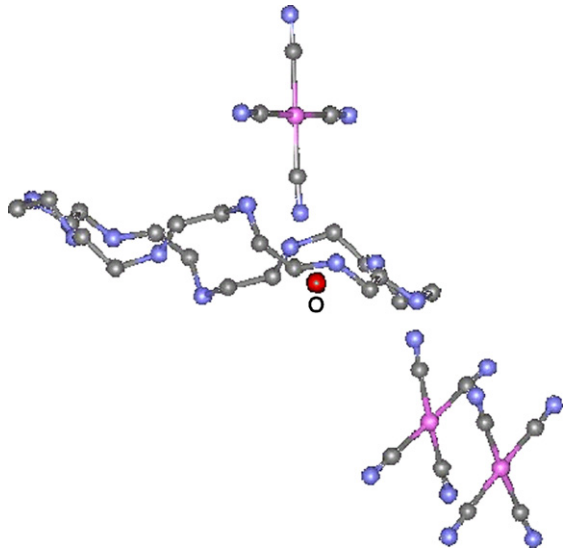

Fig. 11. Detail of the crystal structure of $[H_{10}([30]aneN_{10})][Pt(CN)_4]_5\cdot 2H_2O$ showing the anions involved in hydrogen bonding with the protonated receptor [52].

in D_2O failed to give information about the formation of adduct species of higher nuclearity due to precipitation of the polyammonium salts.

A closer relationship between the events coming up in solution and in the solid state occurs, however, in the system $PdCl_4^{2-}$–$H_{10}([30]aneN_{10})^{10+}$. The solution studies for the different $H_k([3k]aneN_k)^{k+}$ systems were carried out by batch microcalorimetry in 0.1 M HCl aqueous medium (Table 2). The measurements had equilibration times within the time-scale of the experiment for $H_6([18]aneN_6)^{6+}$, $H_7([21]aneN_7)^{7+}$ and $H_8([24]aneN_8)^{8+}$ becoming, however, much slower for the next two terms of the series $H_{10}([30]aneN_{10})^{10+}$ and $H_{11}([33]aneN_{11})^{11+}$. Although all the reactions show slightly

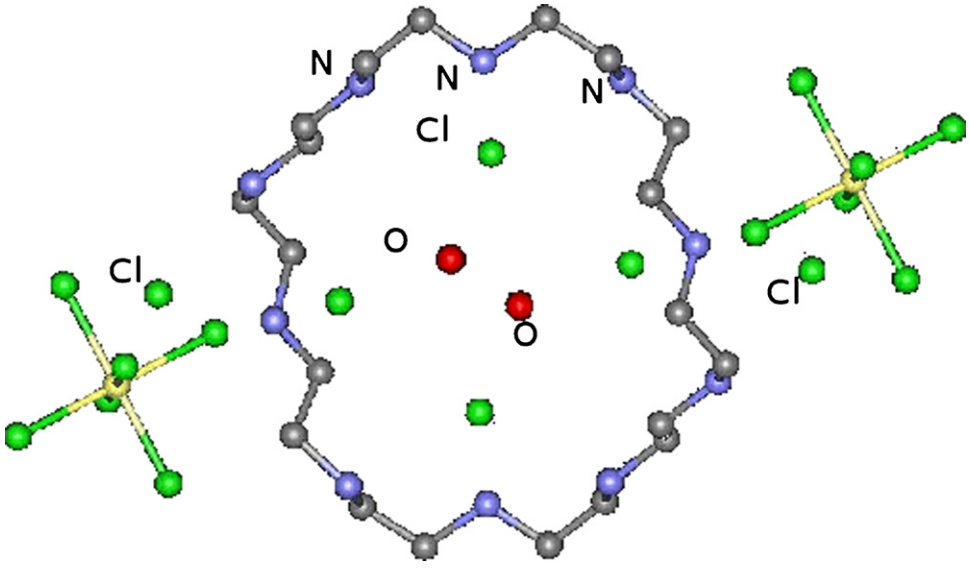

Fig. 10. Detail of the crystal structure of $[H_{10}([30]aneN_{10})[PtCl_6]_2Cl_6\cdot 2H_2O$ showing the outer location of the $PtCl_6^{2-}$ anions. Red dots are water molecules and green are chloride anions [52]. (For interpretation of the references to color in this figure legend, the reader is referred to the web version of the article.)

Table 2
Enthalpy terms and equilibration times for the reactions of fully protonated $[3k]aneN_k$ macrocycles and $PdCl_4^{2-}$ determined in 0.1 M HCl in a BATCH microcalorimeter [50,51]

Reaction	$-\Delta H^\circ$ (kcal mol^{-1})	Time (min)
$H_6([18]aneN_6)^{6+} + PdCl_4^{2-}$	1.5(1)	20
$H_7([21]aneN_7)^{7+} + PdCl_4^{2-}$	1.5(1)	20
$H_8([24]aneN_8)^{8+} + PdCl_4^{2-}$	1.6(1)	20
$H_9([27]aneN_9)^{9+} + PdCl_4^{2-}$	2.9(1)	120
$H_{10}([30]aneN_{10})^{10+} + PdCl_4^{2-}$	3.9(1)	110
$H_{11}([33]aneN_{11})^{11+} + PdCl_4^{2-}$	3.1(1)	50

exothermic enthalpy terms, the values for $(H_{10}[30]aneN_{10})^{10+}$ and $H_{11}([33]aneN_{11})^{11+}$ doubled the other ones. These experimental evidences suggest that $H_{10}([30]aneN_{10})^{10+}$ was the first term of the series for which inclusion of the $PdCl_4^{2-}$ within the macrocyclic cavity occurred. The slower equilibration time should account for conformational reorganizations following host–guest interaction.

The crystal structure of $[(PdCl_4)(H_{10}[30]aneN_{10})](PdCl_4)_2Cl_4$ (Fig. 12) shows that one of the $PdCl_4^{2-}$ is included into the ellipsoidal cavity of the decaprotonated macrocycle along the shorter axes [50,51]. The chlorine atoms stand out of the macrocyclic framework forming hydrogen bonds with the closest nitrogens of the macrocycle. The outer $PdCl_4^{2-}$ anions participate also in hydrogen bonding with the several ammonium groups of the receptors. Although, as previously mentioned, the shape of the macrocycle is greatly defined by coulombic repulsions between protonated nitrogens, attractive charge–charge interactions with the anions and hydrogen bonding do play also their role in determining the conformation of the protonated receptor. As a matter of fact, the conformations found in all the discussed structures are somewhat different. Thus, it can be stated that the coarse fitting of the macrocyclic conformation is performed by

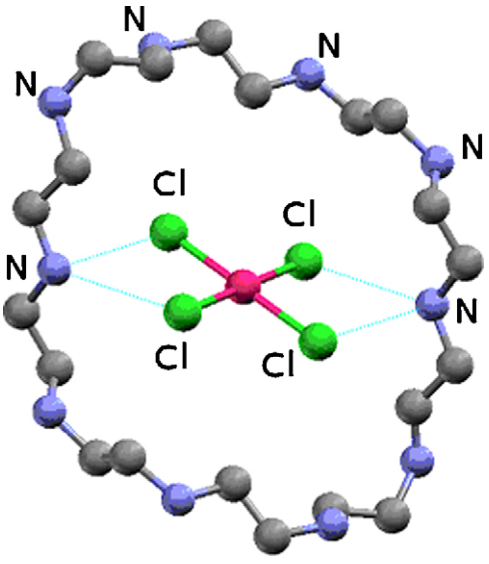

Fig. 12. Drawing of the cation $[(PdCl_4)(H_{10}[30]aneN_{10})]^{8+}$. Hydrogen bonding is indicated with blue-dotted lines. Hydrogens not shown [50,51]. (For interpretation of the references to color in this figure legend, the reader is referred to the web version of the article.)

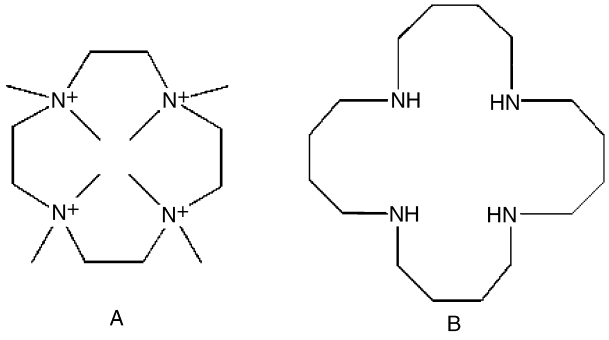

$Me_8[12]aneN_4^{4+}$ $H_4[120]aneN_4^{4+}$

Chart 4.

the charge while hydrogen bonding should be playing a sort of fine tuning.

Although electrostatic attraction is the main driving force for adduct formation, sometimes the supplemental contribution of hydrogen bonding seems to play a key role in the effective formation of the adducts. A very illustrative case was reported by Bianchi et al. for macrocycles $Me_8[12]aneN_4^{4+}$ and $H_4([20]aneN_4)^{4+}$ (see Chart 4) [64,65]. Nitrogen quaternization in $Me_8[12]aneN_4^{4+}$ prevents hydrogen bonding and no appreciable interaction with anions such as ATP^{4-} or $[Co(CN)_6]^{3-}$ was detected for this macrocycle. On the other hand, $H_4([20]aneN_4)^{4+}$ displaying a lower charge density but with possibility of forming hydrogen bonds interacts in water with $[Co(CN)_6]^{3-}$, $[Fe(CN)_6]^{4-}$ or ATP^{4-} with $\log K$s values for the reaction $[H_4([20]aneN_4)]^{4+} + A^{n-} \leftrightarrows [H_4([20]aneN_4)A]^{(4-n)}$ of 2.38, 3.62 and 3.81, respectively.

3. Carboxylate anions

Interaction of carboxylate anions with polyammonium receptors was reported in the very beginning of anion coordination chemistry due to the fundamental biological roles of these anions [14,16,20,66–68]. Since then, the selective targeting of dicarboxylate and polycarboxylate anions has constituted a preferential goal in host–guest chemistry and even nowadays still persists [69–75].

Our first approach to this topic was to consider the interaction of the macrocycle $[21]aneN_7$ (see Chart 2) in its protonated forms with two benzenetricarboxylic acid isomers, with Kemp's acid *cis*,*cis*-1,3,5-trimethyl-1,3,5-cyclohexanetricarboxylic acid (*c*,*c*-TMCT) and with its isomer *cis*,*trans*-1,3,5-trimethyl-1,3,5-cyclohexanetricarboxylic (*c*,*t*-TMCT) (Chart 5) [76,77]. Carboxylates derived from benzenetricarboxylic acids can be considered as ideal models for rigid anionic substrates having well-defined shapes in terms of charge density and hydrogen bonding.

Kemp's triacids also display relatively rigid structures due to its very simple conformational equilibrium which brings the carboxylate groups from equatorial to axial position when first protonation occurs. For comparison the less-rigid citric tricarboxylic acid and 1,2-benzenedicarboxylic (1,2-BDC) and 1,3-benzenedicarboxylic acids (1,3-BDC) were also studied (Chart 5).

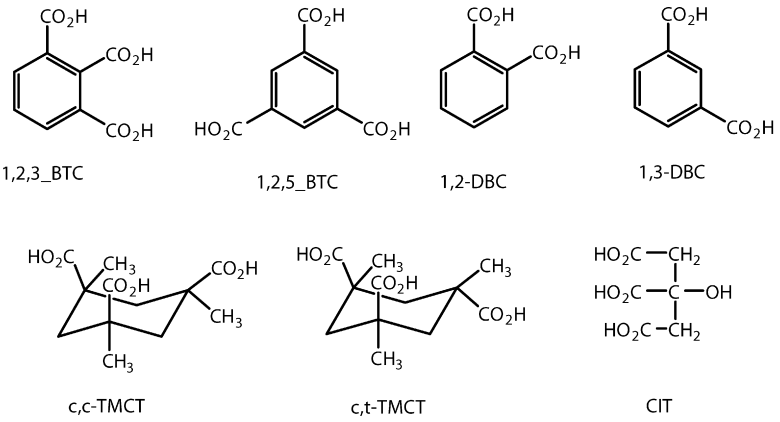

Chart 5.

Table 3
Protonation constants for the tricarboxylic acids 1,2,3-BTC, 1,3,5-BTC, *c*,*c*-TMCTC, *c*,*t*-TMCTC and CIT (0.15 M $NaClO_4$, 298.1 K) [76,77]

Reaction[a]	1,2,3-BTC	1,3,5-BTC	*c*,*c*-TMCT	*c*,*t*-TMCT	Cit
$A + H \leftrightarrows HA$	5.401(2)	4.382(2)	7.289(5)	6.921(5)	5.401(2)
$H + HA \leftrightarrows H_2A$	3.90(1)	3.66(1)	6.20(1)	4.72(1)	3.90(1)
$H + H_2A \leftrightarrows H_3A$	2.65(2)	2.97(2)	3.59(3)	3.82(3)	2.65(3)

Charges omitted for clarity.

This kind of anions introduces an additional problem in the analysis of the stability constants of the systems since they are protic species that will bear proton transfer reaction in the usual pH range of study. Table 3 collects the protonation constants for the tricarboxylic guests. Therefore, a proper comparison of the equilibrium data for these systems has to take into account the actual protonation degrees of host and guest species.

However, as citrate and 1,2,3-benzenetricarboxylate (1,2,3-BTC) have practically the same protonation constants, in this case the interaction constants can be directly compared and show a clear preference of the aromatic tricarboxylate over citrate in all the pH range of complexation. The constants for 1,2,3-BTC are three orders of magnitude greater than those of citrate. The distribution diagrams in Fig. 13 clearly reflect this situation; while for 1,2,3-BTC the adduct species predominate over all the pH range, for citrate the prevailing species are the free carboxylate trianion and its protonated forms.

Owing to their different protonation constants the comparisons for the other acids are not so straightforward. Therefore, it seemed opportune to establish a criterion taking into account this fact that provided a clear picture of selectivity patterns [77,78]. An appropriate way was to calculate the distribution diagram for the mixed systems Anion A–Anion B–[21]aneN7 and represent their overall percentage of formation. This method permits to establish selectivity ratios at any pH and does not require any assumption on the location of protons in the interacting species, which is required to transform cumulative association constants into stepwise ones and is a common source of erroneous interpretation of selectivity. Fig. 14 shows such a diagram for the mixed system [21]aneN7-*c*,*c*-TMTCC-*c*,*t*-TMCT.

This plot indicates that in a 1:1:1 mixture of the two isomers and of the receptor, the *cis*,*cis*-isomer will be selected at a larger extent by the receptor.

A further way to describe these systems is to consider the analytical apparent constants which are calculated, for every pH value, as the quotient between the summation of the complexed species and the summation of the free reagents

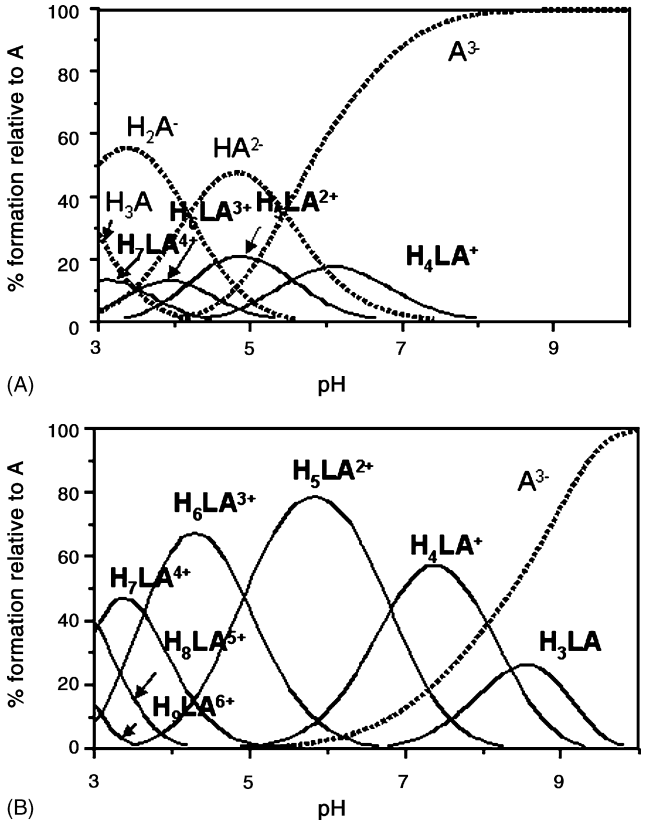

Fig. 13. Distributions diagram for the systems: (A) [21]aneN7 (L)-citrate (A) and (B) [21]aneN7 (L)-1,2,3-BTC (A) [77].

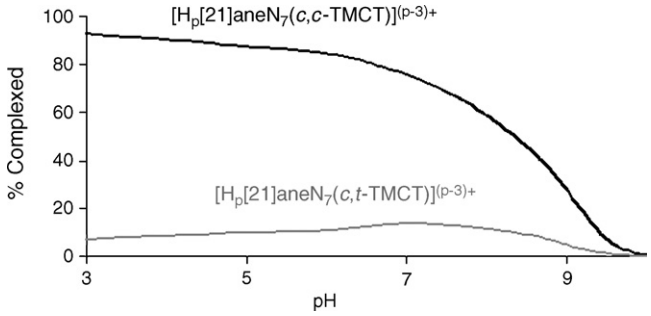

Fig. 14. Calculated overall percentages of complexation in the mixed system [21]aneN$_7$-*c*,*c*-TMCT-*c*,*t*-TMCT. Concentrations of all reagents 10^{-3} M [77].

(Fig. 15) [79].

$$K_{\text{cond}} = \frac{\sum[\text{H}_{j+i}\text{LA}]}{\sum[\text{H}_j\text{L}] \times \sum[\text{H}_i\text{A}]}$$

This way of treating the data provides, for all the pH range of study, equilibrium constants comparable to those obtained by other techniques at fixed pH values. On the other hand thermodynamic selectivity can be calculated at any pH value by just dividing the apparent constants. The selectivity of protonated [21]aneN$_7$ for *c*,*c*-TMCT over *c*,*t*-TMCT would be 15 at pH 7.4, 46 at pH 6.0 and 100 at pH 4.0. The polyammonium host compound behaves as a rather flat charge surface that will match all three carboxylate groups of the *cis*,*cis*-isomer while it would match only two groups in the *cis*,*trans*-isomer as shown in the models (Fig. 16). Since neither the carboxylic/carboxylate substrates nor the polyammonium guest have a suitable electrochemical behavior, competition experiments between the carboxylate anions and hexacyanoferrate(II) were set up in order to check the interactions by an alternative way. These experimental evidences help to confirm the magnitude of the stability constants as well as the stoichiometries and monomer nature of the host–guest adducts formed [77].

The same reasoning explains why 1,2-BDC interacts stronger with [21]aneN$_7$ than the triacid *c*,*t*-TMCT by (Fig. 17).

Other recent examples of shape-selectivity in the selective recognition of tricarboxylic acid isomers are provided by the macrocycle *R*,*R*-Tris-pB2CH (see Chart 6) which contains three trans(1*R*,2*R*)-diaminocyclohexane units connected by *p*-xylene spacers [80] and the two tripodal ligands Tris-cyclen and Tris-

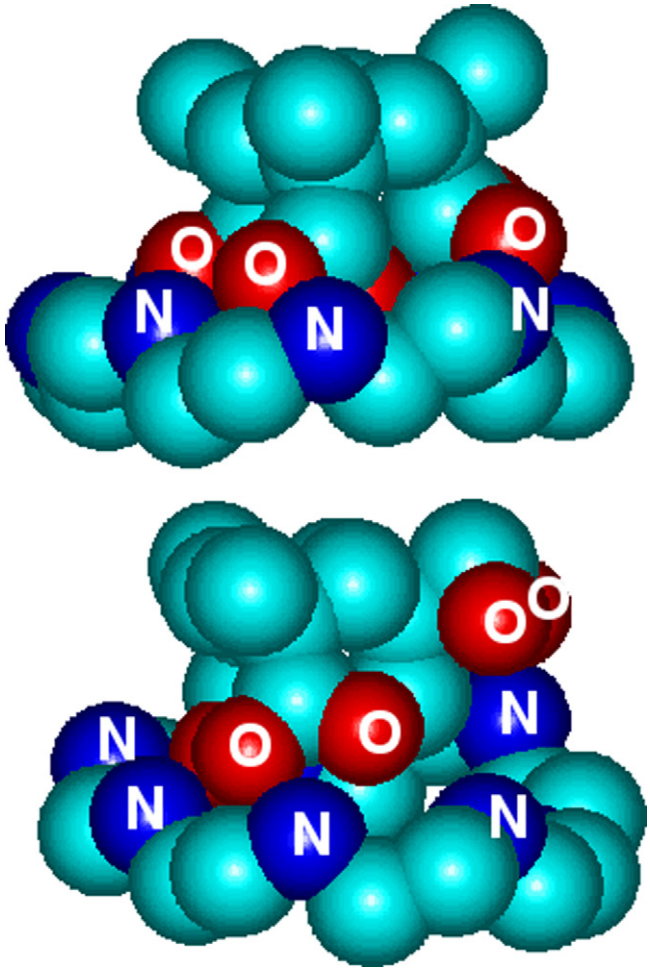

Fig. 16. CPK models showing the matching between protonated [21]aneN$_7$ and *c*,*c*-TMCT (top) and *c*,*t*-TMCT (bottom) [76,77].

isocyclam containing, respectively, three cyclen and three isocyclam hanging moieties [81].

Potentiometric and NMR analysis on the interaction of *R*,*R*-Tris-pB2CH with the 1,3,5-BTC, 1,2,4-BTC and 1,2,3-BTC acids and their relevant anions show that the interaction is highest for the isomer 1,3,5-BTC which perfectly fits within the macrocyclic cavity of the host species (Fig. 18). The studies have been extended to the triacid 1,3,5-benzenetriacetic (1,3,5-BTA) observing in this case the effect of a size mismatch between host and guest species (Fig. 18).

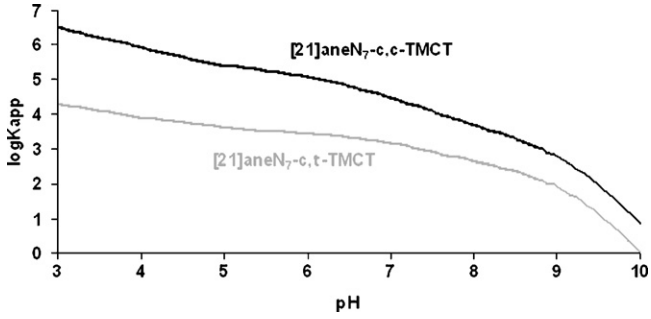

Fig. 15. Logarithms of the apparent stability constants for the systems [21]aneN$_7$-*c*,*c*-TMCT and systems [21]aneN$_7$-*c*,*t*-TMCT.

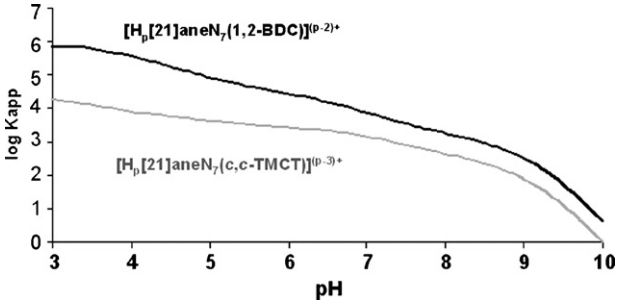

Fig. 17. Plot of the logarithm of apparent stability constants vs. pH for the systems [21]aneN$_7$-1,2-BDE and [21]aneN$_7$-*c*,*c*-TMCT.

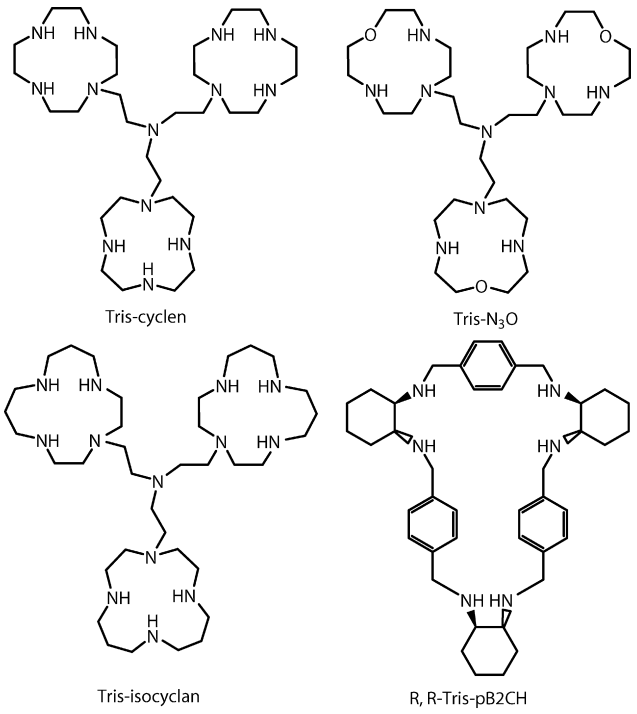

Chart 6.

Recognition of 1,3,5-BTC over 1,2,4-BTC and 1,2,3-BTC was also achieved by means of the two tripodal ligands Tris-cyclen and Tris-isocyclam [81]. The binding properties of these ligands were studied by means of potentiometric, NMR and microcalorimetric measurements showing that both ligands form stable 1:1 complexes with all three substrates, the complex stability depending on the protonation state of receptors and substrates. As shown by molecular dynamic calculations all three anions are encapsulated into the bowl-shaped receptor cavity giving rise to charge–charge and hydrogen bond attractive interactions. 1,3,5-BTC, which displays the same ternary symmetry of Tris-cyclen and Tris-isocyclam, shows the best complementarity with these receptors with which it forms a close network of six salt bridges reinforced by hydrogen bonds involving the six carboxylate oxygens. The lowest energy conformer of $[H_7$Tris-cyclen(1,3,5-BTC)$]^{4+}$ is reported in Fig. 19. Such complementary matching between substrate and receptor is at the origin of the marked recognition of 1,3,5-BTC over 1,2,4-BTC and 1,2,3-BTC.

The calorimetric study pointed out that the complexes with these tricarboxylate substrates are in general stabilized by favorable entropic contributions when the substrates are completely deprotonated and by favorable enthalpic contributions for protonated substrates.

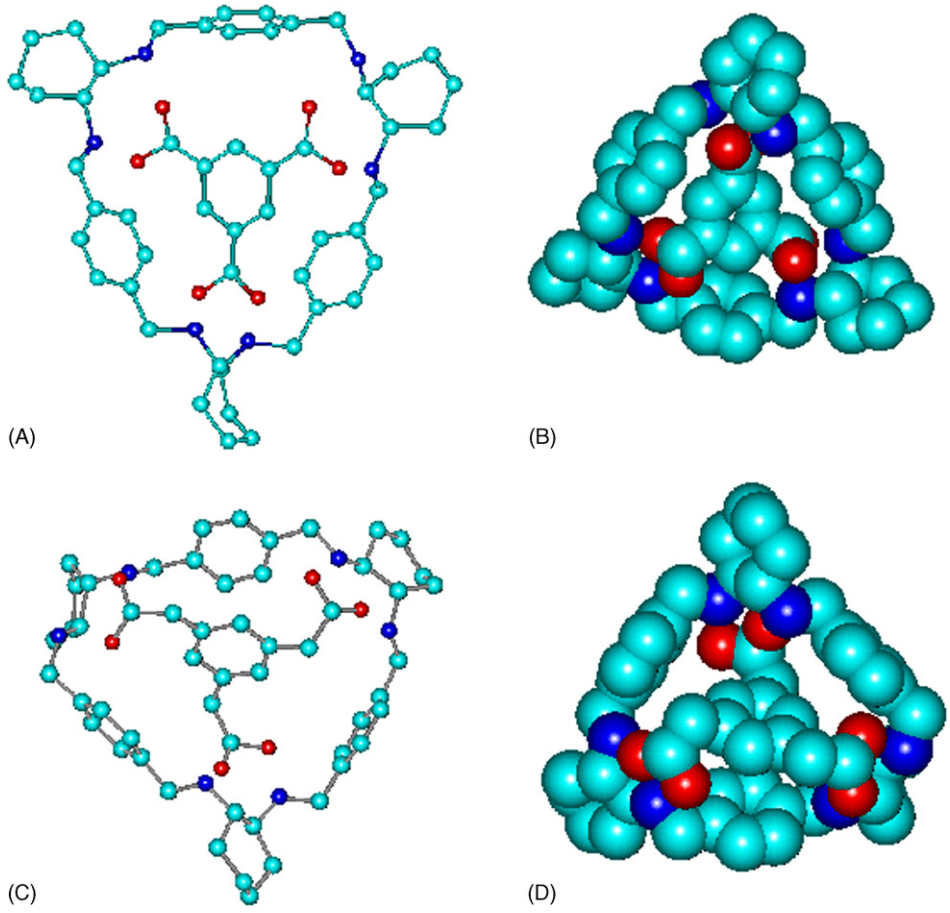

Fig. 18. Ball and stick and CPK molecular models for the system H_3L^{3+} and the tricarboxylate anions derived from 1,3,5-BTC (A and B) and from 1,3,5-BTA (C and D). Reprinted with permission from Ref. [80]. Copyright 2005 American Chemical Society.

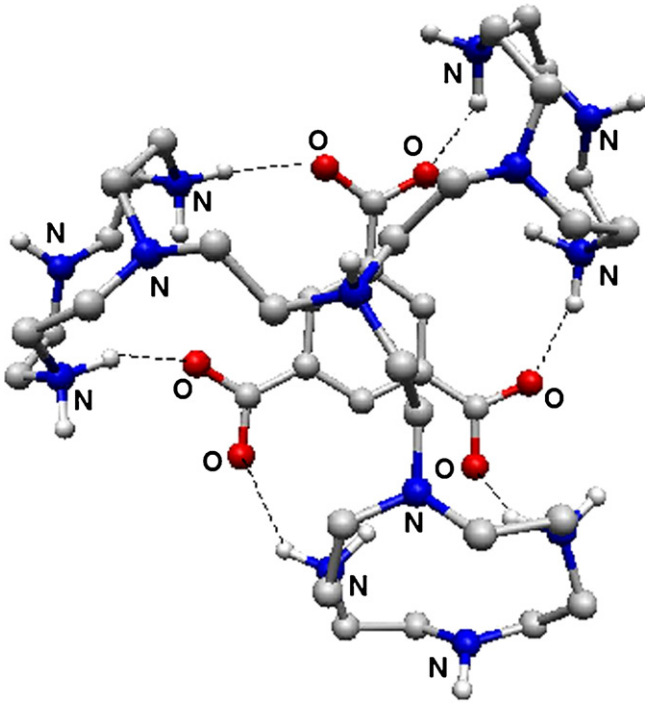

Fig. 19. Lowest energy conformer of the $[H_7Tris\text{-}cyclen(1,3,5\text{-}BTC)]^{4+}$ complex. Dashed lines represent hydrogen bonds. Reprinted with permission from Ref. [81]. Copyright 2005 American Chemical Society.

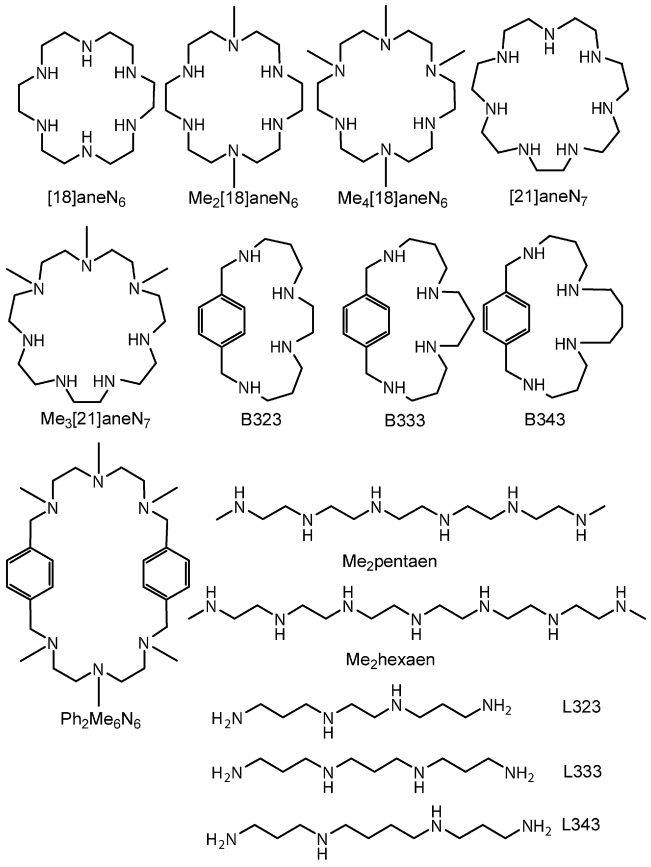

Chart 7.

4. Sulfate, phosphate, pyrophosphate and triphosphate

Among anionic substrates, phosphate anions are of special interest due to their widespread participation in biological systems. Phosphate recognition by proteins has been recently illustrated by a crystal structure of the phosphate binding protein (PBP), which is a periplasmatic protein that transports orthophosphate in bacteria once the anion has crossed the outer membrane cell. In this protein, HPO_4^{2-} is buried in a fully dehydrated form in a crevice 8 Å below the protein surface forming 12 hydrogen bonds contacts with the protein [82,83]. Eleven of these hydrogen bonds involve oxygen atoms of the anion and hydrogen bond donor groups of the protein while in only one the anion OH^- group behaves as a hydrogen bond donor.

In its turn the sulfate binding protein (SBP), which has a similar anion transport role in bacteria, binds sulfate through a seven hydrogen bond network between the oxygen atoms of sulfate and NH groups of the protein backbone, being a tryptophane and a serine residue participating also in the binding [83–85]. The lack of hydrogen bond acceptors in the binding site explains the poor affinity of this protein for phosphate and the sulfate–phosphate discrimination.

Different examples of phosphate and sulfate complexation by synthetic polyammonium receptors in water have been reported in the literature [14,66,68,86–105]. Here we are going to discuss examples of phosphates and sulfate interaction with polyammonium receptors in water for which, in addition to binding constants, also the enthalpy and entropy terms are available [103–105]. In particular, only reliable enthalpy terms measured by means of microcalorimetric titrations will be considered. This kind of data is very important to interpret which is the major contribution affecting the stability of anion complexes in water and which is the role, if any, played by hydrogen bonds.

A complete thermodynamic characterization of the anion complexes formed by phosphate and pyrophosphate with the polyammonium cations deriving from the macrocyclic and acyclic polyamine ligands shown in Chart 7 was performed by means of potentiometric and microcalorimetric measurements, which furnished equilibrium data for complexes in many different protonation states [103].

In spite of their different sizes, molecular architectures and number of binding groups, these ligands form only complexes of 1:1 anion/receptor stoichiometry in solution with both anions.

^1H and ^{13}C NMR spectra performed with solutions of these ligands at various pH values show that the formation of phosphate and pyrophosphate complexes does not alter the protonation patterns and the topology of the charged groups in the ligands and does not modify significantly the overall conformation of the protonated receptors, with the exception of $Ph_2Me_6N_6$ which experience some conformational changes. Only a modest general displacement of NMR signals corresponding to the increase of ligand basicity, brought about by anion complexation, is generally observed. These observations are strongly indicative of the fact that in the formation of such anion complexes the interacting partners maintain their identity and no significant redistribution of protons occurs, that is, under our

experimental conditions, hydrogen bonded ion pairs are favorably formed.

In contrast with the general trend of increasing stability with increasing charge of receptors and anions previously observed for the complexes of these ligands with other inorganic anions like $[Fe(CN)_6]^{4-}$, $[Co(CN)_6]^{3-}$ and $[Pt(CN)_4]^{2-}$ [49,52,53], the stability trends of phosphate and pyrophosphate complexes are not strictly determined by electrostatic contributions. For instance, the stability of the complexes formed by HPO_4^{2-} with the mono-, di- and tri-protonated forms of B343 decreases with increasing charge on the ligand, while the stability of the complexes formed by $H_4(Ph_2Me_6N_6)^{4+}$ with $HP_2O_7^{3-}$, $H_2P_2O_7^{2-}$ and $H_3P_2O_7^{-}$ increases with decreasing charge on the anion. Such unprecedented behavior was ascribed, as later discussed on, to the particular ability of phosphate species in behaving as acceptors and donors of hydrogen bonds.

Considering the stability of the complexes formed by phosphate and pyrophosphate, in a given protonation degree with the same receptor, it can be observed that also in this case no strict trends are found and, in contrast to electrostatic expectations, the less charged anion can form more stable complexes. However, in a general sense, pyrophosphate displays a greater propensity to form complexes, in particular with greater ligands in high protonation degrees and especially with open-chain ligands.

Many of these complexation reactions are almost athermic or endothermic and promoted by favorable entropic contributions ($T\Delta S^\circ > 0$), in agreement with the ideal electrostatic model, although there is also a considerable number of reactions promoted by large favorable enthalpy changes ($\Delta H^\circ < 0$) and accompanied by evident entropy loss. Phosphate, pyrophosphate anions and polyammonium receptors can be involved in the formation of many hydrogen bonds in which both the anions and the receptors can act as acceptors or donors. Hydrogen bonding is largely determined by electrostatic attraction, although significant contribution is also furnished by charge-transfer, dispersive and covalent forces. In particular, when hydrogen bonds take place between chemical species characterized by marked acid/base properties like the present ones, contributions from proton transfer (charge-transfer) from the donor to the acceptor groups may be of considerable importance. There are five possible modes (1)–(5) of hydrogen bonding involving amine or ammonium groups and phosphate, or protonated phosphate anions.

$$\text{–N–H}^{+}\cdots\text{O–} \qquad \Delta H^\circ > 0, T\Delta S^\circ > 0 \tag{1}$$

$$\text{–N–H}^{+}\cdots\text{OH–} \qquad \Delta H^\circ > 0, T\Delta S^\circ \approx 0 \tag{2}$$

$$\text{–N–H}\cdots\text{O–} \qquad \Delta H^\circ > 0, T\Delta S^\circ \approx 0 \tag{3}$$

$$\text{–N–H}\cdots\text{OH–} \qquad \Delta H^\circ > 0, T\Delta S^\circ < 0 \tag{4}$$

$$\text{–N|}\cdots\text{H–O–} \qquad \Delta H^\circ < 0, T\Delta S^\circ < 0 \tag{5}$$

Taking into account that deprotonation of an amine group is a strongly endothermic reaction while protonation of phosphate anions is almost athermic, the partial amine-to-anion proton transfer processes involved in the four hydrogen bonding modes (1)–(4) are expected to give unfavorable enthalpic contributions ($\Delta H^\circ > 0$), while the partial proton transfer process of the bonding mode (5), occurring from the anion to the amine group, is the unique one furnishing favorable enthalpy changes ($\Delta H^\circ < 0$).

Nevertheless, the type of hydrogen bond occurring between anion and receptor is strictly connected with the extent of proton transfer from the donor to the acceptor, which depends on the N–O separation. For instance, the difference between hydrogen bond in the ion pair (1) and in the neutral complex (2) vanishes for short separations. In the case of phosphate and pyrophosphate complexes with polyammonium ligands the strong electrostatic attraction brings the anion and the receptor in contact with each other. Under these conditions both types of hydrogen bonds can be formed depending on the complex structure and the protonation degree of the reacting species, as observed in crystal structures of $H_2P_2O_7^{2-}$ complexes with polyammonium receptors [94,103].

By adopting a similar reasoning, the unusual stability trends observed for the formation of phosphate and pyrophosphate complexes can be explained by assuming the formation of different hydrogen bonds whose contribution is decisive even in a competitive solvent like water which is a good donor and acceptor of hydrogen bonds. Actually, the stability decrease previously highlighted for the complexes formed by HPO_4^{2-} with the mono-, di- and tri-protonated forms of B343 can be interpreted in term of increasing hydrogen bond donor properties (type (1) bonds) of the receptors, leading to unfavorable enthalpic contributions, while the stability increase of the complexes formed by pyrophosphate and $H_4(Ph_2Me_6N_6)^{4+}$, as the charge on the anion decreases from $HP_2O_7^{3-}$ to $H_3P_2O_7^{-}$, can be attributed to the greater donor ability of more protonated anions (type (5) bonds) determining more favorable enthalpic and less favorable entropic contributions.

In a successive work the binding constants, as well as the enthalpy and entropy terms, for the formation of sulfate complexes with protonated forms of [18]aneN$_6$, Me$_2$[18]aneN$_6$, Me$_4$[18]aneN$_6$, [21]aneN$_7$, Me$_3$[21]aneN$_7$, Ph$_2$Me$_6$N$_6$, Me$_2$pentaen, Me$_2$hexaexen (see Chart 7) and other polyamines reported in Chart 8 were determined by means of the same potentiometric and microcalorimetric methods [104].

Also in the case of sulfate only complexes with 1:1 anion/receptor stoichiometry are formed in solution but, in contrast to phosphate complexes, the equilibrium constants for the binding of SO_4^{2-} increase with increasing positive charge on the protonated receptors indicating that electrostatic attraction is the principal force determining the stability of these anion complexes, although also hydrogen bonding is expected to give a favorable contribution. In this case, however, no protonated forms of SO_4^{2-} exist in the studied pH range and, then, SO_4^{2-} can only act as hydrogen bond acceptor preventing the formation of type (5) hydrogen bonds in the complexes, which give rise to the peculiar stability trends found for phosphate complexes.

Both nitrogen methylation and the presence of aromatic groups in the ligand increase the stability of the sulfate complexes with respect to aliphatic not methylated ligands, by reducing the overall solvation of the receptors; less solvated receptors give rise to less energetically expensive desolvation processes, upon complexation, contributing to enhance the complex sta-

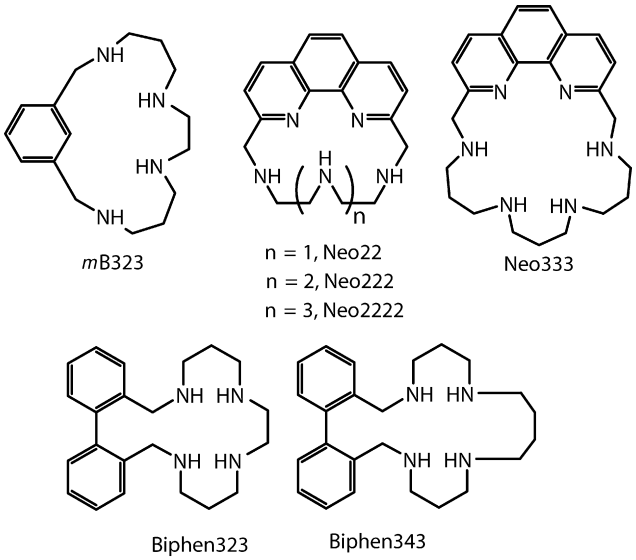

Chart 8.

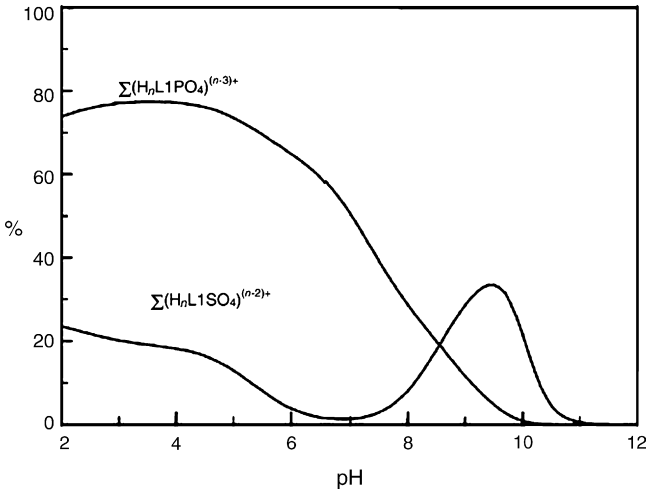

Fig. 20. Calculated overall percentages of complexation in the mixed system PO_4^{3-}/SO_4^{2-}/[21]aneN$_7$. Concentrations of all reagents 10^{-3} M [104]. Reproduced by permission of The Royal Society of Chemistry.

bility. Only the two ligands containing the large phenanthroline groups (Chart 8) form weaker complexes, most likely as a result of repulsive interactions between the negative charge of the anion and the extended electronic π cloud of the aromatic moieties.

For methylated polyamines a considerable contribution to the enhancement of complex stability has to be ascribed to the marked localization of positive charges produced in the ligands by the higher basicity of secondary amine groups in water with respect to tertiary (methylated) ones leading to stronger interactions with the anion. As a matter of fact, for a given charge of the receptor, the complex stability is higher for [18]aneN$_6$ than for the larger [21]aneN$_7$, in agreement with the electrostatic nature of the interaction, but when methylated ligands are considered, different trends can be found. For instance, the equilibrium constants for SO_4^{2-} binding with Me$_2$[18]aneN$_6$, Me$_4$[18]aneN$_6$ and Me$_3$[21]aneN$_7$ are equal, within the experimental errors, for all diprotonated forms, and the same applies for the triprotonated ones. On the other hand, the tetraprotonated forms of Me$_2$[18]aneN$_6$ and Me$_4$[18]aneN$_6$ interact with SO_4^{2-} more strongly that the tetraprotonated form of Me$_3$[21]aneN$_7$, while an opposite trend is observed when considering the pentaprotonated species formed by Me$_4$[18]aneN$_6$ and Me$_3$[21]aneN$_7$.

As shown by the microcalorimetric study, the reactions of SO_4^{2-} binding are endothermic, or almost athermic, and promoted by invariably favorable entropic contributions ($T\Delta S^\circ > 0$), in agreement with the ideal electrostatic model, and in contrast to the previous results for phosphate binding. Since SO_4^{2-} does not form protonated species under the investigation conditions, only hydrogen bonds of types (1) and (3) may occur in the formation of the sulfate complexes justifying the endothermic, or almost athermic character of the binding reactions. Furthermore, protonation of sulfate anion is endothermic and consequently the partial proton transfer processes occurring with the formation of types (1) and (3) hydrogen bonds act in the same direction enhancing the endothermic character of the binding reactions.

Hence, the stability of these sulfate complexes in solution is mostly determined by largely predominant entropic terms produced by the desolvation of the interacting species occurring upon charge neutralization accompanying the pairing processes.

A comparative analysis of the binding ability of these ligands towards sulfate and phosphate, performed by means of calculated selectivity diagrams, furnishes an interesting example of selectivity pattern for [18]aneN$_6$. As shown in Fig. 20, in alkaline solution (pH > 8.5) sulfate is selectively recognized over phosphate, but a selectivity inversion occurs on lowering the solution pH, when the phosphate complexes become largely predominant. Hence, selective recognition of phosphate over sulfate takes place along with increasing phosphate protonation mimicking the function accomplished in living systems by phosphate binding proteins.

The desolvation process occurring upon complexation can be the driving force for anion binding with polyammonium receptors even in the case of phosphate type anions in water. The ligand Bisby, for example (see Chart 9) is folded by the propylenic bridge forming a deep cleft where many water solvent molecules can be hosted, in particular when it is protonated [105].

The cavity of this receptor is also a suitable lodging for large anions, such as phosphate, pyrophosphate and triphosphate (Fig. 21). Inclusion of similar anions into the molecu-

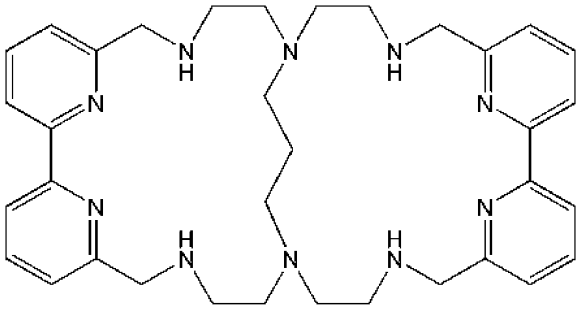

bisby

Chart 9.

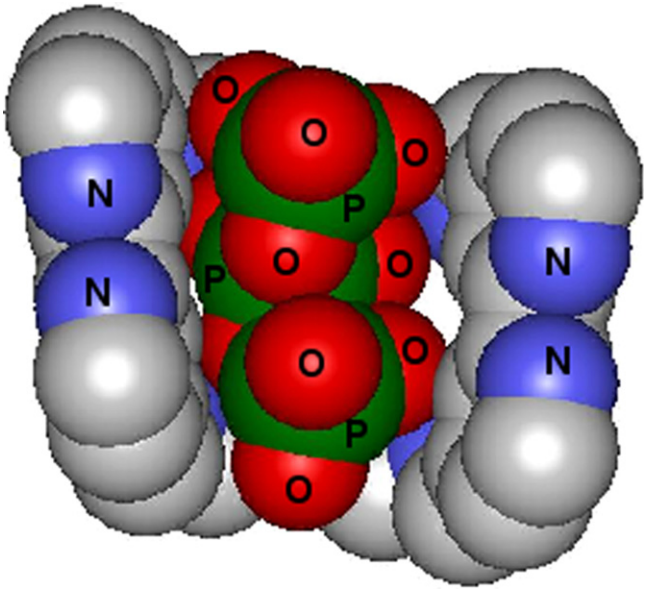

Fig. 21. Proposed model for the interaction of protonated forms of Bisby with triphosphate [105].

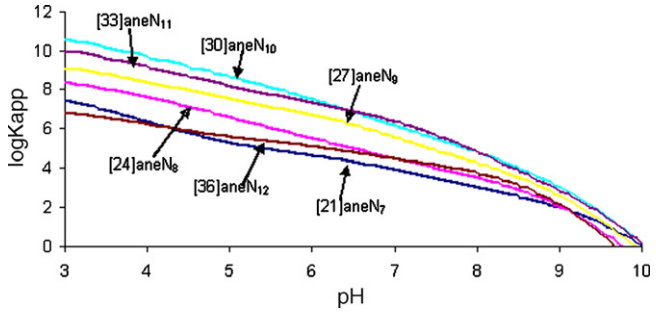

Fig. 22. Plot of the logarithms of the apparent stability constant vs. pH for the system [3*k*]aneN$_k$-ATP (*k* = 7–11) [91].

lar pocket of the protonated receptor causes the exclusion of many water molecules from the cavity which is expected to be accompanied by a favorable entropic effect. Actually, the thermodynamic parameters determined for the complexation of phosphate, pyrophosphate and triphosphate with Bisby in water are invariably promoted by largely favorable entropic contributions while the enthalpic ones are invariably unfavorable even if enthalpically favorable type (5) hydrogen bonds can be formed. In general, the stability of these complexes increases with increasing receptor charge, in agreement with the ideal electrostatic model of ions pairing, but for a given charge of the receptor, anion protonation can produce a stability enhancement, indicating that the formation of type (5) hydrogen bonds are actually acting at some extent.

In conclusion, as shown by the different behaviors illustrated here for the binding of sulfate and phosphates anions with polyammonium receptors in aqueous solution, the formation of hydrogen bonds between anion and receptor can be of considerable importance in such competitive solvent, in particular when protonated forms of the anion are involved. The binding properties of the receptors are determined by the number and localization of the positive charges as well as by the ligand conformation and the presence of hydrophobic aromatic groups.

5. Mononucleotide anions

Polyammonium macrocycles have proved to be interesting synthetic mimics of a variety of phosphoryl transfer enzymes. One of the first ligands to be examined under this point of view was the 24-membered dioxahexazamacrocycle 1,13-dioxa-4,7,10,16,19,23-hexaazacyclotetracosane ([24]aneN$_6$O$_2$) also known as O-bisdien which was found to exhibit both ATPase and kinase activity [106–115].

Following this line of research, the ATP binding and activation capabilities of the series of large [3*k*]aneN$_k$ macrocycles was examined (see Chart 2) [91]. In order to have a more complete picture of the situation, we also analyzed the interaction of these receptors with AMP and ADP and with the anions phosphate and pyrophosphate. The formation constants for all the detected adduct species were calculated by means of potentiometric techniques at constant ionic strength of 0.15 M $NaClO_4$. Re-examination of those constants under the criterion discussed in the latter section indicates that [21]aneN$_7$ is one of the receptors interacting weakest with ATP at any protonation degree while the maximum interaction would occur for the system ATP-[30]aneN$_{10}$ (Fig. 22).

Notwithstanding this fact, HPLC and ^{31}P NMR measurements recorded at pH's 3.0 and 7.0 proved that [21]aneN$_7$ was the macrocycle producing the largest rate enhancement of the hydrolytic cleavage of ATP into ADP and the so-called inorganic phosphate. It is interesting to remark that the interaction of anyone of these receptors with ATP is much higher than with ADP, AMP or phosphate. Therefore, ATP hydrolysis induced by [3*k*]aneN$_k$ polyazacycloalkanes is free, for the major part, of inhibiting agents generated by its own hydrolysis. The only anion that competes in binding strength with ATP and that might exert a real inhibiting effect is pyrophosphate but it was not formed under the experimental condition used in the experiments.

The rates of dephosphorylation were dependent on ATP concentration and pH. At pH 3 the rate of ATP hydrolysis in the presence of [21]aneN$_7$ was $k = 0.029\ min^{-1}$ at 20 °C for an initial ATP concentration 10^{-5} M. At higher temperatures and/or concentrations the rates for this macrocycle were too fast to be monitored using HPLC and NMR techniques. All the other macrocycles showed considerable lower rates being [24]aneN$_8$ the fastest one with $k = 0.0045\ min^{-1}$ ($T = 40$ °C, $[ATP]_0 = 10^{-5}$ M). Either the four larger macrocycles [27]aneN$_9$, [30]aneN$_{10}$, [33]aneN$_{11}$ and [36]aneN$_{12}$ or the smaller [18]aneN$_6$ were clearly slower. At pH 7 all macrocycles showed slower rates than at pH 3. This can be attributed to a lessened participation of general acid catalysis.

The highest efficient of [21]aneN$_7$, particularly at lower pH values, can be attributed to several factors. First, the magnitude of the interaction does not seem to be a key point since the larger macrocycles show less efficiency. Second, if the mechanism proceeds through formation of a covalent intermediate

Table 4
Major and minor axes for the average ellipsoid of polyammonium macrocycles [54]

Macrocycle	Major axis (Å)	Minor axis (Å)
$H_4([18]aneN_6)^{4+}$	7.682	6.212
$H_4([21]aneN_7)^{4+}$	7.653	6.725
$H_6([24]aneN_6O_2)^{61+}$	10.005	6.714
$[H_8([30]aneN_{10})][Co(CN)_6]_2Cl_2{\cdot}10H_2O$	15.486	6.873

phosphoramidate species, the nucleophilicity of the macrocyclic amines should be critical. In the case of the fastest [21]aneN$_7$ macrocycle, evidences of formation of such covalent intermediate were provided by a ^{31}P NMR signal appearing at ca. 10 ppm which was coincident with that displayed by a synthetically prepared phoshoramidate. Factors which favor nucleophilicity are: (i) reduced overall positive charge at a given protonation, (ii) hydrophobicity of the environment where the reaction occurs, (iii) electron donor substituents. As at a given pH [21]aneN$_7$ is less charged than the larger ligands, this should favor a nucleophilic attack. However, the same reasoning should drive to a higher efficiency of the smaller [18]aneN$_6$ and this was not the case.

Therefore, other factors affecting the electronic and stereochemical matching between receptor and substrate have to play a key role in this activity. [24]aneN$_6$O$_2$ (O-bisdien), that produces also a very significant rate enhancement which is persistent from acidic to neutral pH, shares with [24]aneN$_8$ the feature of having the same number of atoms in the macrocyclic ring.

Table 4 collects the minor and major axes defining the elliptical shapes of various macrocycles whose structure have determined by X-ray diffraction analysis.

As seen in Table 4, the macrocycles showing highest efficiencies have very close dimensions of the minor axis. Modeling studies indicated that ATP would be located along this common minor axis. Later we will discuss further this size effect.

Methylation of the nitrogen atoms is a way of increasing the nucleophilicity of the amine groups and in this respect several methylated [3*k*]aneN$_k$ receptors were prepared (Chart 7) [92,97,116].

The effects of methylation on the rate of ATP cleavage are, however, not uniform since apart from the electron donor properties there are other factors also operating. With respect to the stability of the interaction ATP-macrocycle for the adducts formed between ATP and the 18-membered macrocycles, Me$_2$[18]aneN$_6$ is the receptor forming the most stable adducts, while for the ATP adducts of the 21-membered macrocycles the non-methylated [21]aneN$_7$ forms more stable complexes than Me$_3$[21]aneN$_7$. Methylation, apart from providing electron density to the nitrogen atoms, modifies the size and conformation of the macrocycles. These facts can yield on balance stabilizing or non-stabilizing contribution to the formed adducts. Another case in which there is an increase of the stability of the ATP adducts upon permethylation of the nitrogen atoms refers to macrocycles *p*B323 and B323Me$_4$ (Chart 10) [102].

The same happens for the kinetic rates of the dephosphorylation processes. Me$_4$[18]aneN$_6$ produces a greater rate enhancement than [18]aneN$_6$. At pH 3 and 80 °C for [ATP]$_0$ = 0.01 M, Me$_4$[18]aneN$_6$ produces a 20-fold rate acceleration with respect to free ATP while [18]aneN$_6$ just yields a five-fold rate enhancement. However, in the case of the 21-membered macrocycles, methylation of [21]aneN$_7$ to give Me$_3$[21]aneN$_7$ modifies its optimal size and leads to a much poorer hydrolytic rate.

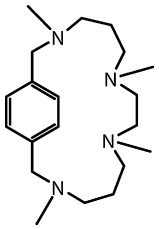

B323Me$_4$

Chart 10.

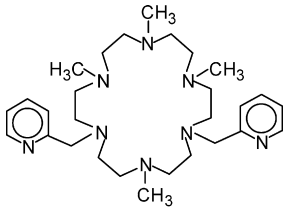

Me$_4$Py$_2$[18]aneN$_6$

Chart 11.

Insertion of two pyridylmethyl hanging groups on Me$_4$[18]aneN$_6$ (Py$_2$Me$_4$[18]aneN$_6$, Chart 11) leads to enhanced binding ability towards ATP at acidic pH [117]. Unfortunately, data regarding the effect on ATP hydrolytic cleavage are not available for the new ligand.

Besides the previous effects, permethylation of amine ligands gives rise to polyammonium receptors with highly reduced ability in forming hydrogen bonds with the substrates. This may lead to unexpected binding selectivity. An interesting case regards the formation of ADP and ATP complexes with polyammonium receptors derived from the cyclophanes Ph$_2$Me$_6$N$_6$ (Chart 7) and Ph$_2$Pip$_2$Me$_4$N$_8$ (Chart 12) [118].

These two ligands present a similar molecular architecture composed of two polyamine subunits linked by aromatic spacers. The presence of aromatic moieties, the short ethylenic chains connecting the amine groups, nitrogen methylation and, in Ph$_2$Pip$_2$Me$_4$N$_8$, the piperazine rings, give rise to rigid macrocyclic frameworks. The protonation patterns of these ligands, determined by means of potentiometric and NMR studies

Ph$_2$Pip$_2$Me$_4$N$_8$

Chart 12.

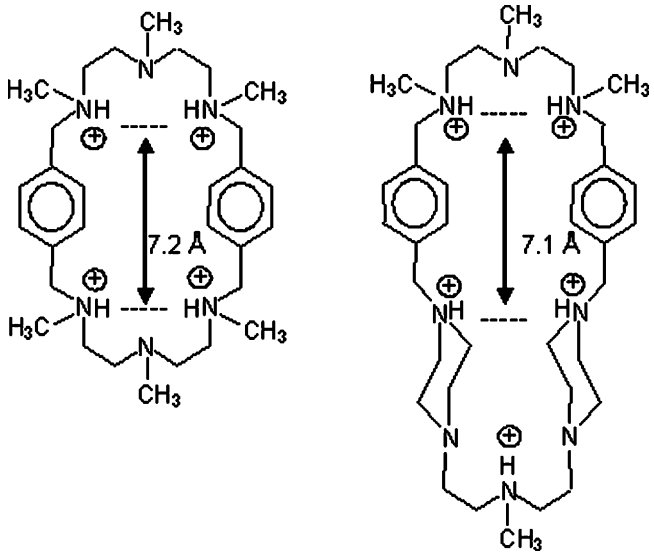

Fig. 23. Charge disposition in $H_4(Ph_2Me_6N_6)^{4+}$ and $H_5(Ph_2Pip_2Me_4N_8)^{5+}$ macrocycles [118]. Reproduced by permission of The Royal Society of Chemistry.

showed that, despite the different number of nitrogen atoms in the molecules, similar arrangements of positive charges are achieved in the polyprotonated species [118,119]. For instance, both in $H_4(Ph_2Me_6N_6)^{4+}$ and in $H_5(Ph_2Pip_2Me_4N_8)^{5+}$, four acidic protons are located on the benzylic nitrogens forming rectangular arrangements of positive charges of very similar dimensions (Fig. 23). Of course, an additional positive charge is present in $H_5(Ph_2Pip_2Me_4N_8)^{5+}$.

Such similarity in the spatial distribution of charge in the two polyammonium cations leads one to suppose that a similar charge–charge matching between the phosphate chains of ATP or ADP and the receptors can be achieved. Moreover, it seems reasonable to expect that $Ph_2Pip_2Me_4N_8$ is a better receptor than $Ph_2Me_6N_6$ since the former, owing to its higher number of amine groups, forms more charged species than the latter under similar conditions. Rather surprisingly, however, while the two nucleotides form stable complexes with various protonated forms of $Ph_2Me_6N_6$, no interaction with $Ph_2Pip_2Me_4N_8$ was detected by means of potentiometric and NMR measurements over the whole pH range. A reasonable interpretation of such behavior can be drawn by considering the crystal structures of the $H_4(Ph_2Me_6N_6)^{4+}$ and $H_5(Ph_2Pip_2Me_4N_8)^{5+}$ cations (Fig. 24). In $H_4(Ph_2Me_6N_6)^{4+}$ the four N–H^+ groups are convergent allowing the receptor to form four hydrogen bonded salt bridges with the phosphate chain of the nucleotides. On the other hand, in $H_5(Ph_2Pip_2Me_4N_8)^{5+}$ the five N–H^+ groups are divergent, preventing the simultaneous interaction with the nucleotides and the formation of complexes. Hence charge–charge attraction, although is the driving force for most ion pairing processes in water, not always produces enough energy to stabilize anion complexes with polyammonium receptors. As shown in this case, as well as in previous cases, the formation of salt bridges reinforced by hydrogen bonds can be the key to achieve efficient anion binding.

Complexation induced ^1H chemical shifts of the adenine protons of ATP and ADP evidenced that a modest π-stacking interaction between the nucleobase and the aromatic groups of

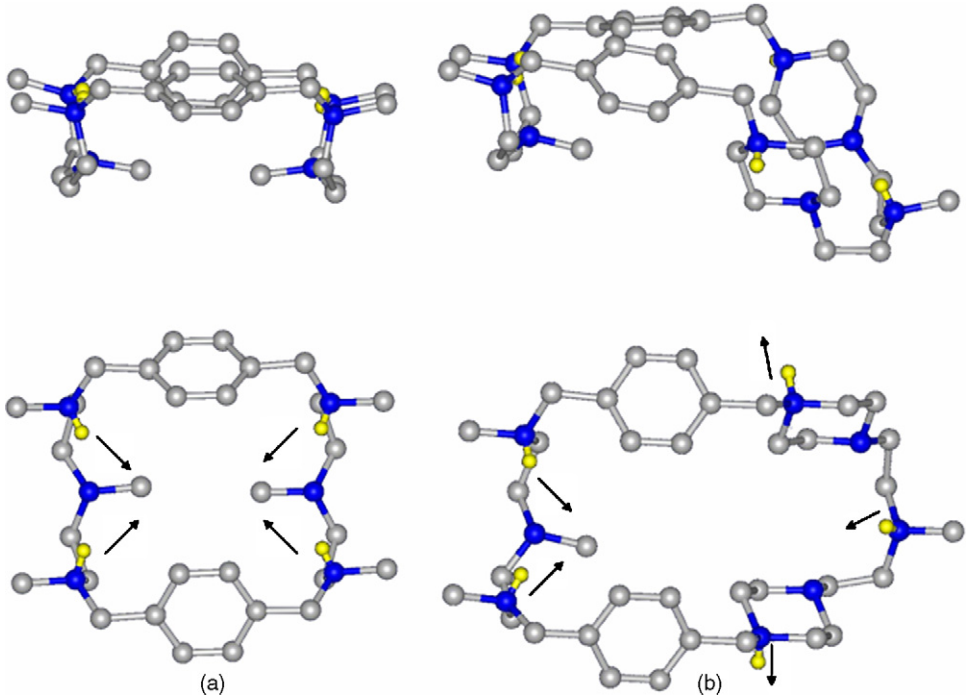

Fig. 24. Lateral and top views of the crystal structure of $H_4(Ph_2Me_6N_6)^{4+}$ (a) and $H_5(Ph_2Pip_2Me_4N_8)^{5+}$ (b). The orientation of N–H^+ groups is indicated by the arrows [119].

the receptors furnishes some stabilization to the nucleotide complexes of $Ph_2Me_6N_6$.

π,π-Stacking is one of the forces that can be used to complement coulombic interactions and hydrogen bonding forces in nucleotide recognition. While the phosphate chain of the nucleotide represents a good electrostatic binding point, the nucleoside part may operate as an adequate site for π,π-stacking interactions with appropriate functionalities of the ligand. One of the first types of synthetic ligands able to behave as multifunctional receptors for nucleotide anions were reported in 1988 by Lehn and his co-workers [120,121]. The receptors consisted of the well-known polyazamacrocycle bisdien that had been functionalized with acridine subunits. Schneider and co-workers presented a multifunctional anion receptor combining hydrophobic and electrostatic interactions [122].

Within this context, a receptor for nucleotides formed by a long hexaamine chain attached through methylene groups to a *m*-xylil spacer was developed (*m*B33233, Chart 13) [123,124]. Potentiometric studies showed that *m*B33233 interacts with ATP, ADP and AMP in the order ATP > ADP > AMP. On the other hand, NMR studies unambiguously proved the participation of π-stacking forces between the nucleoside part of ATP, ADP and AMP and the benzene ring in the stabilization of the adduct species.

Using the intermolecular ^{1}H NMR cross-peaks for establishing the initial host–guest docking, molecular dynamic studies performed for the system L-ADP show π-stacking in all the lowest energy conformers [125]. These studies suggested the possibility that hydrogen bonds between the ammonium groups of the receptors and the phosphate groups of ADP could be formed through water molecules placed between them. So, *m*B33233 displays the right topology and size to recognize the polyphosphate chains of the nucleotides through electrostatic, hydrogen bonding and π-stacking forces.

In order to better understand the influence of the substitution of the aromatic ring in nucleotide interaction, the *ortho*- and *para*-analogs of *m*B33233 were also prepared (see Chart 13). The stability order found followed the sequence *o*B33233 > *m*B33233 > *p*B33233. All of them presented higher stability of the adduct complexes than those formed by their open-chain hexaamine counterpart L33233 (Chart 13).

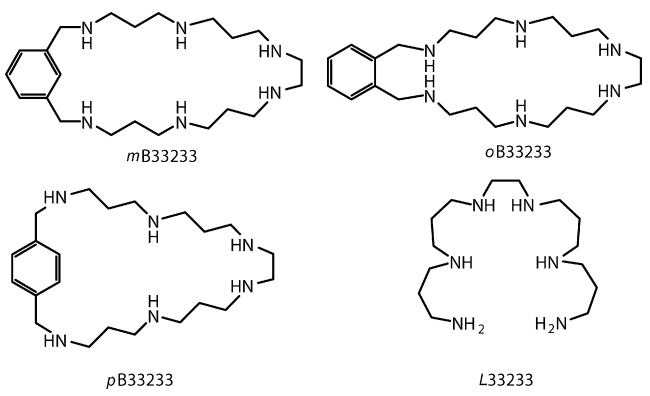

Chart 13.

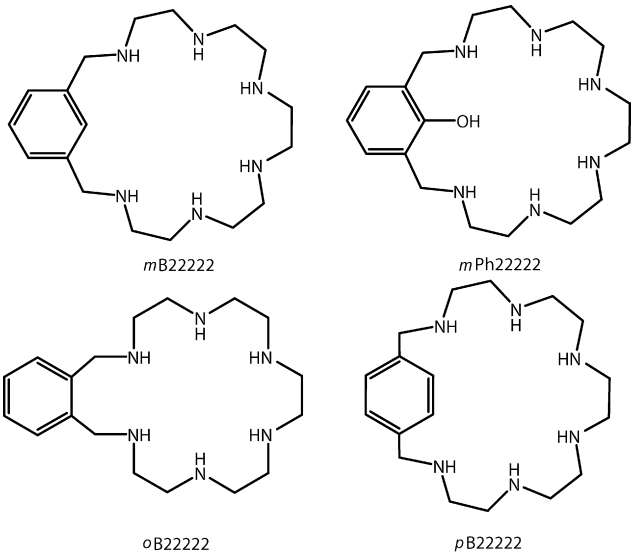

Chart 14.

Interestingly, none of these receptors presented significant rate-enhancements of the hydrolytic cleavage of ATP. As it has been discussed previously, the polyammonium catalysts giving the best performance needed to have a determined cavity size which was defined by 21- or 24-membered macrocyclic rings. Accordingly, a new cyclophane receptor having a 21-membered ring was prepared (*m*B22222, Chart 14) [126].

^{1}H NMR studies also proved the participation of π-stacking interactions in the stabilization of the system ATP-*m*B22222. ^{31}P NMR studies revealed that *m*B22222 produced rate enhancements comparable to those of O-bisdien and slightly lower than those of [21]aneN$_7$ confirming the critical role of size in this catalytic processes (Fig. 25). Interestingly enough, the reaction using *m*B22222 as a catalyst is not only efficient but also very specific since it stops in the formation of ADP and does not proceed significantly further.

The critical size required is manifested in the fact that either the *ortho* or *para*-isomers of *m*B22222, containing 20- and 22-

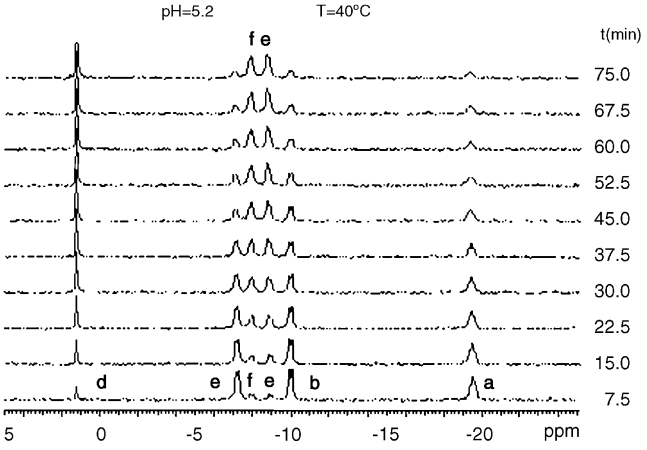

Fig. 25. Time evolution for ^{31}P NMR spectra of solutions containing ATP and *m*B22222 in 10^{-2} M at 40 °C and pH 5.2 (a) P_β (ATP); (b) P_α (ATP); (c) P_γ (ATP); (d) Pi; (e) P_α (ADP); (f) P_β (ADP) [126]. Reproduced by permission of The Royal Society of Chemistry.

membered cavities (*o*B22222 and *p*B22222, Chart 14) yield much poorer enhancements [127]. This lack of activity is particularly noticeable in the case of the *ortho*-derivative.

Molecular dynamics studies suggest that the optimal size is that for which just γ-phosphate of ATP perfectly resides at the macrocyclic cavity. The macrocyclic hole of *m*B22222 is too small for permitting the phosphate group to go through it. Fig. 26 shows the perfect fitting between the phosphate group and the macrocyclic cavity of *m*B22222.

Another macrocycle which presented a 21-membered size was *m*Ph22222 (Chart 14), in which the *meta*-benzene spacer had been substituted by a *meta*-phenolic one. Although not as high as in the *m*B22222-ATP system, relevant rate accelerations were also found for *m*Ph22222 from acidic pH to pH values ca. 7.5. At these pH values, the reaction slows down in concordance with the deprotonation of the phenolic group, which corresponds to the passage from the $H_4(Ph22222)^{4+}$ species to $H_3(Ph22222)^{3+}$ species. Deprotonation of the phenolic group, apart from introducing a negative charge that will somewhat repel the phosphate chain of ATP, yields intramolecular hydrogen bonding between the phenolate group and the protonated benzylic ammonium groups that at this pH are still protonated. This hydrogen bonding leads to a significant size reduction as illustrated in Fig. 27, which does not permit any more the fitting with the phosphate group.

Polyamine ligands, both macrocyclic and acyclic, containing phenanthroline and dipyridine groups were also used for nucleotide binding [99,105,128]. These studies evidenced the importance of π-stacking interactions between the adenine group of ATP and ADP with aromatic moieties of the receptors in determining the stability of nucleotide complexes. For instance, in the case of the acyclic receptors Neo-open and Bipy-open (Chart 15), for the same negative charge of the anions and, respectively, of the receptors, the stability of ATP complexes

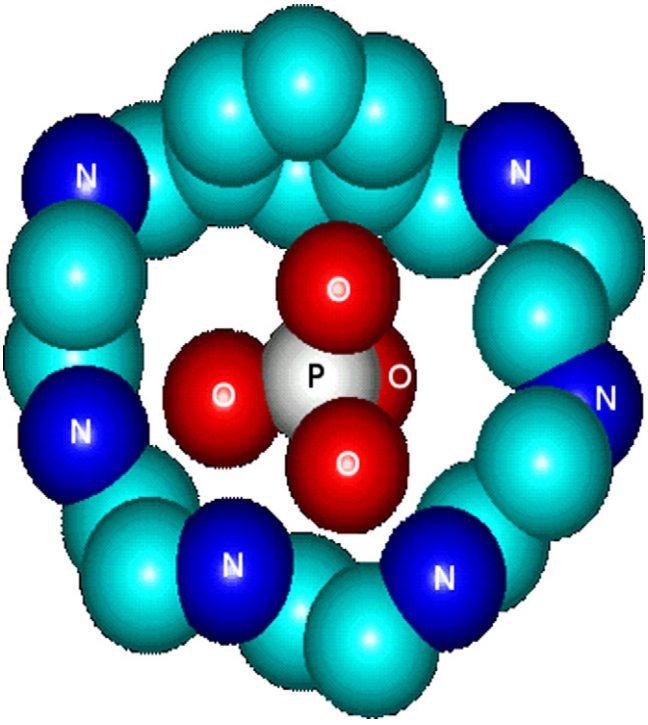

Fig. 26. Comparison between the size of the macrocyclic cavity of *m*B22222 and the γ-phosphate of ATP. The rest of ATP has been obscured for clarity.

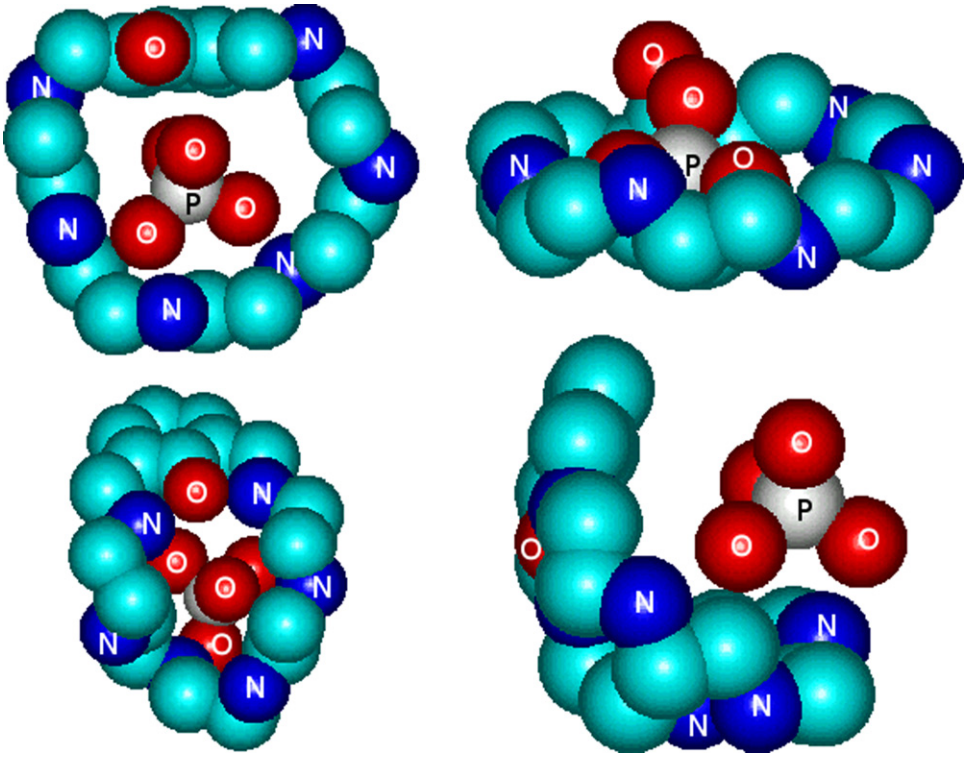

Fig. 27. Model showing the dimensions of $H_4(mPh2222)^{4+}$ and $H_3(mPh2222)^{3+}$ in which phenolate is deprotonated, in comparison to the γ-phosphate of ATP. The remaining of the ATP molecule has been obscured.

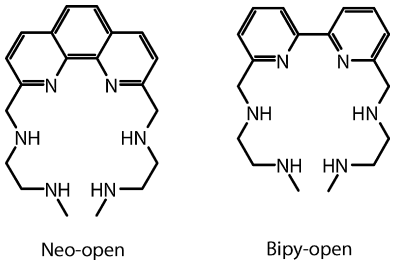

Chart 15.

Table 5
Thermodynamic parameters for the formation of ATP complexes with the ligand Bisby (L) determined in 0.1 mol dm^{-3} Me_4NCl at 298.1 K [105]

Reaction	log K	ΔH° (kcal/mol)	$T\Delta S^\circ$ (kcal/mol)
$H_4L^{4+} + H_2ATP^{2-} \leftrightarrows (H_6LATP)^{2+}$	5.43	8.6	16.0
$H_5L^{5+} + H_2ATP^{2-} \leftrightarrows (H_7LATP)^{3+}$	5.54	12.1	19.7
$H_5L^{5+} + H_3ATP^{-} \leftrightarrows (H_8LATP)^{4+}$	5.29	7.4	14.6

is higher than the stability of the analogous complexes with triphosphate, the stability enhancement being ascribable to the anion–receptor π-stacking interaction observed by means of ^{1}H NMR spectra [99]. In particular, larger complexation-induced chemical shifts of the ^{1}H NMR spectra were found for the receptor Bipy-open containing a larger aromatic moiety.

A complete thermodynamic study including the determination of stability constants, enthalpy changes and derived entropic terms was performed by means of potentiometric and microcalorimetric measurements on the system ATP/Bisby (Chart 9) in order to get further information on the nature of the interaction of nucleotides with polyammonium receptors [105].

As already said in the previous section, this receptor forms a molecular cleft where large anions can be hosted. Molecular modeling showed that in the ATP complex the triphosphate chain of the nucleotide is partially included into such ligand pocket while the adenine moiety remains outside the cavity forming π-stacking interaction with a dipyridine group (Fig. 28). ^{1}H spectra of the complex in solution provide an unambiguous evidence of the formation of such π-stacking interaction, denoted by a significant upfield displacement of the signals of both adenine and dipyridine protons.

A similar host–guest interaction is expected to produce a strong desolvation of both reactants and, in particular, of the receptor, whose cavity can host several water molecules. Accordingly, the complexation reactions are accompanied by a largely favorable entropic terms while the enthalpic ones are invariably unfavorable (Table 5). It is interesting to note that the complex stability constants are not very sensitive to variations of ATP and receptor charge due to some compensation between enthalpic and entropic contributions.

Another important aspect in nucleotide recognition regards the sensing in water of these important biomolecules [106,129–138]. In order to achieve this goal an approach would be to use molecules that do not alter the nature of the nucleotides and that incorporate signaling units. In this sense, open-chain polyammonium receptors containing aromatic moieties are adequate receptors since they can interact with the anionic guest through their positively charged ammonium groups, through hydrogen bonding by their ammonium and amine groups, as well as through hydrophobic and stacking interactions with adenine, provided the aromatic fragments they incorporate are in the correct orientation [121,123,124,139]. In addition, the condensed aromatic rings present in the receptors may serve as luminescent probes for detecting and quantifying the interaction. Indeed, fluorescence emission is one of the most useful signaling properties since its magnitude is highly sensitive to the binding of the guest species. Within this framework, we have studied the possibilities as sensors for anions in water of a series of compounds containing one or two anthryl or naphthyl groups attached to the ends of different polyamine chains (Chart 16) [79,140–143].

With respect to the stability of the ATP adducts, for the receptors sharing a given polyamine chain, those containing one anthrylmethyl fragment interact much more strongly with ATP than those with just one naphthalene. However, they present

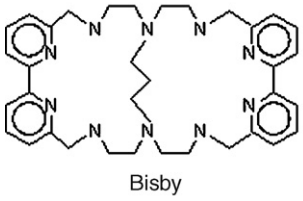

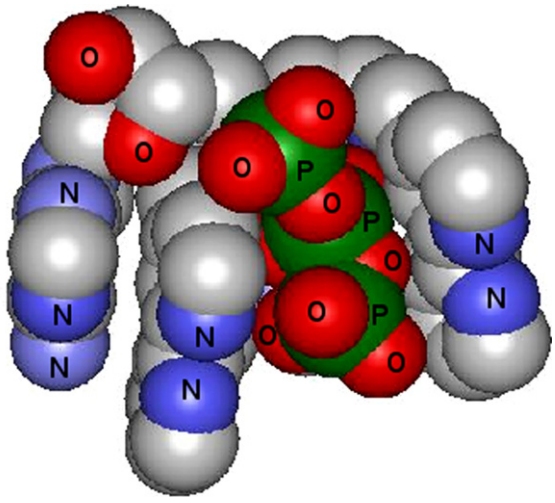

Fig. 28. Proposed model for the interaction of protonated forms of Bisby with ATP [105].

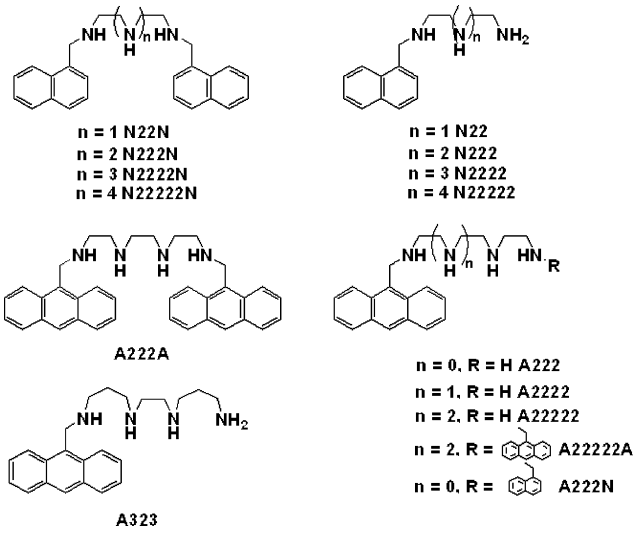

Chart 16.

comparable stability constant values to those containing naphthalene at both ends. NMR studies show that π–π stacking is present throughout all the pH range where interaction occurs. NOE experiments confirm the proximity of the aromatic rings of the receptors and ATP and have allowed for proposing preliminary models for the interaction (see Fig. 29).

Steady-state fluorescence measurements on these systems showed the existence at acidic pH of a quenching effect of the emission of the fluorophores following the protonation of the adenine ring. The analysis of the data made it possible to attribute this quenching to an electron transfer from the naphthalene or anthracene moieties to the protonated adenine ring, this process being more favorable for naphthalene. Time correlated single photon counting showed that even in the presence of ATP, there is an important energy transfer from naphthalene to anthracene in the bis(chromophoric) receptor N222A (Chart 16).

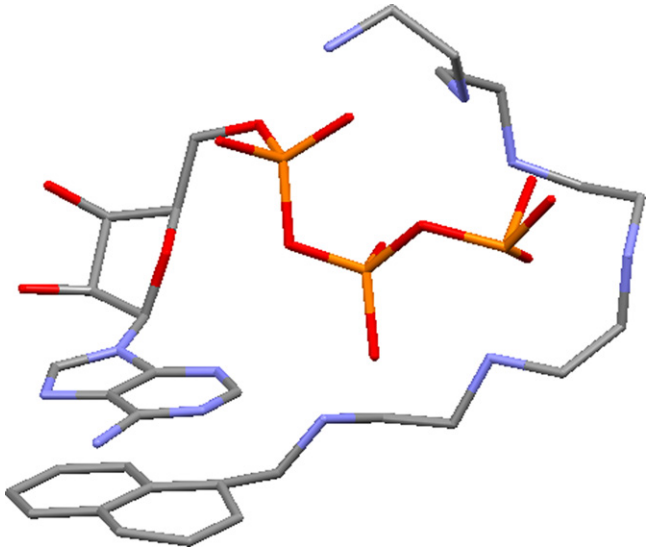

Fig. 29. Molecular model for the interaction of N22222 with ATP showing the stacking between the aromatic fragments [142].

6. NAD$^+$, NADP$^+$, DNA and RNA

Studies on the interaction of the ubiquitous dinucleotides NAD$^+$ and NADP$^+$ with polyammonium receptors are relatively scarce [124,144]. Some years ago we advanced a potentiometry, NMR, cyclovoltamperommetric and molecular dynamics study on the interaction of protonated [21]aneN$_7$ with NAD$^+$ and NADP$^+$ [145]. The stability constants for the 1:1 adducts formed clearly and the plots of the apparent constants clearly indicate that NADP$^+$ is selective recognized over NAD$^+$ by the polyammonium receptor over a wide pH range. ^{31}P NMR spectra suggested that the clue of the selective recognition is the participation of the phosphate group estirified to the 2′-hydroxy group of the AMP moiety of NADP$^+$ in the interaction with the receptor. Such participation is also supported by molecular dynamics studies on the interaction of tetraprotonated [21]aneN$_7$ with NADP$^+$. This phosphate would interact strongly with the two ammonium groups placed adjacent within the tetraprotonated macrocycle (Fig. 30).

On the other hand, formation of receptor-nicotinamide adenine nucleotide adducts alters the electrochemical reduction of NAD$^+$ and NADP$^+$ at carbon electrodes, favoring the formation of dihydronicotinamide species rather than that of the dimer species.

The development of new ligands able to interact with nucleic acids is a topic of great interest within chemistry and biochemistry [146–151]. Cyclophane-type, cyclic polyamines containing phenanthroline moieties, polyaza-polyoxa-macrocycles, open-chain and tripodal polyamines containing condensed aromatic rings or small macrocyclic hanging rings can interact with nucleic acids through salt bridges, hydrogen bonding and stacking interactions. The behavior of the cyclophane-type macrocycles *m*B323 (Chart 8), *m*B33233, *p*B33233 (Chart 13) and *p*B323 (Chart 3) [45,152,153], of the polyamines containing phenanthroline groups Neo22, Neo222, Neo2222 and Neo333 (Chart 8), of the polyaza-polyoza-macrocycle N_6O_4 and N_6O_4OH (Chart 17) [154], of the open-chain polyamines containing one naphthylmethyl group (N22-N2222), two methylnaphthyl groups (N2N-N22222N), the derivatives with anthracene A22222 and A22222A (Chart 16) and the tripodal polyamines TAL, N3TAL, ATAL (Chart 1) [44,45], Tris-cyclen

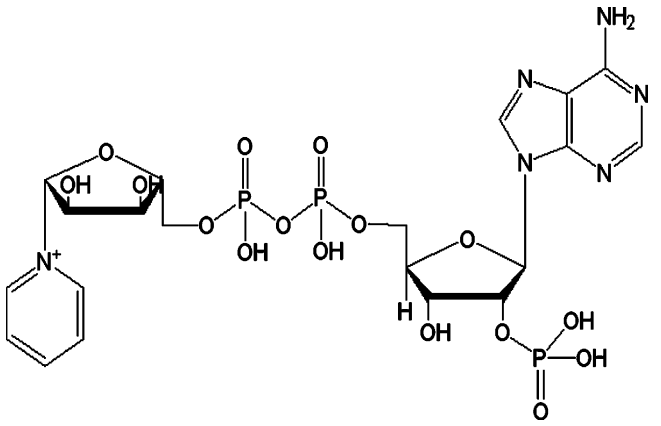

Fig. 30. NADP$^+$.

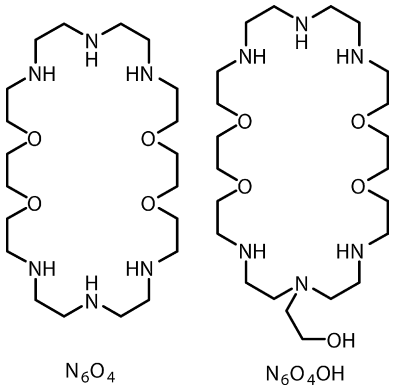

Chart 17.

and Tris-N_3O (Chart 6) [155] were examined for their interaction with double-stranded polyA.polyU as RNA model and poly(dA).poly(dT) as DNA model [156,157]. The effects of the cyclophane receptors *m*B323, *m*B33233, *p*B33233 and of the polyoxa-polyaza-macrocycles N_6O_4 and N_6O_4OH (Chart 17) on the melting behavior of double stranded DNA favor RNA over DNA. Preliminary fluorescence assays with ethidium bromide show similar values for *m*B33233 and *p*B33233 and a slightly higher value for *m*B323, particularly with RNA that is the usual behavior observed also for aliphatic polyamines. On the contrary, the macrocyclic polyamines containing phenanthroline moieties Neo22, Neo222 and Neo2222 display a reversed ability producing larger stabilization of the DNA sequence, while Neo333 produces similar stabilization with both nuclei acids. Neo222 shows more affinity towards both DNA and RNA [155] than the open-chain amine counterpart diethylenetriamine) [45], which suggest that the phenanthroline moiety is indeed intercalating between pairs of DNA bases. Neo222 and Neo2222 show more affinity for DNA then their linear counterparts, while Neo333 does not display significant differences. On the other hand Neo222, Neo2222 and Neo333 lead to smaller affinity towards RNA. Thus, the phenanthroline-based macrocycles are promising ligands for double-stranded DNA.

The preference for RNA over DNA is particularly remarkable for the tripodal polyamine TAL with $\Delta\Delta T = 40\,^{\circ}C$, which shows the strongest preference for RNA from all the hitherto known polyamines [158–160]. This behavior, although not so significant, can be also extended to the other tripodal polyamines ATAL, N3TAL, Tris-cyclen and Tris-N_3O.

The introduction of terminal aryl moieties in the open-chain polyamine chains leads to dramatic changes; with the exception of N22222N all compounds show the reversed larger stabilization of the DNA sequence. This reversal is more noticeable for the ligands in which the chain length allows bis-intercalation particularly N2222N. For this ligand the introduction of the naphthyl groups produces a strong increase in affinity in comparison with the counter-part polyamine without aryl groups (2222) ($\Delta\Delta T_M = 22.5\,^{\circ}C$) for ligand to nucleic acid base pair ratio of 0.1.

The coordination of these polyamines to metal ions introduces distinctive features that will be discussed in the next section.

7. Metal complexes as anion receptors

Complexed metal ions can express their Lewis acid characteristics if they are coordinatively unsaturated or if they have coordination positions occupied by labile ligands that can be easily replaced. If this occurs metal complexes are well suited for interacting with additional Lewis bases which very often are of anionic nature.

This is the strategy of choice of many metalloenzymes dealing with the fixation and activation of substrates. A classical example is the family of enzymes called carbonic anhydrases [161–163]. Carbonic anhydrases are ubiquitous enzymes which catalyze the hydration reaction of carbon dioxide and play roles in processes such as photosynthesis, respiration, calcification and decalcification and pH buffering of fluids. Human carbonic anhydrase II (HCA II) is located in the erythrocytes and is the fastest isoenzyme accelerating CO_2 hydrolysis by a factor of 10^7. Therefore, it is considered to be a perfectly evolved system being its speed controlled just by diffusion. The active site of HCA II is formed by a Zn^{2+} cation coordinated to three nitrogen atoms from histidine residues and by a water molecule which is hydrogen bonded to a threonine residue and to a "relais" of water molecules which interconnects the coordination with histidine 64 (Fig. 31). The pK_a of the coordinated water molecule in this environment is ca. 7 so that at this pH 50% is as hydroxylated as $Zn–OH^-$ generating thus a nucleophile which will attack CO_2 to give the hydrated HCO_3^- form.

The rate determining step is precisely the deprotonation of the coordinated water molecule and the transfer of the proton through the chain of water molecules to His-64 which is assisting the process.

Another example is phosphatases which are the enzymes in charge of the hydrolysis of phosphate monoesters. Metallo phosphatases contain either Zn or Fe or both of them as metal ions being one of their characteristics the presence of at least two metal ions in the active site. *Escherichia coli* alkaline phosphatase contains two Zn^{2+} and one Mg^{2+} metal ions in the active center. In the first step of the catalytic mechanism the phosphate group of the substrate interacts as a bridging η,η'-bis(monodentate) ligand through two of its oxygen atoms with

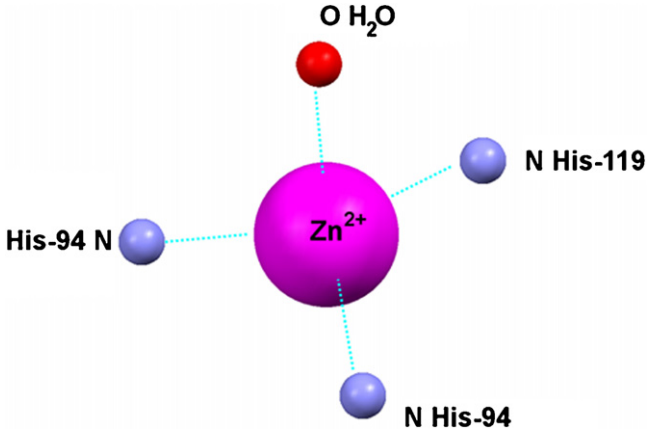

Fig. 31. Metal site of HCA II showing the tetrahedral arrangement of three histidine residues and a water molecule.

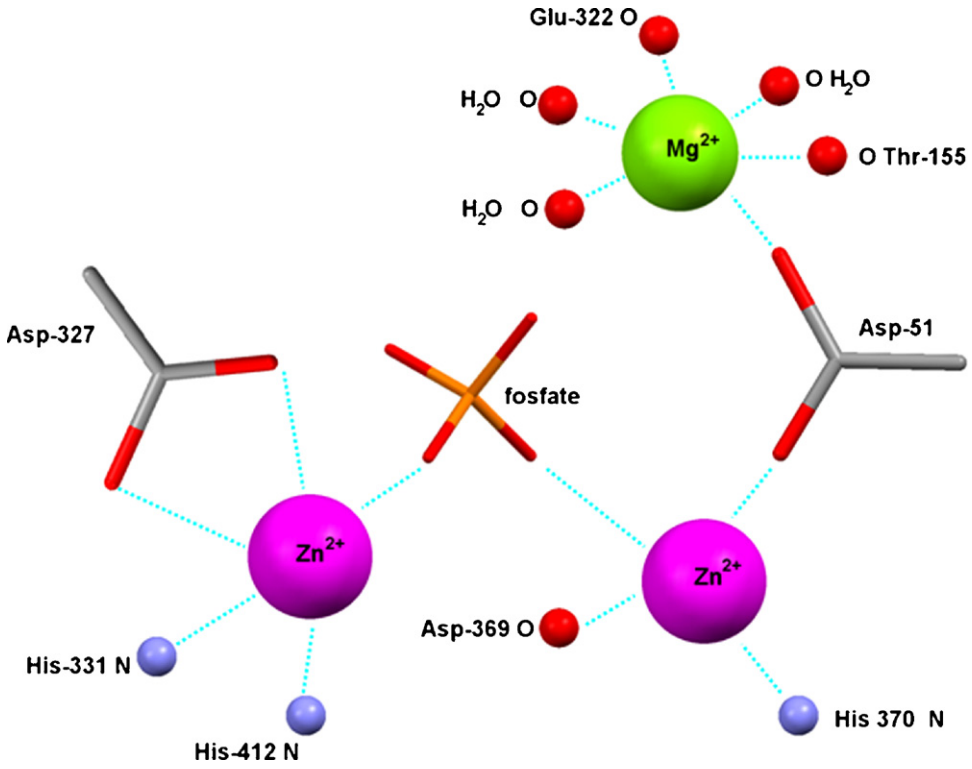

Fig. 32. Active site of alkaline phosphatases. Adapted from Ref. [164].

the two Zn^{2+} ions while its other two oxygen atoms form hydrogen bonds with an arginine residue rightly disposed in the polypeptide chain (Fig. 32).

A last example that we would like to recall regards ribulose-1,5-bisphosphate carboxylase/oxygenase (*rubisco*) which is the most abundant enzyme in Nature. *Rubisco* is a magnesium protein which is present in all the photosynthetic organisms participating in the first stage of the Calvin cycle. A lysine residue interacts with CO_2 forming an elusive carbamate bond which is stabilized by interaction with the Mg^{2+} ion and by hydrogen network with other groups of the polypeptidic chain (Fig. 33). The formed ternary complex interacts with the substrate which is subsequently carboxylated.

In the next paragraphs we will give some examples of abiotic polyammonium receptors mimicking features of these sites.

7.1. Interaction with carbon dioxide and carbonate anions

Metal complexes of cyclophane macrocycles like *p*B323 can match some of the required features for binding and activating anionic species. The crystal structure of the Hg^{2+} complex of the durene-containing macrocycle Du323 (Chart 18), containing a durene spacer, shows as the coordination of one of the Hg^{2+} involves the benzylic nitrogen atoms and the amino groups at the centre of the chain [165]. Geometric reasons prevent the other benzylic nitrogen atom from participating in the binding of the same metal ion. Calorimetric and other solution studies confirmed similar features for the mononuclear Cu(II) and Zn(II) complexes of the macrocycles *m*B323 and *p*B323. Therefore, in these compounds one of the benzylic nitrogen atoms would be also not involved in the coordination to the metal ion, presenting the metal ions unsaturated coordination sites [166–169].

Based on these antecedents we checked the ability of these metal centers for binding additional guests. One of our interests was to analyze the interactions with carbon dioxide and carbonate anions. For doing so we carried out potentiometric titrations in which solutions containing Cu^{2+} and Zn^{2+} metal complexes of *m*B323 and *p*B323 at basic pH were titrated with perchloric

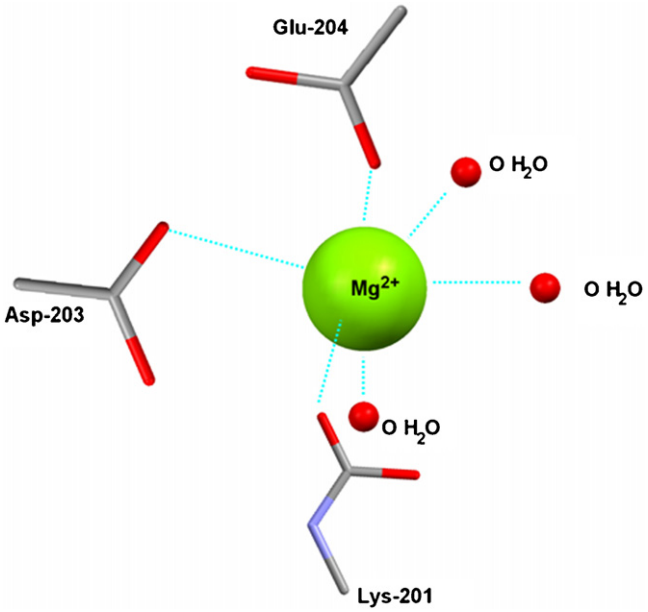

Fig. 33. Active site of the enzyme *rubisco*. Adapted from Ref. [164].

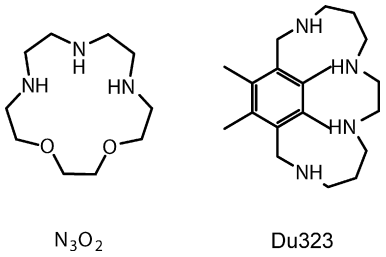

Chart 18.

acid [167]. It was possible to follow the measurements in the pH range 7–11. Below this pH range, CO_2 evolution prevented from obtaining stable readings. The measurements were also performed for the binary system receptor-carbonate. Comparison between the two systems evidenced, particularly in the case of the Zn^{2+}, clear increases of the percentages of complexed carbonate in the presence of the metal ions (Fig. 34).

An interesting example of CO_2 uptake by a synthetic metal complex mimicking the mechanism of carbonic anhydrase (CA) is given by the ligand N_3O_2 (Chart 18) [170].

Both Zn^{2+} and Cu^{2+} complexes with N_3O_2 readily adsorb atmospheric CO_2 in water at alkaline pH, giving rise to $\{[M(N_3O_2)]_3(\mu_3\text{-}CO_3)\}\cdot(ClO_4)_4$ ($M = Zn^{2+}$, Cu^{2+}) complexes. The complexes are isomorphous and their molecular structures show the μ_3-CO_3^{2-} anion bridging the three metal ions through the three oxygen atoms of the carbonate group (Fig. 35).

The CO_2 uptake by these M–N_3O_2 complexes is very fast in comparison with other metal complexes which can fix CO_2 from the air. The fixation is due to the presence in solution of $[M(N_3O_2)OH]^+$ species, which act as nucleophiles towards CO_2, giving rise to $[M(N_3O_2)HCO_3]^+$ complexes. Further reaction with $[M(N_3O_2)OH]^+$ species forms the trinuclear complexes, which can be isolated in very high yields.

In the case of the Zn^{2+} complex, the first step, namely the reversible formation of a hydrogen carbonate adduct, which equilibrates with an aquo-Zn^{2+} complex and HCO_3^- (Fig. 36), resembles the mechanism currently accepted for hydration of CO_2 by CA. Furthermore, the constant for the equilibrium $[Zn(N_3O_2)]^{2+} + HCO_3^- \leftrightarrows [Zn(N_3O_2)(HCO_3)]^+$ ($\log K = 2.2$) is similar to that found for CA.

In order to achieve atmospheric CO_2 fixation at neutral pH, we turned our attention to the active site of *rubisco*. Key features for the recognition and activation of carbon dioxide

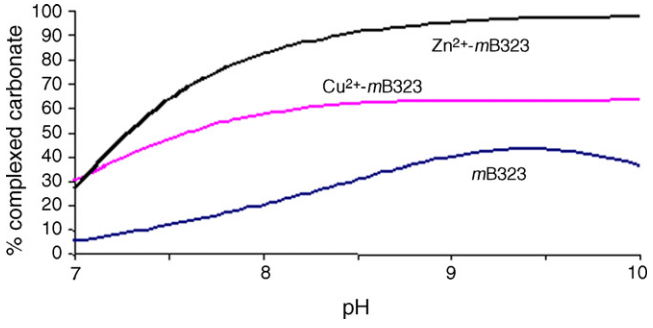

Fig. 34. Percentage of carbonate bound to free *m*B323 and to the Cu^{2+} and Zn^{2+} solutions [167].

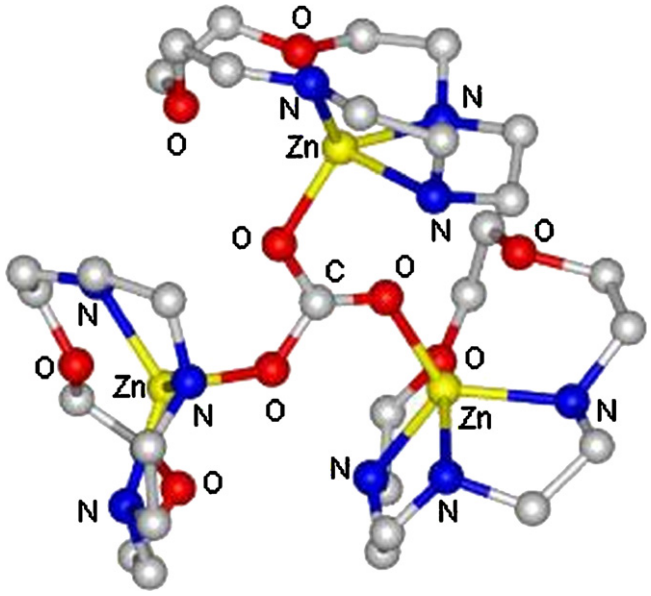

Fig. 35. Crystal structure of the $\{[Zn(N_3O_2)]_3(\mu_3\text{-}CO_3)\}^{4+}$ cation. Similar structures were also obtained for the complexes $\{[Cu(N_3O_2)]_3(\mu_3\text{-}CO_3)\}^{4+}$ and $\{[CuZn_2(N_3O_2)_3](\mu_3\text{-}CO_3)\}^{4+}$. Reprinted with permission from Ref. [170]. Copyright 2005 American Chemical Society.

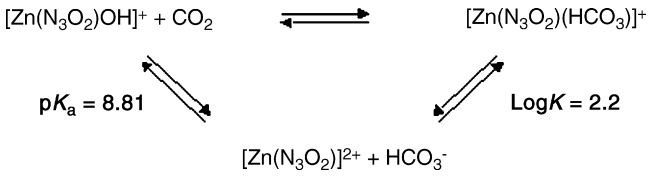

Fig. 36. CO_2 hydration promoted by $[Zn(N_3O_2)]^{2+}$.

where the assistance of the metal ion as Lewis acid, the presence of the basic lysine residue for forming the carbamate bond as well as the presence of other groups able to participate in a hydrogen bond network with the fixed carbon dioxide. Therefore, we prepared a new macrocycles containing the coordinating spacer 2,2′:6′,2″-terpyridine connected at its 5,5″ positions through methylene groups to the highly basic polyamine bridge 1,5,8,11,15-pentaazapentadecane (macrocycle Terpy3223, Chart 19) [171].

Interestingly enough, dilute aqueous solutions of this ligand and $Cu(ClO_4)_2$ in 1:1 molar ratio at pH 9 exposed to an open-air atmosphere yielded after a few minutes acidification down to pH 6.8 and formation of a crystalline material suitable for X-ray analysis. The crystals contained carbamate groups bound to

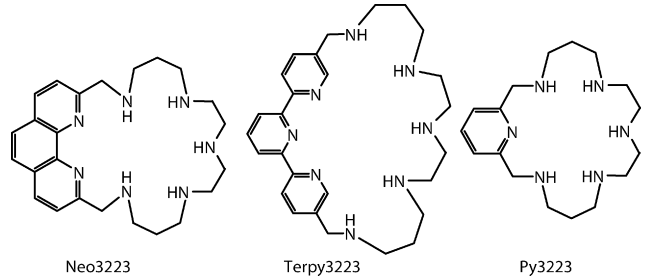

Chart 19.

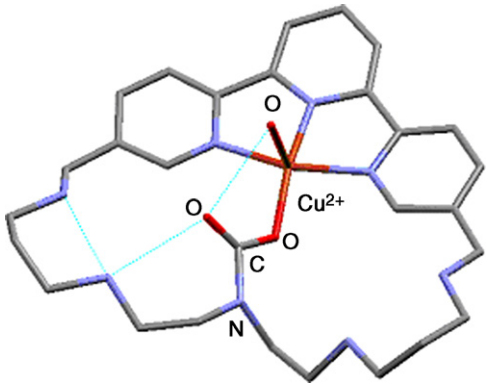

Fig. 37. Schematic representation of the cation $[CuH_2(H_{-1}Terpy3223)(carbamate)]^{3+}$ cation [171].

the Cu^{2+} metal ion and further stabilized by an intramolecular hydrogen bond network that involved amino and ammonium groups of the bridge and the water molecule coordinated to the metal ion (Fig. 37).

When the Cu^{2+}:Terpy3223 molar ratio was 2:1 instead of 1:1, carbon dioxide reacted with the binuclear centre as a η,η′-bridging ligand. Potentiometric studies proved that the species precipitating at neutral pH were among those existing in aqueous solution at this pH. Interestingly enough, this behavior was not reproduced when terpyridine was either removed from the ligand or replaced by a pyridine unit (Py32223, Chart 19). When phenanthroline (Neo3223, Chart 19) was used instead of terpyridine (indications of carbamate formations were detected although the behavior was not as remarkable as in the case of Terpy3223. The assistance of the metal can also be provided by other metal ions. Potentiometric, NMR and UV–vis spectroscopic studies have proved that Zn^{2+} plays a similar role to Cu^{2+} [172].

7.2. Phosphatase mimics

Binuclear Zn^{2+} complexes with synthetic ligands can be used as simple model systems for hydrolytic enzymes such as alkaline phosphatases, phospholipase C and the Klenow fragment of DNA polymerase I, since the bridging coordination of the phosphate groups gives a fundamental contribution to substrate activation. To this purpose, we analyzed the ability of the binuclear Zn^{2+} complex of the polyoxa-polyaza-macrocycle N_6O_4 to promote the hydrolysis of phosphate esters and compared it with the ability of the mononuclear complex with the N_3O_2 ligand, in order to evidence the cooperative effect of the two metal centers in close proximity [173].

Indeed, the hydroxo complexes $[Zn_2(N_6O_4)(OH)_2]^{2+}$ and $[Zn_2(N_3O_2)OH]^{+}$ promote the hydrolysis of bis(*p*-nitrophenyl) phosphate (BNP), the binuclear complex giving rise to a 10-fold enhancement of the rate of hydrolysis with respect to the mononuclear one. Although potentiometric measurements evidenced that BNP does not form stable complexes with any of the two metallo-receptor species, the crystal structure of the complex $[Zn_2(N_6O_4)(\mu\text{-}PP)_2(MeOH)_2](ClO_4)_2$ containing the anion diphenyl-phosphate (PP) (Fig. 38), analogous to BNP,

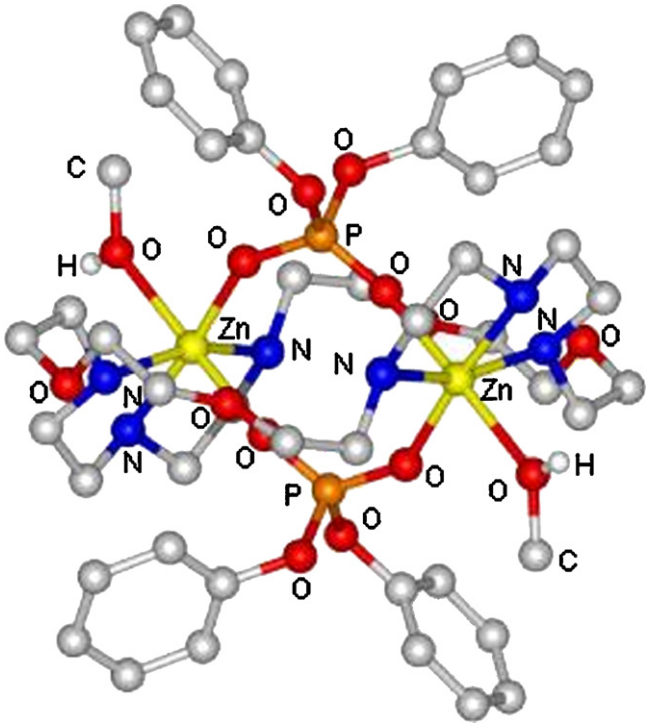

Fig. 38. Crystal structure of the complex cation $[Zn_2(N_6O_4)(\mu\text{-}PP)_2(MeOH)_2]^{2+}$ containing two diphenyl phosphate (PP^{-}) anions. Reprinted with permission from Ref. [173]. Copyright 2005 American Chemical Society.

suggested that two Zn^{2+} ions in $[Zn_2(N_6O_4)(OH)_2]^{2+}$ work cooperatively in the hydrolytic mechanism (Fig. 39) through a bridging interaction of the phosphate group to the two electrophilic metal centers and a simultaneous nucleophilic attack of a Zn–OH function to the substrate.

A similar study was also performed with the two related ligands N_7O_4 and N_8O_4, containing, respectively, one and two additional amine groups with respect to N_6O_4 (Chart 20) [174]. Also in this case the dihydroxo complexes $[Zn_2(L)(OH)_2]^{2+}$ (L = N_7O_4 and N_8O_4) are active in promoting the hydrolysis of BNP but the rate of the process decreases as the size of the macrocycle and the number of amine groups increase. An associative mechanism in which the anionic substrate approaches the binuclear dihydroxo complex and the phosphate group start

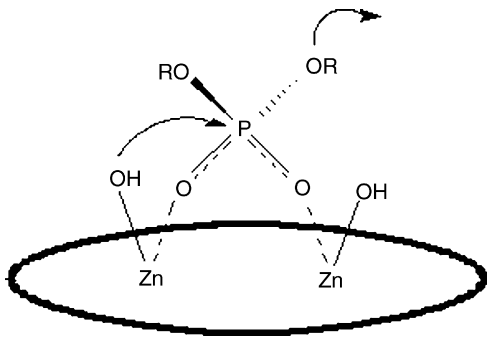

Fig. 39. Suggested mechanism for the hydrolysis of BNP anion by $[Zn_2(N_6O_4)(OH)_2]^{2+}$. Reprinted with permission from Ref. [173]. Copyright 2005 American Chemical Society.

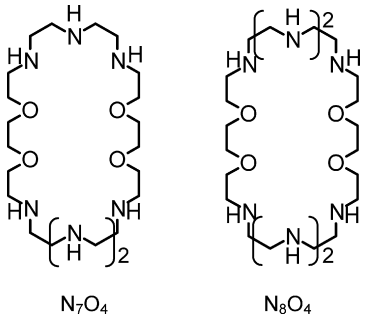

Chart 20.

associating with the two metal centers through bridging coordination was proposed also for N_7O_4 and N_8O_4.

Potentiometric measurements showed that the mono(*p*-nitrophenyl) phosphate produced in the hydrolytic processes forms weak complexes with $[Zn_2(N_6O_4)(OH)_2]^{2+}$ and $[Zn_2(N_7O_4)(OH)_2]^{2+}$, but not with $[Zn_2(N_8O_4)(OH)_2]^{2+}$ [174].

Insertion of aromatic groups into the skeleton of large macrocyclic ligands leads to the formation of binuclear Zn^{2+} with enhanced ability in BNP hydrolysis due to a more efficient association of the complex with the anionic substrate via π-stacking interactions. This is the case of the zinc(II) complexes of the ligands bipy2222 and 2bipy22,22 (Chart 21) [175]. In contrast to the previous polyoxa-polyaza-macrocycles, ternary complexes of bipy2222, and respectively, of 2bipy22,22, with Zn(II) and BNP, of 1:2:1 and 1:2:2 ligand/Zn(II)/BNP stoichiometry, are enough stable to be observed in solution.

The formation of π-stacking interactions between the anionic substrate and the metallo-receptor is nicely visualized by the crystal structure of the $[Zn_2(2bipy22,22)(BNP)_2]^{2+}$ cation (Fig. 40) showing the face-to-face pairing between a nitrophenyl group of BNP and an aromatic group of a dipyridine moiety.

However, the ability to form π-stacking interactions showed by such ligands leads also to the formation of stable complexes with the products of BNP hydrolysis, in particular with mono(*p*-nitrophenyl) phosphate (MNP) dianion, which displays stronger association with the complexes than the less charged BNP monoanion. Consequently, the binding of MNP inhibits the catalytic properties of the complexes.

Similar results were obtained with the mononuclear Zn(II) complex of the small macrocycle bipy22 (Chart 21) in comparison to the analogous complexes with ligand not containing aromatic groups [175].

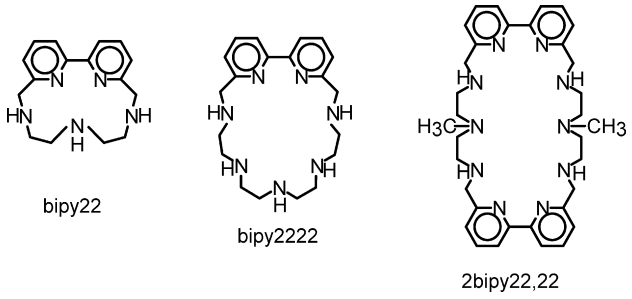

Chart 21.

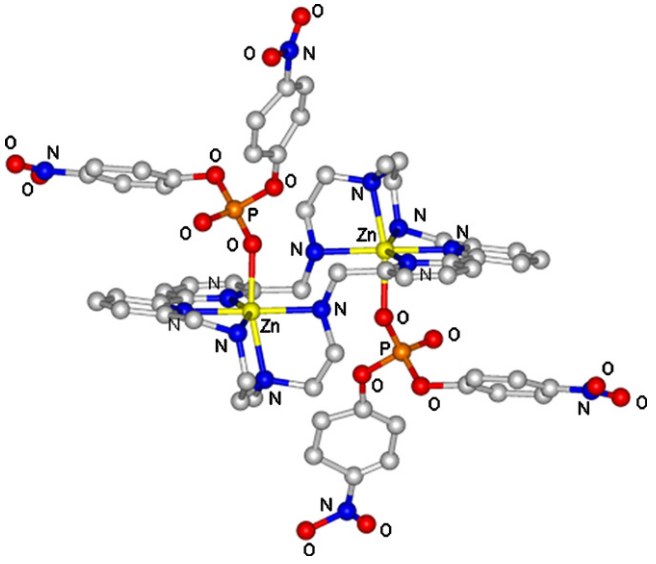

Fig. 40. Crystal structure of the $[Zn_2(2bipy22,22)(BNP)_2]^{2+}$ cation containing two bis(*p*-nitrophenyl) phosphate (BNP) coordinated anions [175].

Another interesting example showing the influence of aromatic groups, inserted in the ligand structure, in promoting BNP hydrolysis was recently obtained by comparing the properties of the three ligands L33233, *m*B33233 (Chart 13) and Neo3223 (Chart 19) [176]. Such ligands present similar binding properties towards Zn^{2+}, giving rise to the formation of mono- and binuclear complexes, in aqueous solution, which form mono- and di-hydroxo species. These hydroxo complexes promote BNP hydrolysis. Despite their similarity, these complexes display quite different ability in the activation of BMP. While the binuclear Zn^{2+} complexes with open L33233 and *m*B33233 (Chart 13) show hydrolytic activity similar to those of complexes with aliphatic ligands, the binuclear complex with Neo3223, containing a large hydrophobic heteroaromatic moiety, gives rise to a remarkably higher rate enhancement being one of the most active synthetic dizinc complexes in BNP hydrolysis. Also in this case a synergistic role in BNP binding of phenanthroline, which can favor the association with the substrate via π-stacking interaction and hydrophobic effects, and of the metal centers, which act cooperatively in substrate binding, has been suggested to rationalize the high activation of BNP.

7.3. Interaction with dicarboxylate anions

The ditopic macrocyclic receptor $Ph_2Pip_4Me_2N_{10}$ forms dinuclear Cu^{2+} complexes with coordinatively unsaturated sites (Chart 22). Due to the presence of the reinforcing piperazine rings $Ph_2Pip_4Me_2N_{10}$ is a quite rigid receptor that will have a fixed distance between the coordination centers. This characteristic was used for discriminating between long and short α,ω-dicarboxylates [177].

The five carbon long hydrocarbon chain of pimelic acid seemed to be appropriate for permitting a non-stressed bridging coordination of the dianion between both metal sites as shown by the crystal structure collected in Fig. 41.

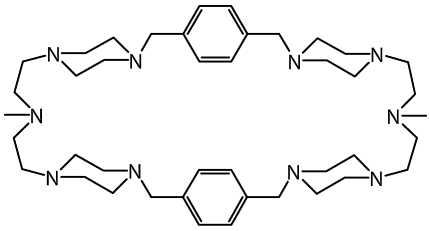

$Ph_2Pip_4Me_2N_{10}$

Chart 22.

In this system a clear switch from supramolecular interaction mode (mode A in Fig. 42) of the carboxylate with the extensively protonated demetallated macrocycle to coordinative interactions (mode C in Fig. 42) with the dinuclear metal complex going through a mixed supramolecular/coordinative mode (mode B in Fig. 42) in which both situations are present when the mononuclear species prevailed in solution, occurred on increasing the pH.

7.4. Interaction with amino acid species

Recently some of us have reported on several pyrazole containing macrocycles (Chart 23) that exhibited a significant interaction for L-glutamate and L-aspartate in pure water with some selectivity for L-glutamate over L-aspartate at the physiological pH value of 7.4 [178]. In particular, the macrocycle having benzylated the central nitrogen of the chain shows a remarkable interaction with L-glutamate.

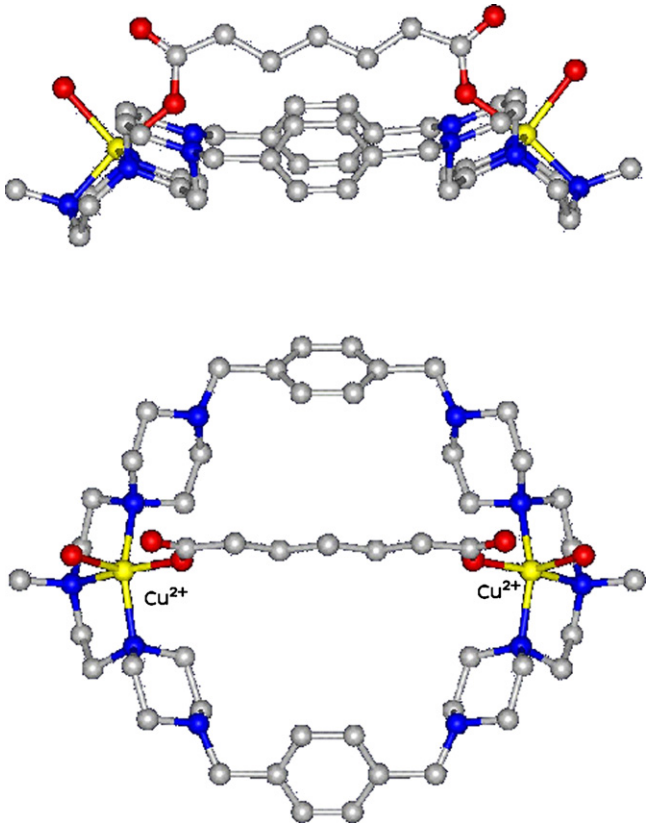

Fig. 41. Ball and stick representation of the crystal structure of the $[Cu_2(Ph_2Pip_4Me_2N_{10})(H_2O)(pim)]^{2+}$ cation. Reprinted with permission from Ref. [177]. Copyright 2005 American Chemical Society.

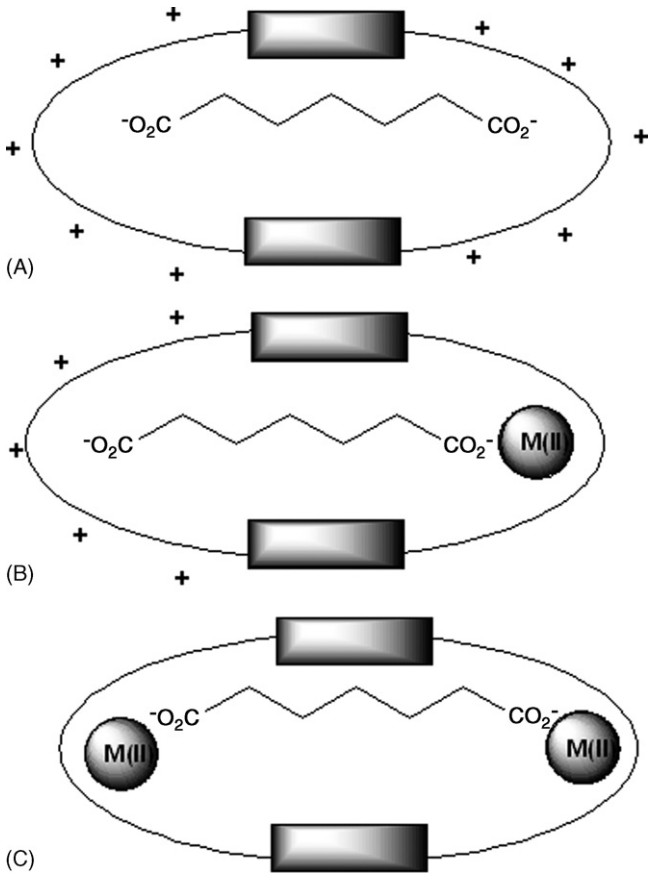

Fig. 42. Sketch of the interactions modes operating as a function of pH in the system Cu^{2+}–$Ph_2Pip_4Me_2N_{10}$-pim [177].

NMR studies supported the participation of π-cation interactions in this particular interaction. This was consistent with the higher interaction observed for $bn_2pz_2N_6$ with respect to pz_2N_6. However, the introduction of two metal ions in the ditopic ligand was not effective for coordinating amino acid species. The reason seems to be that there are enough donor atoms in the

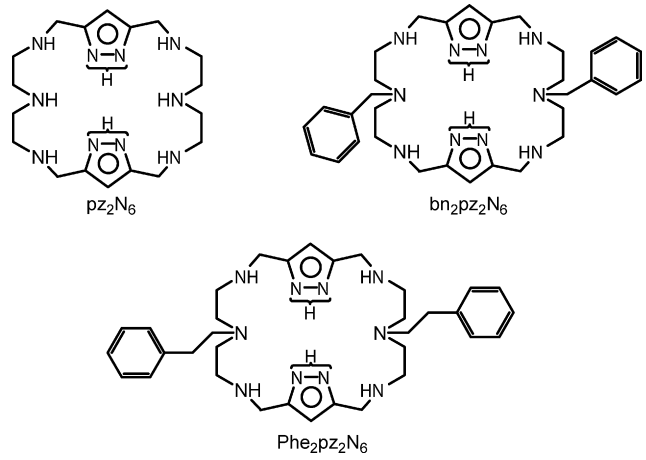

pz_2N_6 $bn_2pz_2N_6$ $Phe_2pz_2N_6$

Chart 23.

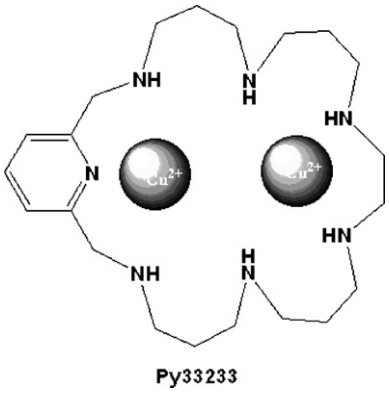

Py33233

Chart 24.

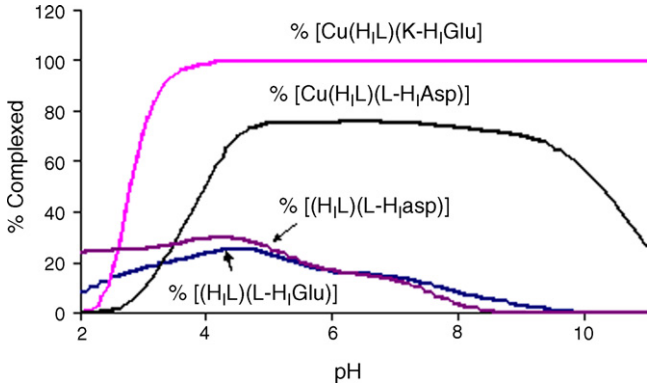

Fig. 43. Plot of the percentages of complexed glutamate and aspartate by Py33233 as free receptor and as Cu^{2+} complex [180]. Reproduced by permission of The Royal Society of Chemistry.

macrocycle for fulfilling the coordination spheres of the metal ions and therefore the affinity for the amino acids is rather low. Formation of ternary complexes was however observed in the case of the neurotransmitter dopamine. The catechol moiety competes effectively with the nitrogen atoms of the macrocycle and can remove those at the axial positions which are the ones forming the weaker bonds [179].

Therefore, Cu^{2+} complexes with lower coordination numbers are required for being effective amino acid receptors. The binuclear Cu^{2+} complex of the polyamine Py33233 (Chart 24) seems to be a good candidate since it has only seven nitrogens for coordinating the two metal ions.

Potentiometric studies carried out on the binary systems L-Glu-Py33233 and L-Asp-Py33233 show a moderate degree of interaction between the charged receptor and the amino acid species although there is no discrimination between the two amino acids [180]. When the receptor is the dinuclear Cu^{2+} complex there is a much larger interaction with both amino acids which is accompanied by a clear selectivity for L-Glu over L-Asp as shown by the percentages of amino acid complexation (Fig. 43). Paramagnetic NMR studies have indicated that L-glutamate coordinates both metal ions as a bridging ligand through its carboxylate groups.

This selective discrimination has been used for building up a modified electrode able to selectively detect L-glutamate.

7.5. Interaction of metal complexes with nucleotides and nucleic acids

The last paragraph in this section will concern interaction of polyamine metal complexes with nucleotides and nucleic acids. The potentiometric studies of the ternary systems M–polyamine (L)–nucleotide (A) require from a previous knowledge of the binary systems involved. First, the protonation constants of the polyamine and of the nucleotides should be known. Secondly the species forming in the binary system M–L, M–A and L–A should be established and their stability constants determined under the same experimental conditions than the ones used for the study of the ternary systems. As an example we will consider the system Cu^{2+}-4,7,10,13-tetrazatridecane-1,16-diamine (L32223)-AMP (A) (see Chart 25) [181].

In the binary systems L32223(L)-AMP (A) formation of species $[H_q(L3223)(AMP)]^{(q-2)+}$ with protonation degrees varying from $q=3$ to 8 were observed. On the other hand, 32223 forms with Cu^{2+} complexes of 1:1 and 2:1 metal ligand stoichiometries are formed. The insertion of all these data, together with the protonation constants of the polyamine, AMP and the formation constants of Cu^{2+}-AMP as known parameters in the titrations performed for the ternary systems in which different Cu^{2+}-L32223-AMP molar ratios were used gave as a result the formation of mixed species of stoichiometries $[CuH_rL(AMP)]^{r+}$ with r varying from 4 to 0 and binuclear ones $[Cu_2H_rL(AMP)]^{(2+r)+}$ with r between +1 and −1. Distribution diagrams for this system showed the prevalence of the ternary complexes throughout the whole pH range of study.

Some of us have recently shown that the presence of a not-coordinated metal ion can play a decisive role in the activation of ATP cleavage in the presence of metal complexes forming ternary complexes with the nucleotide [181]. This is the case of the protonated mononucler Zn^{2+} complexes with the ligand Terpy2222 (Chart 26) [182]. This ligand forms both mono- and binuclear Zn^{2+} complexes depending on the metal-to-ligand molar ratio and the solution pH. The first Zn^{2+} ion interacting with the ligand binds to the terpyridine moiety while the second one occupies the polyamine chain. Both mono- and binuclear complexes form stable ternary complexes with ATP but

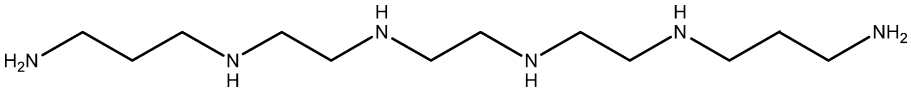

L32223

Chart 25.

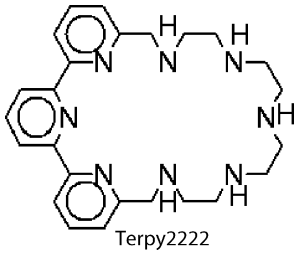

Chart 26.

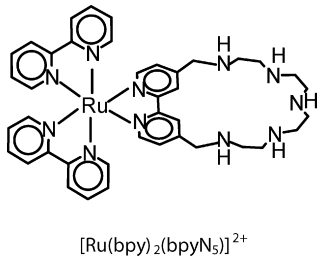

Chart 27.

do not show any significant ability in ATP hydrolysis. Only the tetraprotonated $[ZnH_4(Terpy2222)(ATP)]^{2+}$ species in presence of not-coordinated Zn^{2+} ions gives rise to fast ATP cleavage to produce ADP and phosphate. The analysis of the time dependence of the ^{31}P NMR spectra recorded at different pH's clearly showed that only the tetraprotonated species is able to activate ATP hydrolysis, while both three- and penta-protonated ones are completely inactive. The hydrolytic process proceeds through the formation of a phosphoramidate (PN) intermediate which is then fast hydrolyzed to hydrogen-phosphate. The hydrolysis rate ($k_{OBS} = 3.2 \times 10^{-2}$ min^{-1} at pH 4 is among the highest observed for ATP dephosphorylation promoted by polyammonium receptors.

The fact that ATP cleavage takes place only in the presence of a "second" Zn(II) ion with second order kinetic suggests that the transition state could be stabilized by this metal ion, probably through coordination of the metal to unprotonated amine groups of the macrocycle and to the γ-phosphate of ATP, leading to a higher activation of the γ-phosphorus to the nucleophilic attack. At the same time, the PN intermediate could be stabilized via coordination to the metal, accounting for the observed relatively high percentage of PN accumulating during the cleavage process.

The present system, therefore, represents a unique case of ATP dephosphorylation promoted by the simultaneous action of a metal complex, which is used essentially to anchor the anionic substrate, and of a second metal, which acts as cofactor, assisting the phosphoryl transfer from ATP to an amine group of the receptor.

Sometimes, although formation of binuclear complexes is not observed in the binary Cu^{2+}–L systems it can be induced by the presence of the second ligand. For instance, in the case of the polyamine N2222N, with each of its two ends functionalized with a naphthylmethyl fragment (Chart 16), melting point measurements showed that addition of a second Cu^{2+} ion had a dramatic influence on the interaction with nucleic acids [153]. In this case N2222N alone does not form binuclear Cu^{2+} complexes however, the presence of AMP as secondary ligand will help the formation of the mixed binuclear species. This will explain the large allosteric effect observed in the interaction of nucleic acids upon addition of the second mole of metal.

We have reported above that ligands Neo22, Neo222, Neo2222 (Chart 8), Tris-cyclen and Tris-N_3O (Chart 6) lead to strong stabilization of double-stranded nucleic acids, with preference for DNA over RNA. Similar stabilization effects were also found for Cu^{2+} complexes of these ligands, but with reversed trend in favor of RNA [154,155]. The trinuclear complexes of Tris-cyclen and Tris-N_3O gives rise to stronger stabilization with respect to complexes of the other three ligands, accounting for the interaction of all three metal centers with the nuclei acid. Nevertheless, as far as the nuclease activity of these metal complexes is considered we observed that the complexes with Tris-cyclen and Tris-N_3O have low efficiency in promoting DNA cleavage in contrast to the effective action of displayed by the complexes with the ligands containing phenanthroline moieties and, in particular, by the mononuclear complex with Neo2222.

7.6. A photocatalytic system

The anion binding ability of the protonated forms of $[Ru(bpy)_2(bpyN_5)]^{2+}$ coupled with the photoinduced energy and electron transfer properties of the $[Ru(bpy)_3]^{2+}$ complex core make $[Ru(bpy)_2(bpyN_5)]^{2+}$ (Chart 27) a potential catalyst for many light-induced reactions involving anionic substrates hosted into the receptor cavity.

For instance $[Ru(bpy)_2(bpyN_5)]^{2+}$ is effective in promoting the photocatalytic oxidation of iodide to iodine by O_2 promoted by light absorption [183]. The absorption spectra of solutions containing $[Ru(bpy)_2(bpyN_5)]^{2+}$ and I^- are the summation of the spectra of both components, and thus there is no evidence for the formation of ion-pair charge transfer. However, the fluorescence emission of compound $[Ru(bpy)_2(bpyN_5)]^{2+}$ is partially quenched in the presence of I^-. When air equilibrated solutions of $[Ru(bpy)_2(bpyN_5)]^{2+}$ in the presence of I^-, at pH 4.3, are irradiated at 436 nm, formation of I_3^- is immediately observed by the increasing of its characteristic absorption band centered at 350 nm, while saturation of the solutions with dioxygen increases the quantum yield by ca. five-fold. It is interesting to note that no catalytic activity was detected for the parent compound $[Ru(bpy)_3]^{2+}$ irradiated in the presence of I^-.

These results can be accounted for by the processes displayed in Fig. 44. Excitation of compound $[Ru(bpy)_2(bpyN_5)]^{2+}$ in the MLCT band allows the transfer of one electron from I^- to the Ru(II) complex, leading to the formation of an iodine radical and to a Ru(II) complex with a reduced dipyridine radical anion. The iodine radical gives I_3^- as a final product by a sequence of well-known reactions [184–186]. The cycle is completed by reoxidation of the dipyridine radical by dioxygen.

In the case of $H_4\mathbf{L}^{6+}$, the net reaction can be accounted for by the equations

$$2[Ru^{II}(bpy)_2(H_4bpyN_5))]^{6+} + 3I^- \xrightarrow{h\nu} 2[Ru^{II}(bpy^-)(bpy)(H_4(bpyN_5))]^{5+} + I_3^-$$

which is thermodynamically favorable by 0.3 eV.

As demonstrated by the inertness of the parent $[Ru(bpy)_3]^{2+}$ compound, the existence of the positively charged macrocyclic receptor moiety is an indispensable requirement to fix the iodine in a position close to the metal, in order to allow the electron transfer process.

8. Influences of anions in crystalline growth

We would like to conclude this review with an example of the role played by anionic species in determining the arrangement of crystal structures. Recently, some of us studied the capacity of the ditopic cyclophane receptor 232*o*B*o*232 (**L**) (Chart 28) to interact with Cu(II) and Zn(II) in aqueous solution [187]. Along the course of that study, three new crystal structures were produced which correspond with the stoichiometric formulae $[H_4\mathbf{L}](ZnCl_4)_2{\cdot}2H_2O$ (**1**), $[Cu_2\mathbf{L}Cl_2](ClO_4)_2{\cdot}6H_2O$ (**2**) and $[Zn_2\mathbf{L}Cl_2](CF_3SO_3)_2{\cdot}0.6H_2O$ (**3**). In Fig. 44 are plotted views of the crystal packings of all three structures. The analysis of

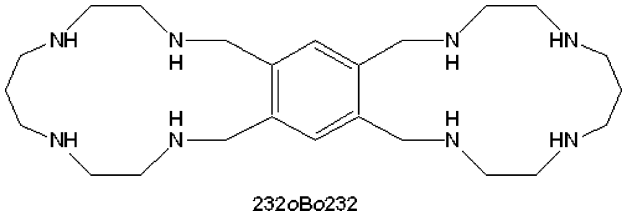

232oBo232

Chart 28.

the crystallographic data of the three crystal structures clearly shows that the overall architectures of the crystals are controlled by the anions present in the moiety, π–π-stacking interactions between the aromatic rings and hydrogen bonding interactions involving the anions and the water used as the solvent (Fig. 45).

Tetrahedral anions like $ZnCl_4^{2-}$ in (**1**) or ClO_4^- in (**2**) are encapsulated in the macrocyclic cleft of the butterfly-shaped macrocycle neutralizing the excess of charge and favoring a boat-conformation. This boat conformation favors on the other hand, π–π-stacking interaction between the aromatic rings of different macrocyclic units. On the contrary, large triflate anions, which have less charge density and cannot be included in the cavity, favor a chair disposition of the ditopic macrocycle so that the charged metal centers are disposed as far away as possible. In the case of crystal structure (**2**), a very particular 3D hydrogen bond network of pentamer and rhomboid units involving the coordi-

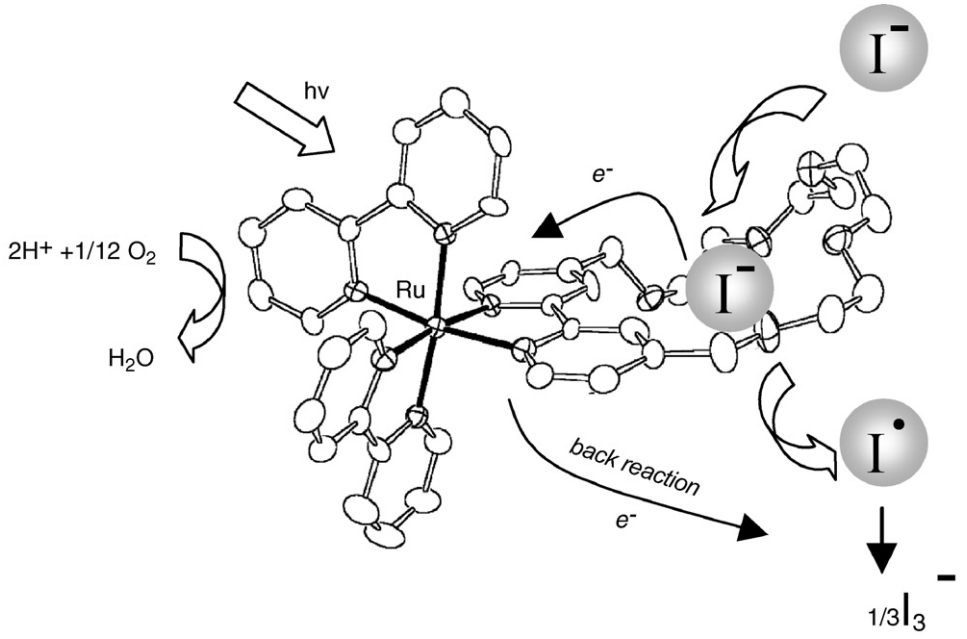

$$2\,[Ru^{II}(bpy)_2(H_4bpyN_5))]^{6+} + 3I^- \xrightarrow{h\nu} 2\,[Ru^{II}(bpy^-)(bpy)(H_4(bpyN_5))]^{5+} + I_3^-$$

$$2\,[Ru^{II}(bpy^-)(bpy)(H_4(bpyN_5))]^{5+} + \tfrac{1}{2}O_2 + 2H^+ \longrightarrow 2\,[Ru^{II}(bpy)_2(H_4bpyN_5))]^{6+} + H_2O$$

$$3I^- + \tfrac{1}{2}O_2 + 2H^+ \xrightarrow{h\nu} I_3^- + H_2O$$

Fig. 44. Photocatalytic cycle for the oxidation of iodide to iodine by dioxygen promoted by $[Ru(bpy)_2(bpyN_5)]^{2+}$. Reprinted with permission from Ref. [183]. Copyright 2005 American Chemical Society.

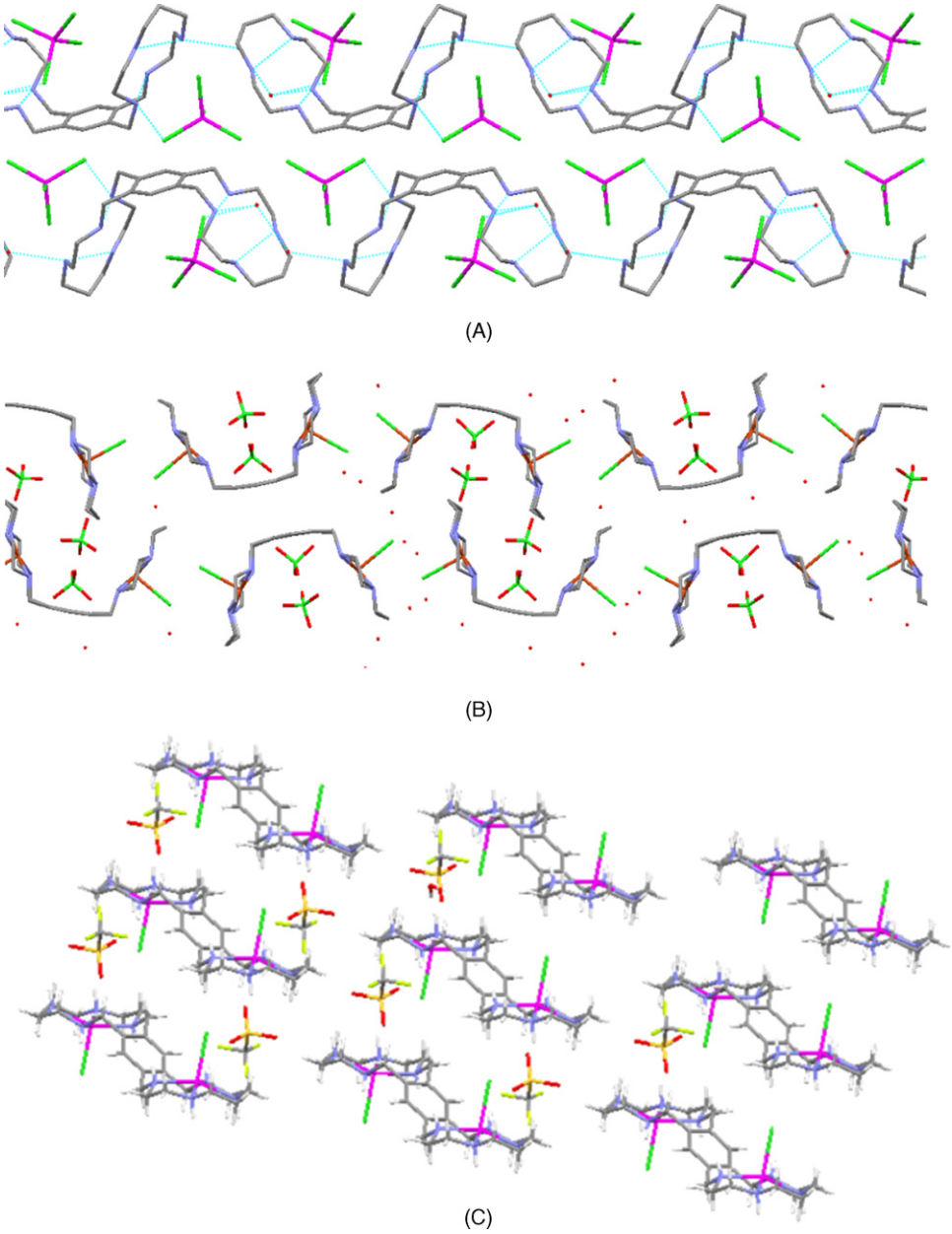

Fig. 45. Details of the crystal packing of structures (**1**) (A), (**2**) (B) and (**3**) (C) showing the effects of anions on the crystal arrangements. Dots stand for water molecule [187].

nated and free water molecules, coordinated chloride anions and perchlorate counter-anions was observed. The water molecules are placed in the channels formed between the macrocyclic units.

9. Conclusion and outlook

Although polyammonium cations were among the earliest class of compounds being explored as anion binders, their chemical versatility and their easy derivatization make them still to be one of the kinds of anion receptors most widely employed in the supramolecular chemistry of anions. In polyamines having high degrees of conformational freedom, rigidity and preorganization can be gained as a result of the own protonation process of the polyamine. Positive charges tend to locate far away from each other thereby influencing and reinforcing the receptor conformation. Precisely, the attraction between oppositely charged partners is the main driving force in anion coordination by polyammonium receptors. Such prime binding force can be modulated and tuned by weaker contributions among which hydrogen bonding plays an important role. Inclusion of aromatic moieties in the polyamine structure switches on new weaker forces such as π–π stacking between electron deficient and electron rich electronic clouds. Interaction can lead to supramolecular catalysis and activation. With the present review focusing on work mainly performed in our laboratories in the last years we have shown several examples concerning metallocyanide anions, car-

boxylate, phosphate as well as nucleotide and oligonucleotide interaction and activation. All this examples refer to pure water. Finally, gaining inspiration from the biological world we have shown the strong interrelation between classical coordination and anion coordination chemistry. Many metalloenzymes recognize and/or activates anionic species forming ternary complexes in which the target anionic species bind to a coordinatively unsaturated metal center. We have provided examples of abiotic systems reminiscent of enzyme centers with interesting anion recognition and catalytic behaviors.

Polyammonium receptors will continue to be at the core of anion recognition in the coming years and due to their tremendous chemical versatility will continue to offer new challenges to the scientists in the field. Many of these systems will make use of the chemical possibilities offered by the ensemble of metal ions and polyamine ligands.

Acknowledgements

The authors of the review would like to express their acknowledgement to all the colleagues and students who have actively participated in this project throughout the last years and whose names appear in the references. Financial support from the Spanish MEC and Generalitat Valencia and Italian MIUR is acknowledged.

References

[1] C.J. Pedersen, J. Am. Chem. Soc. 89 (1967) 7017.
[2] B. Dietrich, J.-M. Lehn, J.P. Sauvage, Tetrahedron Lett. 10 (1969) 2885.
[3] B. Dietrich, J.-M. Lehn, J.P. Sauvage, J. Blanzat, Tetrahedron 29 (1973) 1629.
[4] D.J. Cram, J.M. Cram, Science 183 (1974) 803.
[5] D.J. Cram, J.M. Cram, Acc. Chem. Res. 11 (1978) 8.
[6] J.-M. Lehn, Acc. Chem. Res. 11 (1978) 49.
[7] J.-M. Lehn, Angew. Chem., Int. Ed. Engl. 27 (1988) 89.
[8] J.-M. Lehn, Supramolecular Chemistry. Concepts and Perspectives, VCH, Weinheim, 1995.
[9] B. Dietrich, Pure Appl. Chem. 65 (1993) 1457.
[10] A. Bianchi, K. Bowman-James, E. García-España (Eds.), Supramolecular Chemistry of Anions, Wiley–VCH, New York, 1997.
[11] C.H. Park, H.E. Simmons, J. Am. Chem. Soc. 90 (1968) 2431.
[12] E. Graf, J.-M. Lehn, J. Am. Chem. Soc. 98 (1976) 6403.
[13] J.-M. Lehn, E. Sonveaux, A.K. Willard, J. Am. Chem. Soc. 100 (1978) 4914.
[14] B. Dietrich, M.W. Hosseini, J.-M. Lehn, R.B. Sessions, J. Am. Chem. Soc. 103 (1981) 1282.
[15] F. Peter, M. Gross, M.W. Hosseini, J.-M. Lehn, R.B. Sessions, J. Chem. Soc., Chem. Commun. 20 (1981) 1067.
[16] M.W. Hosseini, J.-M. Lehn, J. Am. Chem. Soc. 104 (1982) 3525.
[17] J.-P. Kintzinger, J.-M. Lehn, E. Kauffman, J.L. Dye, A.I. Popov, J. Am. Chem. Soc. 105 (1983) 7549.
[18] F. Peter, M. Gross, M.W. Hosseini, J.-M. Lehn, J. Electroanal. Chem. 144 (1983) 279.
[19] F.P. Schmidtchen, Angew. Chem., Int. Ed. Engl. Engl. 6 (1977) 720.
[20] (a) E. Kimura, A. Sakonaka, T. Yatsunami, M. Kodama, J. Am. Chem. Soc. 103 (1981) 3041;
(b) E. Kimura, Top. Curr. Chem. 128 (Biomimetic Bioorg. Chem.) (1985) 113.
[21] F.P. Schmidtchen, G. Muller, J. Chem. Soc., Chem. Commun. 16 (1984) 1115.
[22] C. Seel, A. Galan, J. De Mendoza, Top. Curr. Chem. 175 (1995) 101.
[23] P.A. Gale, Coord. Chem. Rev. 213 (2001) 79.
[24] P.D. Beer, E.J. Hayes, Coord. Chem. Rev. 240 (2003) 167.
[25] R. Vilar, Angew. Chem., Int. Ed. Engl. 42 (2003) 1460.
[26] J.M. Llinares, D. Powell, K. Bowman-James, Coord. Chem. Rev. 240 (2003) 57.
[27] S. Kubik, C. Reyheller, S. Stüwe, J. Inclusion Phenom. Mol. Recognit. Chem. 52 (2005) 137.
[28] Top. Curr. Chem. 255 (2005) (special issue in anion sensing).
[29] E. Martell, R.M. Smith, R.J. Motekaitis, NIST Critically Selected Stability Constants of Metal Complexes Database, NIST Standard Reference Database, Version 4, 1997.
[30] M. Fujita, Chem. Soc. Rev. 27 (1998) 417.
[31] S. Leininger, B. Olenyuk, P.J. Stang, Chem. Rev. 100 (2000) 853.
[32] M. Haj-Zaroubi, N.W. Mitzel, F.P. Schmidtchen, Angew. Chem., Int. Ed. Engl. 41 (2002) 104.
[33] A. Bencini, A. Bianchi, E. García-España, M. Micheloni, J.A. Ramírez, Coord. Chem. Rev. 188 (1999) 97.
[34] C. Nave, M.R. Truter, J. Chem. Soc. 96 (1974) 2351.
[35] M. Studer, A. Riesen, T.A. Kaden, Helv. Chim. Acta 72 (1989) 1253.
[36] M. Chadim, P. Díaz, E. García-España, J. Hodacova, P.C. Junk, J. Latorre, J.M. Llinares, C. Soriano, J. Zavada, New J. Chem. 27 (2003) 1132.
[37] A. Bianchi, S. Mangani, M. Micheloni, V. Nanini, P. Orioli, P. Paoletti, B. Seghi, Inorg. Chem. 24 (1985) 1182.
[38] A.P. Davis, J.J. Perry, R.P. Williams, J. Am. Chem. Soc. 119 (1997) 1793.
[39] S.-I. Sasaki, D. Citterio, S. Ozawa, K. Suzuki, J. Chem. Soc., Perkin Trans. 2 (2001) 2309.
[40] H. Ihm, S. Yun, H.G. Kim, J.K. Kim, K.S. Kim, Org. Lett. 4 (2002) 2897.
[41] S. Yun, H. Ihm, H.G. Kim, C.-W. Lee, B. Indrajit, K.S. Oh, Y.J. Gong, J.W. Lee, J. Yoon, H.C. Lee, K.S. Kim, J. Org. Chem. 68 (2003) 2467.
[42] K.J. Wallace, W.J. Belcher, D.R. Turner, K.F. Syed, J.W. Steed, J. Am. Chem. Soc. 125 (2003) 9699.
[43] Z. Yin, Y. Zhang, J. He, J.-P. Cheng, Tetrahedron 62 (2006) 765.
[44] M.T. Albelda, E. García-España, L. Gil, J.C. Lima, C. Lodeiro, J. Seixas de Melo, M.J. Melo, A.J. Parola, F. Pina, C. Soriano, J. Phys. Chem. B 107 (2003) 6573.
[45] N. Lomadze, H.-J. Schneider, M.T. Albelda, E. García-España, B. Verdejo, Org. Biomol. Chem. (2006).
[46] W. Peschke, F.P. Schmidtchen, Tetrahedron Lett. 36 (1995) 5155.
[47] E. García-España, M. Micheloni, P. Paoletti, A. Bianchi, Inorg. Chim. Acta Lett. 102 (1985) L9.
[48] A. Bianchi, E. García-España, S. Mangani, M. Micheloni, P. Orioli, P. Paoletti, J. Chem. Soc., Chem. Commun. 10 (1987) 729.
[49] A. Bencini, A. Bianchi, E. García-España, M. Giusti, S. Mangani, M. Micheloni, P. Orioli, P. Paoletti, Inorg. Chem. 26 (1987) 3902.
[50] A. Bencini, A. Bianchi, P. Dapporto, E. García-España, M. Micheloni, P. Paoletti, P. Paoli, J. Chem. Soc., Chem. Commun. (1990) 753.
[51] A. Bencini, A. Bianchi, M. Micheloni, P. Paoletti, P. Dapporto, P. Paoli, E. García-España, J. Inclusion Phenom. Mol. Recognit. Chem. 12 (1992) 291.
[52] A. Bencini, A. Bianchi, P. Dapporto, E. García-España, M. Micheloni, J.A. Ramírez, P. Paoletti, P. Paoli, Inorg. Chem. 31 (1992) 1902.
[53] J. Aragó, A. Bencini, A. Bianchi, A. Doménech, E. García-España, J. Chem. Soc., Dalton Trans. 2 (1992) 319.
[54] M.A. Bernardo, A.J. Parola, F. Pina, E. García-España, V. Marcelino, S.V. Luis, J.F. Miravet, J. Chem. Soc., Dalton Trans. 6 (1995) 993.
[55] J. Aragó, A. Bencini, A. Bianchi, E. García-España, M. Micheloni, P. Paoletti, J.A. Ramírez, P. Paoli, Inorg. Chem. 30 (1991) 1843.
[56] M.F. Manfrin, N. Sabbatini, L. Moggi, V. Balzani, M.W. Hosseini, J.-M. Lehn, J. Chem. Soc., Chem. Commun. 8 (1984) 555.
[57] M.F. Manfrin, L. Moggi, V. Castelvetro, V. Balzani, M.W. Hosseini, J.-M. Lehn, J. Am. Chem. Soc. 107 (1985) 6888.
[58] F. Pina, L. Moggi, M.F. Manfrin, V. Balzani, M.W. Hosseini, J.-M. Lehn, Gazz. Chim. Ital. 119 (1989) 65.
[59] M.A. Bernardo, J.A. Guerrero, E. García-España, S.V. Luis, J.M. Llinares, F. Pina, J.A. Ramírez, C. Soriano, J. Chem. Soc., Perkin Trans. 2 (1996) 2335.

[60] L. Rodriguez, S. Alves, J.C. Lima, A.J. Parola, F. Pina, C. Soriano, M.T. Albelda, E. García-España, J. Photochem. Photobiol. A 159 (2003) 253.
[61] P. Arranz, M.T. Albelda, E. García-España, J.C. Lima, C. Lodeiro, J.S. De Melo, A.J. Parola, F. Pina, J. Chem. Soc., Dalton Trans. (2002) 3024.
[62] J.H. Yoe, A.L. Jones, Ind. Eng. Chem. Anal. Ed. 16 (1944) 11.
[63] A. Bianchi, A. Doménech, E. García-España, S.V. Luis, Anal. Chem. 65 (1993) 3137.
[64] A. Bianchi, M. Micheloni, P. Paoletti, Inorg. Chim. Acta 151 (1988) 266.
[65] A. Bianchi, M. Micheloni, P. Orioli, P. Paoletti, S. Mangani, Inorg. Chim. Acta 146 (1988) 153.
[66] B. Dietrich, J.-M. Lehn, C. Pascard, E. Sonveaux, Helv. Chim. Acta 67 (1984) 91.
[67] M.W. Hosseini, J.-M. Lehn, Helv. Chim. Acta 69 (1986) 587.
[68] F.P. Schmidtchen, A. Gleik, A. Schummer, Pure Appl. Chem. 61 (1989) 1335.
[69] (a) R.J. Fitzmaurice, G.M. Kyne, D. Douheret, J.D. Kilburn, J. Chem. Soc., Perkin Trans. 1 (2002) 841;
(b) C. De Stefano, O. Giuffrè, S. Sanmartano, J. Chem. Soc., Faraday Trans. 94 (1998) 2395;
(c) A. De Robertis, C. De Stefano, C. Foti, S. Sammartano, A. Gianguzza, J. Chem. Soc., Faraday Trans. 91 (1995) 1619.
[70] J.L. Sessler, D. An, W.-S. Cho, V. Lynch, J. Am. Chem. Soc. (Commun.) 125 (2003) 13646.
[71] F. Sancenón, R. Martinez-Manez, M.A. Miranda, M.-J. Segui, J. Soto, Angew. Chem., Int. Ed. Engl. 42 (2003) 647.
[72] M.W. Hosseini, Coord. Chem. Rev. 240 (2003) 157.
[73] J. Nelson, M. Nieuwenhuyzen, I. Pal, R.M. Town, Dalton Trans. 2 (2004) 229.
[74] X. Cui, R. Delgado, H.M. Carapuca, M.G.B. Drew, V. Felix, Dalton Trans. 20 (2005) 3297.
[75] L. Fabbrizzi, F. Foti, A. Taglietti, Org. Lett. 7 (2005) 2603.
[76] A. Bencini, A. Bianchi, M.I. Burguete, E. García-España, S.V. Luis, J.A. Ramírez, J. Am. Chem. Soc. 114 (1992) 1919.
[77] A. Bencini, A. Bianchi, M.I. Burguete, P. Dapporto, A. Doménech, E. García-España, S.V. Luis, P. Paoli, J.A. Ramírez, J. Chem. Soc., Perkin Trans. 2 (1994) 569.
[78] A. Bianchi, E. García-España, J. Chem. Educ. 76 (1999) 1727.
[79] M.T. Albelda, M.A. Bernardo, E. García-España, M.-L. Godino, S.V. Luis, M.J. Melo, F. Pina, C. Soriano, J. Chem. Soc., Perkin Trans. 2 (1999) 2545.
[80] J. Hodacova, M. Chadim, J. Závada, J. Aguilar, E. García-España, S.V. Luis, J.F. Miravet, J. Org. Chem. 70 (2005) 2042.
[81] C. Bazzicalupi, A. Bencini, A. Bianchi, L. Borsari, C. Giorgi, B. Valtancoli, C. Anda, A. Llobet, J. Org. Chem. 70 (2005) 4257.
[82] H. Lueke, F.A. Quiocho, Nature 347 (1990) 402.
[83] J.J. He, F.A. Quiocho, Science 251 (1991) 1497.
[84] J.W. Pflugrath, F.A. Quiocho, Nature 314 (1985) 257.
[85] J.W. Pflugrath, F.A. Quiocho, J. Mol. Biol. 200 (1988) 163.
[86] B. Dietrich, T.M. Fyles, J.-M. Lehn, L.G. Pease, D.L. Fyles, J. Chem. Soc., Chem. Commun. (1978) 934.
[87] E. Kimura, M. Kodama, T. Yatsunami, J. Am. Chem. Soc. 104 (1982) 3182.
[88] R.I. Gelb, L.B. Schwartz, L.J. Zompa, Inorg. Chem. 25 (1986) 1527.
[89] (a) M.W. Hosseini, J.-M. Lehn, Helv. Chim. Acta 71 (1988) 749;
(b) E. Kimura, Y. Kuramoto, T. Koike, H. Fujioka, M. Kodama, J. Org. Chem. 55 (1990) 42.
[90] A. Bencini, A. Bianchi, M.I. Burguete, A. Doménech, E. García-España, S.V. Luis, M.A. Niño, J.A. Ramírez, J. Chem. Soc., Perkin Trans. 2 (1991) 1445.
[91] A. Bencini, A. Bianchi, E. García-España, E.C. Scott, L. Morales, B. Wang, T. Deffo, F. Takusagawa, M.P. Mertes, K.B. Mertes, P. Paoletti, Bioorg. Chem. 20 (1992) 8.
[92] A. Andrés, J. Aragó, A. Bencini, A. Bianchi, A. Doménech, V. Fusi, E. García-España, P. Paoletti, J.A. Ramírez, Inorg. Chem. 32 (1993) 3418.
[93] A.W. Czarnik, Acc. Chem. Res. 27 (1994) 302.
[94] Q. Lu, R.J. Motekaitis, J.J. Reibenspies, A.E. Martell, Inorg. Chem. 34 (1995) 4958.
[95] Q. Lu, J.J. Reibenspies, A.E. Martell, R.J. Motekaitis, Inorg. Chem. 35 (1996) 2630.
[96] D.A. Nation, J. Reibenspies, A.E. Martell, Inorg. Chem. 35 (1996) 4597.
[97] A. Bencini, A. Bianchi, C. Giorgi, P. Paoletti, B. Valtancoli, E. García-España, J.M. Llinares, J.A. Ramírez, Inorg. Chem. 35 (1996) 1114.
[98] J.B. English, A.E. Martell, R.J. Motekaitis, I. Murase, Inorg. Chim. Acta 258 (1997) 183.
[99] C. Bazzicalupi, A. Bencini, E. Berni, A. Bianchi, P. Fornasari, C. Giorgi, A. Masotti, P. Paoletti, B. Valtancoli, J. Phys. Org. Chem. 14 (2001) 432.
[100] T. Clifford, A. Danby, J.M. Llinares, S. Mason, N.W. Alcock, D. Powell, J.A. Aguilar, E. García-España, K. Bowman-James, Inorg. Chem. 40 (2001) 4710.
[101] V. McKee, J. Nelson, R.M. Town, Chem. Soc. Rev. 32 (2003) 309.
[102] M.T. Albelda, J.C. Frias, E. García-España, S.V. Luis, Org. Biol. Chem. 2 (2004) 816.
[103] C. Bazzicalupi, A. Bencini, A. Bianchi, M. Cecchi, B. Escuder, V. Fusi, E. García-España, C. Giorgi, S.V. Luis, G. Maccagni, V. Marcelino, P. Paoletti, B. Valtancoli, J. Am. Chem. Soc. 121 (1999) 6807.
[104] P. Arranz, A. Bencini, A. Bianchi, P. Díaz, E. García-España, C. Giorgi, S.V. Luis, M. Querol, B. Valtancoli, J. Chem. Soc., Perkin Trans. 2 (2001) 1765.
[105] C. Anda, A. Bencini, E. Berni, A. Bianchi, P. Fornasari, A. Llobet, C. Giorni, P. Paletti, B. Valtancoli, Inorg. Chim. Acta 356 (2003) 167.
[106] M.W. Hosseini, J.-M. Lehn, M.P. Mertes, Helv. Chim. Acta 66 (1983) 2454.
[107] M.W. Hosseini, J.-M. Lehn, M.P. Mertes, Helv. Chim. Acta 68 (1985) 818.
[108] M.W. Hosseini, J.-M. Lehn, J. Chem. Soc., Chem. Commun. (1985) 1155.
[109] M.W. Hosseini, J.-M. Lehn, L. Maggiora, K.B. Mertes, M.P. Mertes, J. Am. Chem. Soc. 109 (1987) 537.
[110] P.G. Yohannes, K.E. Plute, M.P. Mertes, K.B. Mertes, Inorg. Chem. 26 (1987) 1751.
[111] M.W. Hosseini, J.-M. Lehn, J. Am. Chem. Soc. 109 (1987) 7047.
[112] H. Jahansouz, Z. Jiang, R.H. Himes, M.P. Mertes, K.B. Mertes, J. Am. Chem. Soc. 107 (1985) 8288.
[113] R.C. Bethel, G. Lowe, M.W. Hosseini, J.-M. Lehn, Bioorg. Chem. 16 (1988) 418.
[114] G.M. Blackburn, G.R.J. Thatcher, M.W. Hosseini, J.-M. Lehn, Tetrahedron Lett. 28 (1987) 2779.
[115] Z. Jiang, P. Chalabi, K.B. Mertes, H. Jahansouz, R.H. Himes, M.P. Mertes, Bioorg. Chem. 17 (1989) 313.
[116] A. Andrés, C. Bazzicalupi, A. Bencini, A. Bianchi, V. Fusi, E. García-España, C. Giorgi, N. Nardi, P. Paoletti, J.A. Ramírez, B. Valtancoli, J. Chem. Soc., Perkin Trans. 2 (1994) 2367.
[117] C. Bazzicalupi, A. Bencini, A. Bianchi, V. Fedi, V. Fusi, C. Giorgi, P. Paoletti, L. Tei, B. Valtancoli, J. Chem. Soc., Dalton Trans. 7 (1999) 1101.
[118] C. Bazzicalupi, A. Bencini, A. Bianchi, V. Fusi, C. Giorgi, A. Granchi, P. Paoletti, B. Valtancoli, J. Chem. Soc., Perkin Trans. 2 (1997) 775.
[119] C. Bazzicalupi, A. Bencini, A. Bianchi, V. Fusi, C. Giorgi, P. Paoletti, A. Stefani, B. Valtancoli, J. Chem. Soc., Perkin Trans. 2 (1995) 275.
[120] M.W. Hosseini, A.J. Blacker, J.-M. Lehn, J. Chem. Soc., Chem. Commun. (1988) 596.
[121] M.W. Hosseini, A.J. Blacker, J.-M. Lehn, J. Am. Chem. Soc. 112 (1990) 3896.
[122] A.V. Elissev, H.-J. Schneider, J. Am. Chem. Soc. 116 (1994) 6081.
[123] J. Aguilar, E. García-España, J.A. Guerrero, S.V. Luis, J.M. Llinares, J.F. Miravet, J.A. Ramírez, C. Soriano, J. Chem. Soc., Chem. Commun. 21 (1995) 2237.
[124] J. Aguilar, E. García-España, J.A. Guerrero, S.V. Luis, J.M. Llinares, J.F. Miravet, J.A. Ramírez, C. Soriano, Inorg. Chim. Acta 246 (1996) 287.
[125] J. Aguilar, B. Celda, V. Fusi, E. García-España, S.V. Luis, M.C. Martínez, J.A. Ramírez, C. Soriano, R. Tejero, J. Chem. Soc., Perkin Trans. 2 (2000) 1323.
[126] J. Aguilar, A.B. Descalzo, P. Díaz, E. García-España, S.V. Luis, M. Micheloni, J.A. Ramírez, P. Romani, C. Soriano, J. Chem. Soc., Perkin Trans. 2 (2000) 1187.
[127] J. Aguilar, P. Díaz, L. Gil, E. García-España, unpublished results.

[128] C. Bazzicalupi, A. Beconcini, A. Bencini, V. Fusi, C. Giorgi, A. Masotti, B. Valtancoli, J. Chem. Soc., Perkin Trans. 2 (1999) 1675.
[129] J. Rebek Jr., Science 235 (1987) 1478.
[130] A.D. Hamilton, D.J. Van Engen, J. Am. Chem. Soc. 109 (1987) 5035.
[131] M. Shionaya, T. Ikeda, E. Kimura, S. Motoo, J. Am. Chem. Soc. 116 (1994) 3848.
[132] T. Sakakibara, S. Murakami, N. Hattori, M. Nakajima, K. Imai, Anal. Biochem. 250 (1997) 157.
[133] P. Ronner, E. Friel, K. Czerniawski, S. Fraenkle, Anal. Biochem. 275 (1999) 208.
[134] T. Kamidate, S. Niwa, N. Nakata, Anal. Chim. Acta 424 (2000) 169.
[135] J. Edwards, R. Sprung, R. Sprague, D. Spence, Analyst 126 (2001) 1257.
[136] A. Denessiouk, V.-V. Rantanen, M.S. Johnson, Proteins: Struct., Funct., Genet. 44 (2001) 282.
[137] F. Dai, J.A. Kelley, H.P. Zhang, N. Malinowski, M.F. Kavlick, J. Lietzau, L. Welles, R. Yarchoan, H. Ford Jr., Anal. Biochem. 288 (2001) 52.
[138] R. Marczak, V.T. Hoang, K. Noworyta, M.E. Zandler, W. Kutner, F. D'Souza, J. Mater. Chem. 12 (2002) 2123.
[139] H. Fenniri, M.W. Hosseini, J.-M. Lehn, Helv. Chim. Acta 80 (1997) 786.
[140] S. Alves, F. Pina, M.T. Albelda, E. García-España, C. Soriano, S.V. Luis, Eur. J. Inorg. Chem. 2 (2001) 405.
[141] M.A. Bernardo, S. Alves, F. Pina, J. Seixas de Melo, M.T. Albelda, E. García-España, J.M. Llinares, C. Soriano, S.V. Luis, J. Supramol. Chem. 13 (2001) 435.
[142] M.T. Albelda, J. Aguilar, S. Alves, R. Aucejo, P. Díaz, C. Lodeiro, J.C. Lima, E. García-España, F. Pina, C. Soriano, Helv. Chim. Acta 86 (2003) 3118.
[143] J.S. de Melo, M.T. Albelda, P. Díaz, E. García-España, C. Lodeiro, S. Alves, J.C. Lima, F. Pina, C. Soriano, J. Chem. Soc., Perkin Trans. 2 (2002) 991.
[144] P. Schiessel, F.P. Schmidtchen, J. Org. Chem. 59 (1994) 509.
[145] A. Doménech, E. García-España, J.A. Ramírez, B. Celda, M.C. Martínez, C. Soriano, D. Monleón, R. Tejero, A. Bencini, A. Bianchi, J. Chem. Soc., Perkin Trans. 2 (1999) 23.
[146] W.D. Wilson, in: G.M. Blackburn, M.J. Gait (Eds.), Nucleic Acids in Chemistry and Biology, second ed., Oxford University Press, New York, 1996, p. 329.
[147] C. Denison, T. Kodadek, Chem. Biol. 5 (1998) R129.
[148] T. Hermann, W. Westhof, Curr. Opin. Biotech. 8 (1998) 278.
[149] M. Afshar, C.D. Prescott, G. Varani, Curr. Opin. Biotech. 10 (1999) 59.
[150] C. Chow, F.M. Bogdan, Chem. Rev. 97 (1997) 148.
[151] J.B. Chaires, Curr. Opin. Struct. Biol. 8 (1998) 314.
[152] D.K. Chand, H.-J. Schneider, J.A. Aguilar, F. Escartí, E. García-España, S.V. Luis, Inorg. Chim. Acta 316 (2000) 71.
[153] N. Lomadze, E. Gogritchainai, H.-J. Schneider, M.T. Albelda, J. Aguilar, E. García-España, S.V. Luis, Tetrahedron Lett. 43 (2002) 7801.
[154] D.K. Chang, H.-J. Schneider, A. Bencini, A. Bianchi, C. Giorgi, S. Ciattini, B. Valtancoli, Chem. Eur. J. 6 (2000) 4001.
[155] A. Bencini, E. Berni, A. Bianchi, C. Giorgi, B. Valtancoli, D.K. Chand, H.-J. Schneider, Dalton Trans. (2003) 793.
[156] W.D. Wilson, F.A. Tanious, M. Fernandez-Saiz, C.T. Rigl, in: K.R. Fox (Ed.), Methods in Molecular Biology: Drug–DNA Interaction Protocols, Humana Press Inc., Totowa, N.Y., 1997, p. 90.
[157] W.D. Wilson, L. Ratmeyer, M. Zhao, L. Strekowski, D. Boykin, Biochem. 32 (1993) 4908.
[158] Q. Vicens, E. Westhof, Chembiochem. 4 (2003) 1018.
[159] F. Walter, Q. Vicens, E. Westhof, Curr. Opin. Chem. Biol. 3 (1999) 694.
[160] for DNA polyamine interactions see H. Deng, V.A. Bloomfield, J.M. Benevides, G.J. Thomas, Nucl. Acids Res. 28 (2000) 3379.
[161] L. Bertini, H.B. Gray, S.J. Lippard, J.S. Valentine (Eds.), Bioinorganic Chemistry, University Science Books, Mill Valley, California, 1994.
[162] S.J. Lippard, J.M. Berg, Principles of Bioinorganic Chemistry, University Science Books, Mill Valley, California, 1995.
[163] R.H. Holm, E.I. Solomon (Eds.), Chem. Rev. 96 (1996) 2237 (special issue in bioinorganic enzymology).
[164] Protein Data Bank, http://www.pdb.org.
[165] E. García-España, J. Latorre, S.V. Luis, J.F. Miravet, P.E. Pozuelo, J.A. Ramírez, C. Soriano, Inorg. Chem. 35 (1996) 4591.
[166] A. Andrés, C. Bazzicalupi, A. Bianchi, E. García-España, S.V. Luis, J.F. Miravet, J.A. Ramírez, J. Chem. Soc., Dalton Trans. (1994) 2995.
[167] S. Andrés, B. Escuder, A. Doménech, E. García-España, S.V. Luis, V. Marcelino, J.M. Llinares, J.A. Ramírez, C. Soriano, J. Phys. Org. Chem. 14 (2001) 495.
[168] M.I. Burguete, B. Escuder, J.C. Frías, E. García-España, S.V. Luis, J.F. Miravet, J. Org. Chem. 63 (1997) 1810.
[169] B. Altava, M.I. Burguete, S.V. Luis, J.F. Miravet, E. García-España, V. Marcelino, C. Soriano, Tetrahedron 53 (1997) 4571.
[170] C. Bazzicalupi, A. Bencini, A. Bencini, A. Bianchi, F. Corana, V. Fusi, C. Giorgi, P. Paoli, P. Paoletti, B. Valtancoli, C. Zanchini, Inorg. Chem. 35 (1996) 5540.
[171] E. García-España, P. Gaviña, J. Latorre, C. Soriano, B. Verdejo, J. Am. Chem. Soc. 126 (2004) 5082.
[172] B. Verdejo, J. Aguilar, E. García-España, P. Gaviña, J. Latorre, C. Soriano, J.M. Llinares, A. Doménech, Inorg. Chem. 45 (2006) 2803.
[173] C. Bazzicalupi, A. Bencini, A. Bianchi, V. Fusi, C. Giorgi, P. Paoletti, B. Valtancoli, D. Zanchi, Inorg. Chem. 36 (1997) 2784.
[174] A. Bencini, E. Berni, A. Bianchi, V. Fedi, C. Giorgi, P. Paoletti, B. Valtancoli, Inorg. Chem. 38 (1999) 6323.
[175] C. Bazzicalupi, A. Bencini, E. Berni, A. Bianchi, P. Fornasari, C. Giorgi, B. Valtancoli, Inorg. Chem. 43 (2004) 6255.
[176] J. Aguilar, A. Bencini, E. Berni, A. Bianchi, E. Garcia-España, L. Gil, A. Mendoza, L. Ruiz-Ramirez, C. Soriano, Eur. J. Inorg. Chem. (2004) 4061.
[177] C. Bazzicalupi, A. Bencini, A. Bianchi, V. Fusi, E. García-España, C. Giorgi, J.M. Llinares, J.A. Ramírez, B. Valtancoli, Inorg. Chem. 38 (1999) 620.
[178] C. Miranda, F. Escartí, L. Lamarque, M.J.R. Yunta, P. Navarro, E. García-España, M.L. Jimeno, J. Am. Chem. Soc. 126 (2004) 823.
[179] L. Lamarque, P. Navarro, C. Miranda, V.J. Arán, C. Ochoa, F. Escartí, E. García-España, J. Latorre, S.V. Luis, J.F. Miravet, J. Am. Chem. Soc. 123 (2001) 10560.
[180] B. Verdejo, J. Aguilar, A. Domenech, C. Miranda, P. Navarro, E. García-España, H.R. Jimenez, C. Soriano, Chem. Commun. (2005) 3086.
[181] J. Aguilar, P. Díaz, F. Escartí, E. García-España, L. Gil, C. Soriano, B. Verdejo, Inorg. Chim. Acta 339 (2002) 307.
[182] C. Bazzicalupi, A. Bencini, A. Bianchi, A. Danesi, C. Giorgi, C. Lodeiro, F. Pina, S. Santarelli, B. Valtancoli, Chem. Commun. (2005) 2630.
[183] C. Lodeiro, F. Pina, A.J. Parola, A. Bencini, A. Bianchi, C. Bazzicalupi, S. Ciattini, C. Giorgi, A. Masotti, B. Valtancoli, J. Seixas de Melo, Inorg. Chem. 40 (2001) 6813.
[184] F. Pina, M. Ciano, L. Moggi, V. Balzani, Inorg. Chem. 24 (1985) 844.
[185] F. Pina, M. Maestri, R. Ballardini, Q.G. Mulazzani, M. D'Angelantonio, V. Balzani, Inorg. Chem. 25 (1986) 4249.
[186] F. Pina, J. Sotomayor, L. Moggi, J. Photochem. Photobiol. A 53 (1990) 411.
[187] M. Chadim, P. Díaz, E. García-España, J. Hodacova, J. Latorre, M. Liu-González, S.V. Luis, J.M. Llinares, J. Zavada, Inorg. Chem. 44 (2005) 7503.